The implication of microglial sialic acid-binding immunoglobulin-like lectin-E (Siglec-E) in neuroinflammation

Dissertation

zur

Erlangung des Doktorgrades (Dr. rer. nat.)

der

Mathematisch-Naturwissenschaftlichen Fakultät

der

Rheinischen Friedrich-Wilhelms-Universität Bonn

vorgelegt von

Janine Claude

aus

Heidelberg

Bonn, September 2013

Angefertigt mit Genehmigung der Mathematisch Naturwissenschaftlichen Fakultät der Rheinischen Friedrich-Wilhelms Universität Bonn.

1. Gutachter: Prof. Dr. Harald Neumann
2. Gutachter: Prof. Dr. Joachim Schultze

Tag der Promotion: 7. Februar 2014
Erscheinungsjahr: 2014

Table of contents

I List of figures

II Abbreviations

A	ab	antibody
	AD	Alzheimer’s disease
	ALS	amyotrophic lateral sclerosis
B	BAL	bronchoalveolar lavage
	BCR	B cell receptor
	BME	Basal Medium Eagle
	BSA	bovine serum albumin
C	CD	cluster of differentiation
	CMV	cytomegalovirus
	CNS	central nervous system
	CX3CL1	CX3 chemokine ligand 1
	CX3CR1	CX3 chemokine receptor 1
D	DAMP	danger-associated molecular pattern
	DAP12	DNAX activation protein of 12 kDa
	DAPI	4',6-diamidino-2-phenylindole
	DC	dendritic cell
	dest.	destillata
	DHE	dihydroethidium
	DMEM	Dulbeccos`s Modified Eagle Medium
	DMSO	dimethyl sulfoxide
	DTT	Dithiothreitol
E	E8	embryonic day 8
	EAE	experimental autoimmune disease
	EDTA	Ethylenediaminetetraacetic acid
F	Fc	fragment crystallisable
G	GAD	glutaraldehyde
	GFAP	Glial Fibrillary Acidic Protein
	GFP	Green fluorescent protein
H	HBS	Hepes buffered saline
	HBSS	Hank’s Balanced Salt Solution

I	I	isoleucine
	ICAM-1	intercellular adhesion molecule-1
	IgSF	immunoglobulin superfamily
	IFN	Interferon
	IL	Interleukin
	ITAM	immunoreceptor tyrosine-based activation motif
	ITIM	immunoreceptor tyrosine-based inhibition motif
K	kb	kilobases
	KCl	potassium chloride
	KDN	keto-deoxynonulosonic acid
L	L	leucine
	LPS	lipopolysaccharide
M	MAC-1	macrophage antigen 1
	MIS	a myeloid inhibitory siglec
	mRNA	messenger ribonucleic acid
N	NAD(P)H	reduced nicotinamide adenine dinucleotide (phosphate)
	NCAM	neural cell adhesion molecule
	Neu	neuraminic acid
	NO	nitric oxide
	NOX2	NADPH oxidase
O	OVA	ovalbumin
P	PAMP	pathogen-associated molecular pattern
	PD	Parkinson’s disease
	PE	phycoerythrin
	PFA	paraformaldehyde
	PGK	phosphoglycerate-kinase
	PI3K	phosphatidyl-inositol-3-kinase
	pLL	poly-L-lysine
	PSA	polysialic acid
Q	qRT-PCR	Quantitative real-time polymerase chain reaction
R	RANTES	regulated on activation, normal T cell expressed and secreted
	RNA	ribonucleic acid
	ROS	reactive oxygen species

S	SAMP	self-associated molecular pattern
	SHIP	Src homology 2 domain-containing inositol polyphosphate 5´phosphatase
	SHP	Src homology 2 domain-containing protein tyrosine phosphatase
	Siglec	sialic acid-binding immunoglobulin like lectin
	SOD1	superoxide dismutase 1
T	TBE	Tris/Borate/EDTA
	TGF-β	transforming growth factor-β
	TLR	Toll-like receptor
	TNF-α	tumour necrosis factor-α
	TRIF	TIR domain containing adaptor inducing IFN-β
V	V	valine
Y	Y	tyrosine

III Abstract

Microglia are the resident immune cells of the central nervous system (CNS). They display a whole set of recognition receptors on their cell surface to sense intact or lesioned cells in the CNS. A subfamily of these receptors are sialic acid-binding immunoglobulin like lectins (Siglecs). Siglecs can either exert activatory or inhibitory signals. Siglec-E is a member of this receptor family and has an immunoreceptor tyrosine based inhibitory motif (ITIM) in the cytoplasmic tail to suppress activatory microglial signals.

To study Siglec-E transcription and expression profile *ex vivo*, primary and stem cell-derived microglia were used. Via RT-PCR and flow cytometry it was shown that Siglec-E is expressed on microglia and was up-regulated following IFN-γ treatment. To study the functional role of Siglec-E, lentiviral knock-down and overexpression of Siglec-E was performed. Lentiviral overexpression of Siglec-E decreased whereas knock-down increased the phagocytosis rate of neural debris and its associated reactive oxygen burst. The extracellular domain of Siglec-E linked to the Fc-part of immunoglobulin bound to the sialic acid residues of the neuronal glycocalyx. Therefore, primary hippocampal neurons were co-cultured with the modified microglia. Overexpression and knock-down of Siglec-E led to an increase and decrease in relative neurite length, respectively. The neuroprotective effect of Siglec-E was abrogated after removal of the sialic acid residues on the neuronal glycocalyx. Treatment with the anti-oxidant Trolox abolished the neurotoxic effect of the Siglec-E knock-down on neurite length.

In summary, our data suggest an immunomodulatory function of Siglec-E on microglia, which leads to a neuroprotective phenotype by decreasing the production of reactive oxygen species and a reduced phagocytosis rate of neural debris.

1. Introduction

1.1 Microglia

1.1.1 History of microglia

The first scientist who described cells of the CNS, which did not show the appearance of neurons, in 1846 was the German pathologist Rudolf Virchow (1821 – 1902). He assumed that these cells fulfil the function of a connective tissue of the brain and ascribed them two functions: to support the neurons and to participate in the repair of the tissue. Nowadays it is known that two major cell types populate the CNS: nerve cells and glial cells. Glial cells consist of astrocytes, oligodendrocytes and microglia. The discrimination of microglia against astrocytes and oligodendrocytes as a separate cell type was discovered by Rio-Hortega in the early 20th century by his silver carbonate staining method (Figure 1.1) (del Rio-Hortega and Penfield 1927). Rio-Hortega described those cells as a cell population differing from other glial cell types like astrocytes and neurons and was the first scientist postulating the concept of the mesodermal origin of microglial cells (del Rio-Hortega 1932).

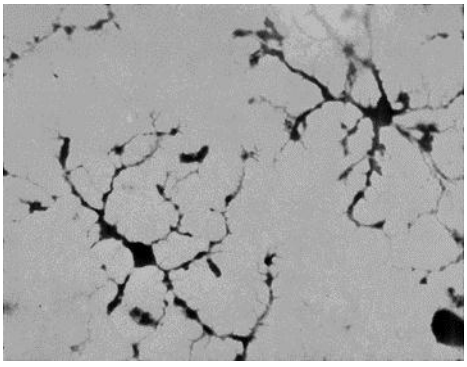

Figure 1.1: Silver staining of microglial cells by del Rio-Hortega (del Rio-Hortega 1919). With his silver carbonate staining del Rio-Hortega was the first scientist who distinguished between glial cell types.

1.1.2 Origin of microglia

The recent consensus is that microglia emanate from myeloid cells. Alliot and colleagues were able to show microglial progenitors positive for the macrophage/microglia markers macrophage-1 antigen (Mac-1), F4/80 and fragment crystallisable receptor (Fc-R) at the proto-somitic stage at embryonic day 8 (E8) in the neural folds where the embryo consists of 4-8 somites (Alliot et al. 1991).

A more recent study provides additional evidence that microglia derive from myeloid progenitors that arise before E8 from the yolk sac. Furthermore perinatal circulating hematopoietic precursors seem not to play a role in the homeostasis of microglia and invasion of bone marrow-derived cells only occurs upon injury (Ginhoux et al. 2010). Kierdorf and collegues were able to demonstrate that microglia emerge from erythromyeloid precursors from the yolk sac which can be identified at 9 days post conception as cluster of differentiation (CD) 45^- c-kit^+ cells. The further development seems to be dependent on the transcription factors Pu.1 and Irf8 (Kierdorf et al. 2013).

1.1.3 Morphology and function of microglia

Microglia constitute 5-20 % of the adult brain cell population depending on the species; in the adult mouse brain approximately 10 % of the cells are microglia (Lawson et al. 1990). The whole mouse brain harbours about 3.5×10^6 microglia. Of the glial cell population they represent about 20 %. Compared to the other glia they are the smallest.

Microglia are distributed throughout the brain and spinal cord and are more abundant in the grey compared to the white matter. Particularly dense populated areas are the hippocampus, basal ganglia, substantia nigra and parts of the telencephalon. Microglia are found as well in greater numbers in the cerebral cortex, thalamus and hypothalamus (Lawson et al. 1990). They form the first line of defence in the CNS.

Resting ramified microglia of the adult brain have only little or no visible cytoplasm. In their cytoplasm they have vacuoles suggesting their phagocytic activity and diverse finely-branched processes that have additional protrusions (Ransohoff and Perry 2009). Microglia concentrate in perivascular and perineuronal positions. On their cell surface they only express few surface markers of the monocyte-macrophage line, e.g. fragment crystallisable (Fc) and complement receptor whereas amoeboid

microglia have surface markers of the monocyte-macrophage lineage and an abundant cytoplasm (Barron 1995).

In vivo two-photon studies showed that microglia occur in two major forms but the metamorphosis between these conformational extremes is fluent. The “ramified” microglia have highly motile processes and branches (Figure 1.2). By constant withdrawal and *de novo* formation of their processes they are able to scan their microenvironment without movement of the cell body. Thereby, they do not disturb any fine-wired neuronal structures. Their duty is the homeostatic surveillance (Davalos et al. 2005; Nimmerjahn et al. 2005). Resting ramified microglia receive inhibitory signals via for example their CX3CR1 receptor. The ligand CX3 chemokine ligand 1 (CX3CL1) is secreted by neurons in the CNS (Cardona et al. 2006). Vice versa microglia produce immunosuppressive factors like Interleukin (IL) 10 and transforming growth factor-β (TGF-β) as well as neurotrophic factors to support neuronal function and survival (Hanisch 2002; Ransohoff and Perry 2009).

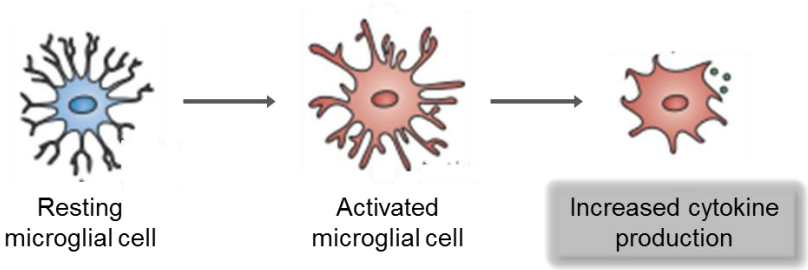

Figure 1.2: Different states of microglia. Resting microglia scan their environment and have a highly ramified structure. Upon activation they retract their processes and change to the amoeboid stage (modified from Perry et *al.*, 2007).

If the inhibitory CX3CR1 impulse is absent microglia become neurotoxic. Other stimuli can also trigger the activation of microglia such as the bacterial cell wall component lipopolysaccharide (LPS), viral ribonucleic acid (RNA) or the exposure to plasma proteins (Bechmann et al. 2007; Lehnardt 2010). Receptors recognizing these structures are of the Toll-like receptor (TLR) family or complement receptor MAC-1 triggered by opsonised bacteria (Stevens et al. 2007). Microglia express TLR 1-9. Their activation leads to increased secretion of Interferon (IFN)-α, IFN-β, IL-1β

and tumour necrosis factor (TNF)-α as well as reactive oxygen species (ROS) and nitric oxide (NO). After activation microglia regress their processes and undergo a metamorphosis to the so-called “amoeboid” state. The expression of specific surface receptors is activated and they become motile. Once activated, microglial cells are enabled to phagocyte and to present antigens to circulating T cells (Chan et al. 2007; Lehnardt 2010). The reorientation can occur in minutes to seconds (Hanisch and Kettenmann 2007).

Microglia eliminate cellular debris and redundant cells, which underwent apoptosis, without inducing inflammation. Find-me signals like ATP and UDP on damaged neurons enable the movement of microglia via the receptor $P2Y_6$ (Koizumi et al. 2007). Scavenger receptors perceive the translocation of phosphatidylserine from the inner leaflet onto the outer leaflet of the plasma membrane. The translocation leads to the recognition of an apoptotic cell (Ravichandran 2003; Ravichandran and Lorenz 2007). In the end this process triggers the removal of dying cells or their debris.

1.2 ITIM receptors

1.2.1 Microglial carbohydrate receptors in neuroinflammation

Microglia have different sets of receptors on their surface to fulfil their duties in the CNS. Additionally to the before mentioned TLRs, complement, cytokine and chemokine receptors microglia express carbohydrate-binding receptors on their surface. One family of these carbohydrate-binding receptors are the lectins, which can be further subdivided into three different classes: galectins, selectins and Siglecs (Schnaar 2004). Siglecs are carbohydrate receptors signalling via either an immunoreceptor tyrosine-based activation motif (ITAM) or an immunoreceptor tyrosine-based inhibition motif (ITIM).

1.2.2 Definition and function of ITIM receptors

The first ITIM was identified in the cytoplasmic domain of the receptor FcγRIIB (Van Den Herik-Oudijk et al. 1994). ITIMs can be traced back to relatively primitive metazoa. Genes encoding ITIM-containing molecules belong to the immunoglobulin superfamily (IgSF) or the C-type lectin family. They are derived from a common set of

ancestor genes having expanded and diverged from fish to mammals (Daeron et al. 2008).

Vivier and colleagues defined ITIMs as short sequences harbouring a tyrosine (Y) which is followed by a hydrophobic residue (isoleucine (I), valine (V) or leucine (L)) at position Y+3 and preceded by a less conserved hydrophobic residue at position Y-2 (Vivier and Daeron 1997).

ITIM-containing molecules are involved in the control of a large spectrum of biological processes, mostly but not exclusively related to immunity. They act on several cell types such as T cells (Nagaishi et al. 2006), macrophages (Takizawa and Manz 2007) and platelets (Cicmil et al. 2002; Rathore et al. 2003). Only recently it was shown that they participate in the promotion of proliferation (Kono et al. 2008) as well as apoptosis of cancer cells (Voisin et al. 2008).

1.2.3 Signalling pathway

ITIMs are the counterpart to activatory ITAM motifs. ITAM receptors are phosphorylated at their tyrosine residues by members of the Src kinase family (SKF) and then become a binding site for Syk protein kinases. When co-aggregated with an ITAM receptor ITIMs become phosphorylated by a tyrosine kinase of the Src-family, which enables them to recruit phosphatases, either Src homology 2 domain-containing inositol polyphosphate 5´phosphatase (SHIP) or more common the Src homology 2 domain-containing protein tyrosine phosphatases (SHP)-1 and SHP-2. They are recruited via the binding of their SH2 domain(s) to the phosphorylated ITIM. The activated SHP1 then dephosphorylates intracellular signalling intermediates leading to the termination of an activatory signal generated by an ITAM receptor (Figure 1.3).

The residue at position Y-2 determines the binding of SHP-1 and SHP-2 (Burshtyn et al. 1997; Olcese et al. 1996; Vely et al. 1997). For FcγRIIB a loss-of-function study identified the leucine at position Y+2 as mandatory for recruitment of SHIP-1 and SHIP-2 *in vitro* and *in vivo* (Bruhns et al. 2000).

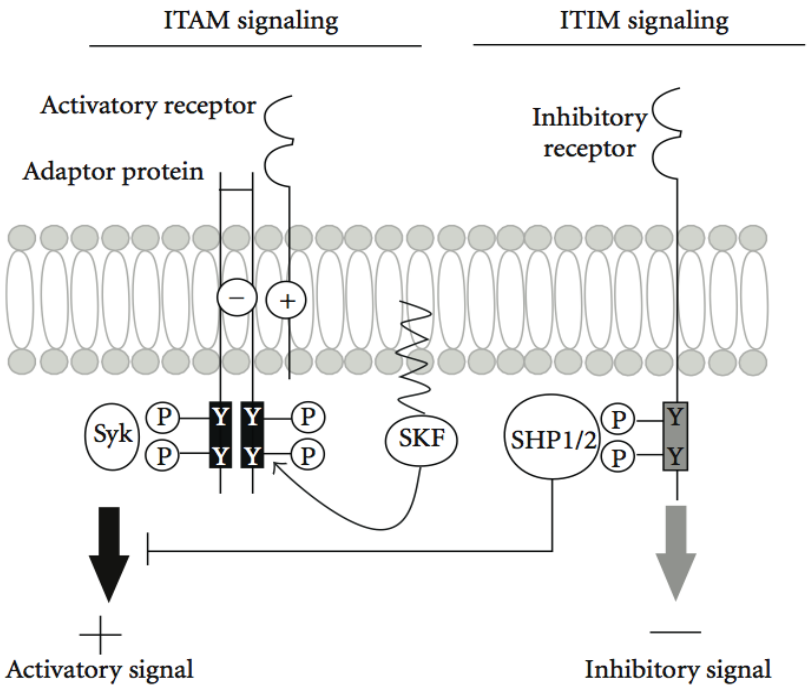

Figure 1.3: Signalling pathway of ITIM receptors. ITIM receptors inhibit the activatory signals of ITAM receptors (Linnartz et *al.*, 2010).

1.3 Siglecs

1.3.1 Sialic acid

The cell surface is covered by a broad variety of glycans that are attached to proteins and lipids. The exposed termini of oligosaccharides are often capped sialic acid-residues believed to have evolved relatively late in evolution. Fossil records report of sialic acid in deuterostome lineage animals such as starfish (Schauer and Kamerling 1997).

The term sialic acid is a general term for sugars encompassing nine carbons. Mammals possess different types of sialic acids and sialic acid can occur in different linkages. Usually, they are exposed at the non-reducing ends of oligosaccharide chains attached to the surface of a wide variety of proteins and cell types. One of their functions is to act as ligands on the cell surface to mediate selective cell-cell communication and interaction. In addition, they prevent cell-cell-interactions by

masking subterminal sugars (Kelm and Schauer 1997; Schauer and Kamerling 1997).

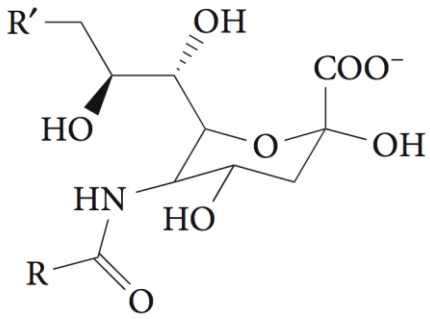

Sialic acid	R	R′
Neu5Ac	CH_3	OH
Neu5Gc	CH_2OH	OH
Neu5,9Ac_2	CH_3	OAc
Neu5Gc9Ac	CH_2OH	OAc

Figrue 1.4: Schema of sialic acid with a nine carbon backbone. In mammals sialic acid is commonly modified at the R and R' positions with the residues indicated in the grey box (modified from Crocker et *al.*, 2007).

In some pathogens the expression of sialic acid is essential for pathogenicity and survival within the microenvironment of the host. Via sialic acid pathogens mimic the surface of host cells and thereby circumvent the detection by the host immune system; they prevent complement activation and attenuate antibody (ab) production. Some pathogenic bacteria synthesize their own sialic acids, others transfer sialic acids from the host cell surface using a *trans*-sialidase (Crocker and Varki 2001a).

Another hypothesis is that the sialic acid residues on pathogens interact with the inhibitory CD33-related Siglecs to trigger a reduced activation response and as an outcome an improved pathogen survival within the host (Crocker and Varki 2001b).

1.3.2 Nomenclature and subfamilies of Siglecs

I-type lectins are defined as glycan-binding proteins that belong to the immunoglobulin superfamily. Among the I-type lectins there is a distinct subfamily of surface receptors that share structural and functional similarities - the Siglecs. Siglecs were separately discovered by two studies on a macrophage lectin-like adhesion molecule named sialoadhesin and a B-cell restricted member of the

immunoglobulin superfamily CD22 (Crocker and Gordon 1986; Stamenkovic and Seed 1990). Siglecs are characterized by a V-set Ig-like domain mediating sialic acid recognition and binding. Following this domain they have one or more C2-set Ig-like domains. Criteria for the inclusion of receptors in this specific group are (i) the ability to bind sialylated glycans and (ii) a significant sequence similarity within the N-terminal V-set and joining C2-set domains (Crocker et al. 1998).

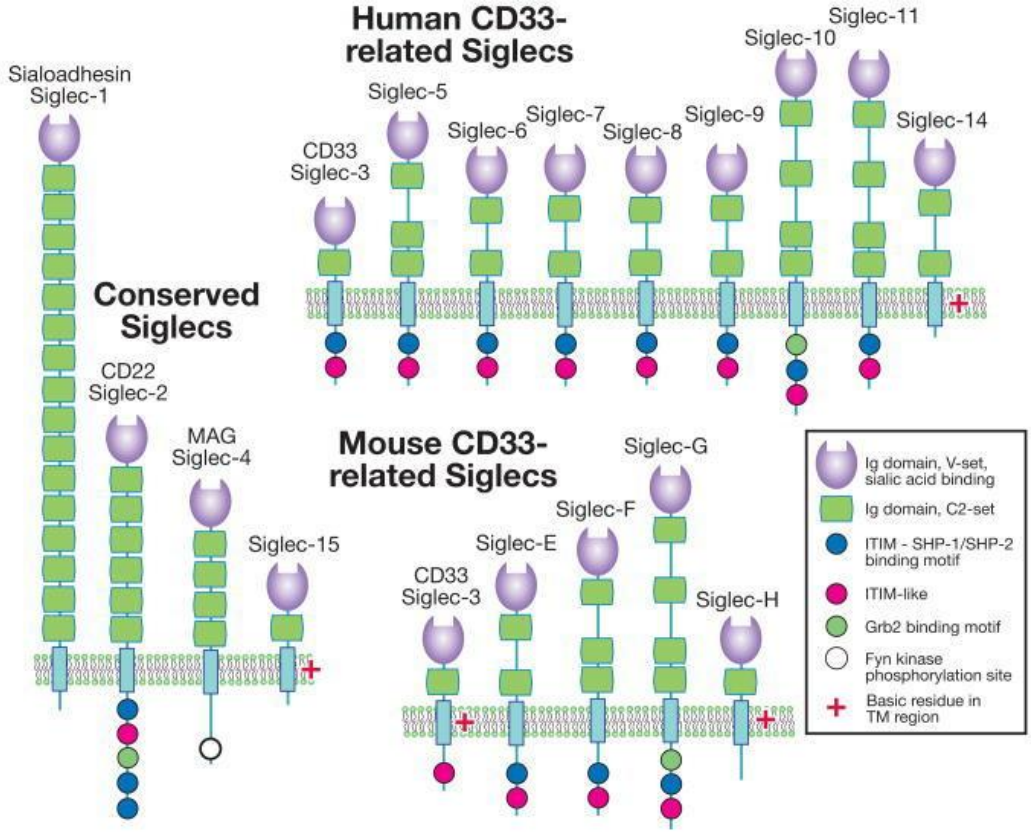

Figure 1.5: Overview of the Siglec family. The human Siglecs 2, 3 and 5-12 and the murine Siglecs 2 and Siglec-E, -F and –G have ITIM sequences in their cytoplasmic tail whereas the human Siglecs 14-15 and murine Siglecs 15 and –H have ITAMs and associate with the adaptor protein DNAX activation protein of 12 kDa (DAP12) (modified from Varki et al, 2009).

During the last few years several human and mouse members of the Siglec family have been identified through genomic studies and functional analyses. Siglecs can be subdivided into two distinct groups: the common Siglecs and the CD33-related Siglecs. The former group consists of the human founding members of the Siglec family: sialoadhesin (Siglec-1), a macrophage adhesion molecule; CD22 (Siglec-2), a

B-cell inhibitory receptor; CD33 (Siglec-3), a marker of myeloid cells and myelin-associated glycoprotein (MAG or Siglec-4). The latter are highly related to CD33 and to each other among this group and share about 50-80 % sequence similarity. They are a separate group not only from a functional point of view but concerning evolutionary perspectives as well. The nomenclature for CD33-related Siglecs is numerical in humans and alphabetical in mice (Crocker 2002) (Figure 1.5).

1.3.3 Composition and expression of Siglecs

Siglecs are type I transmembrane proteins, which are characterized by an N-terminal V-set Ig-like domain, which mediates sialic acid binding. The preference for a certain type of sialic acid is determined by a sequence of six amino acids in the C-C´ loop of the V-set domain (Yamaji et al. 2002). The V-set is followed by a varying number of C2-set Ig-like domains from which is believed that they have evolved through repeated gene duplications. In the mouse the number varies between 4 C2-set Ig-like domains in Siglec-G and only one in Siglec-H. For the human sialoadhesin even 16 C2-set Ig-like domains have been reported (Crocker et al. 2007) (Figure 1.5).

Collectively, the CD33-related Siglecs are expressed broadly in the innate immune system, but are strikingly absent from most T lymphocytes (Crocker and Varki 2001b). Some Siglecs are expressed on a broad range of cells; others are expressed in a much more specific pattern, e.g. human Siglec-9 is found on neutrophils, monocytes and a fraction of natural killer (NK) and B cells and a subset of T cells (Zhang et al. 2000). Quite the contrary is true for Siglec-8, which is expressed on circulating eosinophils and hence in a much more restricted pattern (Floyd et al. 2000). Some cell types express more than one type of Siglec receptors. But of the CD33-related Siglecs, every receptor exhibits a specific expression pattern among hematopoietic cells.

Concerning their cytosolic tail, Siglecs vary in sequence and length, although most of the CD33-related Siglecs share regions of sequence similarity surrounding their two conserved ITIMs. The genes encoding human Siglecs are on chromosome 20p (sialoadhesin) or 19q (all other Siglecs) and those encoding the murine Siglecs are on chromosomes 2 and 7 (Crocker 2002).

1.3.4 Function in the immune system

Siglecs recognize different forms and linkages of sialic acids that are commonly found on the cell surface. Siglec binding sites can be masked by *cis* interactions with sialic acids on the same cell, which then prevent them from mediating cell-cell interactions. Studies indicate that most Siglecs on resting cells indeed exist in a masked form. Unmasking them may occur during cellular activation (Crocker et al. 1995; Crocker and Gordon 1986). Therefore, *cis* interactions could potentially regulate Siglec functions (Figure 1.6).

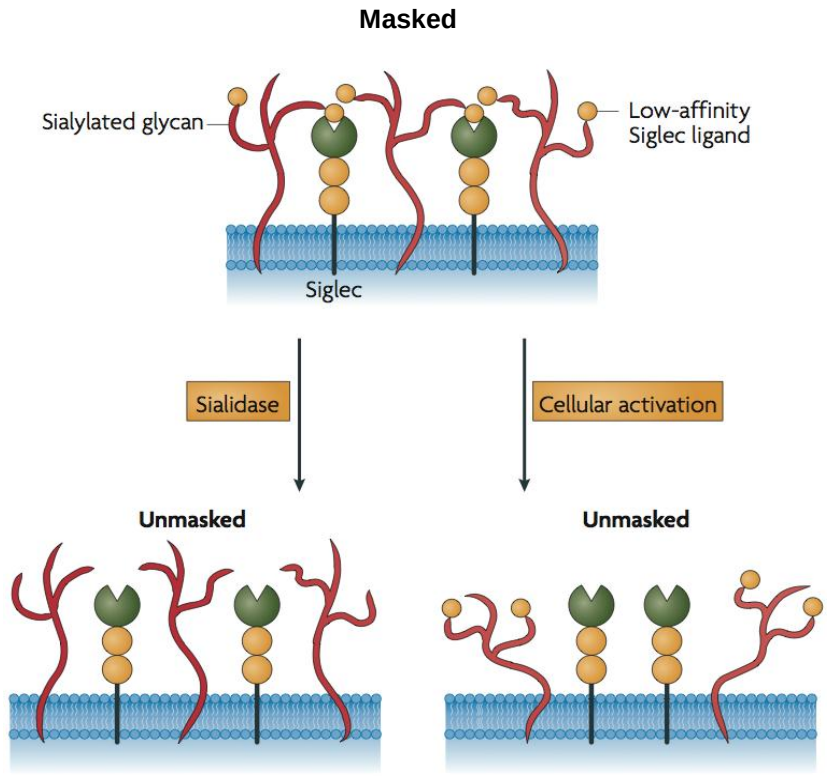

Figure 1.6: *Cis* and *trans* interactions of Siglecs. Most Siglecs found on cells are in a masked form due to *cis*-interactions with sialic acids expressed on the cell surface of the same cell. Treatment with sialidase or cellular activation leads to unmasking of the Siglecs and enables them to bind to their ligand in *trans* (modified from Crocker et *al.*, 2007).

In case the receptor becomes unmasked it can bind to its target in *trans* on another cell surface; the signalling cascade via the cytosolic ITIM gets activated and the inhibitory effect that antagonizes the ITAM receptor is executed. It is believed that

Siglecs could play a role in the regulation of the innate immune system. For example, CD22 is a B-cell inhibitory receptor and contains three ITIMs. The ITIMs associate with the B-cell receptor (BCR) and inhibit cellular activation (Crocker 2002). In contrast, another study could show that a sialic-acid-based CD22-specific inhibitor caused heightened activation of B cells in response to BCR cross-linking, which is accompanied by hypophosphorylation of CD22 and reduced recruitment of SHP-1 (Kelm et al. 2002).

Artificially cross-linking of FcγRI with antibodies results in reduced Ca^{2+} influx (Ulyanova et al. 2001). Similarly, when clustering Siglec-7 with a cross-linking antibody, cytotoxicity of NK cells can be inhibited (Falco et al. 1999). Addition of an antibody against human CD33 or against Siglec-7 to haematopoietic cell cultures leads to reduced cell growth and inhibition of dendritic cell development (Ferlazzo et al. 2000; Vitale et al. 1999).

Additionally sialic acids might act as broadly expressed “self” ligands that interact with CD33-related Siglecs on myeloid cells. Thereby, they could prevent inappropriate self-reactivity.

1.3.5 Siglec-E

Siglec-E was first identified by Ulyanova and colleagues in 2001. In the beginning Siglec-E was called MIS (a myeloid inhibitory siglec) (Ulyanova et al. 2001). Siglec-E consists of seven exons spanning approximately 9.1 kilobases (kb). The messenger ribonucleic acid (mRNA) transcript has a length of 2.0 kb and the encoded protein is 467 amino acids long and has a molecular weight of ~80-85 kilo Dalton (kDa). *In vivo* it exists as a disulfide-linked oligomeric complex with at least two molecules of Siglec-E (Yu et al. 2001). From the sequence, an extracellular domain composed of 331 amino acids, a hydrophobic transmembrane domain containing 27 amino acids, and a cytoplasmic tail of 93 amino acids was predicted. The sequence starts with a hydrophobic signal peptide and harbours ten potential N-glycosylation sides (asparagine (N)-X-serine (S)/threonine (T)) in the extracellular region of the protein. By its migration properties in a SDS-PAGE it was confirmed that Siglec-E is indeed glycosylated. It most closely resembles the human Siglecs 7 and 9 with an overall

sequence identity of 52 % and 53 % and exhibits combined features of both (Zhang et al. 2004) (Figure 1.5 and 1.7).

Siglec-E binds alpha2-8 linked sialic acid preferentially to alpha2-3 and alpha2-6-linked sialic acid (Zhang et al. 2004). The amino acids, which are indispensable for binding of sialic acid, are conserved in Siglec-E at position 126 (arginine), at position 25 (phenylalanine) and at position 134 (tyrosine). Additionally, cysteine residues, which are conserved in the Siglec family, are found in Siglec-E (Yu et al. 2001).

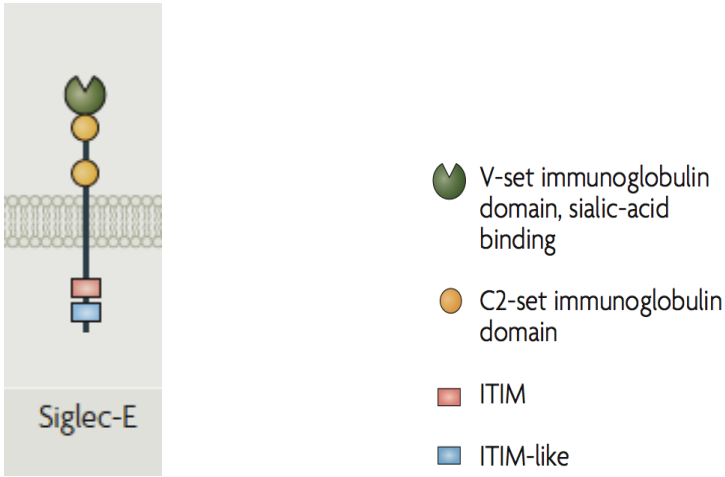

Figure 1.7: Murine Siglec-E. The murine receptor Siglec-E is a type I transmembrane protein with three extracellular domains. The N-terminal domain mediates sialic acid binding and is followed by two Ig-like domains. In its intracellular part it harbours one ITIM sequence and one ITIM-like sequence (modified from Crocker et *al.*, 2007).

Siglec-E is highly expressed in the spleen and on mature cells of the innate immune system, including the cell types that express either hSiglec-7 and/or -9 such as phagocytic cells and on antigen-presenting cells including macrophages and dendritic cells (DCs) (Zhang et al. 2004).

The ITIMs of Siglec-E recruit SHP-1 and SHP-2. SHP-1 is recruited either through its membrane-proximal ITIM (centred at Y-432) or the membrane-distal ITIM (centred at Y-455) (Ulyanova et al. 2001). The membrane-proximal ITIM alone is sufficient for binding of SHP-1 (Zhang et al. 2004). Each SH2 domain of SHP-1 is capable of binding to the membrane-proximal ITIM, whereas only the first (N-terminal) SH2 domain is able to bind to the membrane-distal ITIM. The degree of association with

Siglec-E correlates with the extent of Siglec-E tyrosine phosphorylation (Ulyanova et al. 2001).

A study of Boyd and colleagues demonstrated that the expression of Siglec-E is induced after stimulation with TLRs in a MyD88-specific manner. Once up-regulated, it can control/inhibit TLR-induced NF-κB and the induction of the antiviral cytokines Interferon-β (IFN-β) and RANTES (regulated on activation, normal T cell expressed and secreted). Hence Siglec-E seems to be capable of controlling the antiviral response to TLRs and thereby helps to maintain a healthy cytokine balance following infection (Boyd et al. 2009).

In a recent publication another functional aspect of Siglec-E was shown. Siglec-E deficient mice showed a higher neutrophil recruitment to the lung in an acute lung inflammation model induced by aerosolised LPS (McMillan et al. 2013). This effect was mediated by negative regulation of the adhesive function of the integrin CD11b by Siglec-E, indicating an important role of Siglec-E in the regulation of the inflammatory response to lung inflammation to prevent an over-activation of the immune system.

1.4 Aim of the study

Microglia are cells of the innate immune system and build the first line of defence in the CNS. Their duty is on the one hand homeostasis and defence against pathogens on the other. To be able to fulfil their duties, they have immune receptors on their surface, recognizing pathogen and disease-associated molecular patterns, but have molecules to sense intact tissue, too. Siglecs are one of these receptor families on microglia. One member of this family is the murine Siglec-E.

So far there are no data about Siglec-E on microglial cells. Therefore, the aim of this study was to investigate the role of Siglec-E on microglia in neuroinflammation. The questions to be answered were, which regulatory role Siglec-E might play on microglia in the CNS and what are the consequences for neurons in the brain in a co-culture setting.

For this purpose, we first had to prove that there is indeed Siglec-E expression on microglia. To get an idea about the functional role, we performed lentiviral knock-down and overexpression studies. The modified microglia were analysed for changes in cytokine transcription and surface marker expression. We looked for differences in phagocytic behaviour and the associated burst of reactive oxygen species in these modified microglia.

After we discovered that a recombinant Siglec-E:Fc fusion protein is able to bind to sialic acids on neuronal surfaces, we started co-culture experiments with primary neurons in which we mimicked the state of neuronal damage. Scavenging experiments were done with an anti-oxidant. By measuring the neurite length we evaluated the effect of Siglec-E knock-down and overexpression.

2. Materials and Methods

2.1 Materials

2.1.1 Chemicals and Reagents

Chemical	Company
Agarose	Biozym, Germany
Ampicillin	Sigma, Germany
Amplex® Red	Invitrogen, Germany
Avertin (2, 2, 2-tribromoethanol)	Sigma, Germany
B-27® Supplement	Gibco, Germany
Basal Medium Eagle (BME) (1x), liquid	Gibco, Germany
Boric Acid (H_3BO_3)	Sigma, Germany
Bromophenol Blue	Sigma, Germany
CellTracker™ CM-DiI, 1 mg	Life Technologies, Germany
Chloroquine diphosphate salt	Sigma-Aldrich, Germany
DABCO	Sigma, Germany
4',6-diamidino-2-phenylindole (DAPI)	Sigma Aldrich Chemie GmbH, Germany
ddH_2O	Roth, Germany
dihydroethidium (DHE)	Invitrogen GmbH, Germany
D-Glucose (45 %)	Sigma, Germany
DMEM/F12 (1:1)	Gibco, Germany
DMSO for molecular biology, >= 99.9 %	Sigma, Germany
dNTP Mix (10 mM)	Sigma, Germany
DTT (10 mM)	Invitrogen, Germany
Dulbecco's Modified Eagle Medium (D-MEM) (1x), liquid (4.5 g/L D-glucose)	Gibco, Germany
Ethanol (C_2H_6O)	Roth, Germany
Ethidium Bromide (10g/l)	Roth, Germany
Ethylendiamintetraacetate (EDTA)	Roth, Germany

Fetal Bovine Serum (FBS)	Gibco, Germany
Fetal Bovine Serum, ultra-low IgG	Gibco, Germany
Ficoll-400	Bio-Rad, Germany
First Strand Buffer (5x)	Invitrogen, Germany
Glycerol	Sigma, Germany
Hank's Balanced Salt Solution (HBSS) (1x)	Gibco, Germany
HBSS (10x)	Gibco, Germany
Hexanucleotide Mix (10x)	Roche, Germany
L-Glutamine (200 mM)	Sigma, Germany
LB Agar	Sigma, Germany
LB Broth	Sigma, Germany
Lipofectamine™ Transfection Reagent	Gibco, Germany
MEM nonessential amino acid solution (100x)	Gibco, Germany
MEM sodium pyruvate solution (100 mM)	Gibco, Germany
Mowiol	Kremer Pigmente, Germany
okadaic acid	Sigma, Germany
Opti-MEM® I Reduced-SerumMedium (1x), liquid	Gibco, Germany
Paraformaldehyde (PFA)	Sigma, Germany
Penicillin/Streptomycin (100x)	Gibco, Germany
Percoll™	GE Healthcare, Germany
Polybrene	Sigma, Germany
poly-L-Lysine	Sigma, Germany
Sodium chloride (NaCl)	Roth, Germany
Sodiumhydrogenphosphate (NaH_2PO_4*H_2O)	Roth, Germany
Sodiumhydrogenphosphate (NaH_2PO_4*$7H_2O$)	Roth, Germany
Sodium hydroxid (NaOH)	Roth, Germany
Sucrose	Roth, Germany
SYBR Green Master Mix (2x)	Applied Biosystems, Germany
tert-amyl alcohol (2-methyl-2-butanol)	Fisher, Germany
Tris base	Roth, Germany
Tris buffer, 0.2 M	Roth, Germany
Trypan Blue	Gibco, Germany
Xylene Cyanole	Sigma, Germany
Zeocin	InvivoGen, USA

2.1.2 Buffers and solutions

10x (0.125 M) Phosphate buffered saline (PBS), pH 7.3	0.007 M	$NaH_2PO_4*H_2O$
	0.034 M	$NaH_2PO_4*7H_2O$
	0.6 M	NaCl
	up to 1 litre ddH_2O	
2x HBS	8 g	NaCl
	0.38 g	KCl
	0.1 g	Na_2HPO_4
	5 g	Hepes
	1 g	glucose
	up to 500 ml ddH_2O	
	adjust pH to 7.05	
4% Paraformaldehyde (PFA), pH 7.3	20 g	PFA
	30 ml	NaOH
	50 ml	PBS (10x)
	up to 1 litre ddH_2O	
Mowiol	4.8 g	mowiol
	12 g	glycerol
	12 ml	ddH_2O
	24 ml	0.2 M tris buffer
	1.32 g	DABCO
10x Tris/Borate/EDTA (TBE) buffer	1.78 M	tris-Base
	1.78 M	boric Acid
	0.04 M	EDTA
	up to 2 litres ddH_2O	

6x Loading buffer	0.5 M	EDTA
	60 % (w/v)	sucrose
	0.04 % (w/v)	bromophenol blue
	0.04 % (w/v)	xylene cyanole
	2 % (v/v)	Ficol-400
1% Agarose gel	0.5 g	agarose
	4 µl	ethidium bromide
	50 ml	TBE (1x)
Real time polymerase chain reaction (RT-PCR) mix	3 µl	cDNA (200 ng/µl)
	12.5 µl	SYBR Green Master Mix (2x)
	2 µl	primer Mix (10 pmol/µl)
	7.5 µl	ddH_2O
Reverse transcription (RT) mix	5 µg	total RNA
	1 µl	hexanucleotide Mix (10x)
	1 µl	dNTP Mix (10 mM)
	2 µl	DTT (10 mM)
	4 µl	5x RT first strand buffer
	1 µl	reverse transcriptase (200 U/ml)
	up to 20 µl ddH_2O	
Avertin stock solution	25 g	avertin (2, 2, 2-tribromoethanol)
	15,5 ml	tert-amyl alcohol (2-methyl-2-butanol)

2.1.3 Cell culture media and reagents

N2 medium	500 ml	DMEM/F12 (1:1)
	0.048 mM	L-Glutamine (200 mM)
	15.3 µg/ml	D-Glucose (45%)
	1 % (v/v)	Penicillin/Streptomycin (100x)

MEF medium	450 ml	DMEM high glucose
	10 % (v/v)	Fetal Bovine Serum
	1 % (v/v)	L-Glutamine (200 mM)
	1 % (v/v)	MEM nonessential amino acid solution (100x)
	1 % (v/v)	MEM sodium pyruvate solution (100 mM)
Trans-MEF medium	500 ml	DMEM high glucose
	5 % (v/v)	Fetal Bovine Serum
	1 % (v/v)	L-Glutamine (200 mM)
	1 % (v/v)	MEM nonessential amino acid solution (100x)
	1 % (v/v)	MEM sodium pyruvate solution (100 mM)
	50 nM	chloroquine
Primary microglia medium	450 ml	BME
	10 % (v/v)	Fetal Bovine Serum
	1 % (v/v)	L-Glutamine (200 mM)
	2 % (v/v)	D-Glucose (45%)
	1 % (v/v)	Penicillin/Streptomycin (100x)
Neuron medium	500 ml	BME
	1 % (v/v)	Fetal Bovine Serum
	1 % (v/v)	D-Glucose (45%)
	2 % (v/v)	B-27

2.1.4 Cell lines and bacterial strains

Cell line/Bacterial Strain	Source
Chinese Hamster Ovary (CHO) cells	Jerome Mertens (AG Brüstle)
Embryonic Stem Cell-derived Microglia (ESdM)	Clara Beutner (AG Neumann)
GL261	Hertie-Institute for clinical neurology, Germany
HEK293FT	Invitrogen, Germany
OneShot® Top10 Chemically Competent E. coli	Invitrogen, Germany

SMA560	Hertie-Institute for clinical neurology, Germany

2.1.5 Antibodies, enzymes, recombinant proteins and stimulants

2.1.5.1. Primary Antibodies

Antibody	Host	Reactivity	Company
anti-mouse-Fc	rabbit	mouse	Dianova, Germany
βIII-tubulin	mouse	mouse	Sigma, Germany
CD11b-biotinylated	rat	mouse	BD Biosciences, Germany
CD11b-phycoerythrin (PE)	rat	mouse	eBioscience, USA
CD11c-biotinylated	hamster	mouse	BD Biosciences, Germany
CD16/32	rat	mouse	BD Biosciences, Germany
CD18-biotinylated	rat	mouse	BD Biosciences, Germany
CD31-biotinylated	rat	mouse	BD Biosciences, Germany
CD34-biotinylated	rat	mouse	BD Pharmingen, Germany
CD45-biotinylated	rat	mouse	BD Biosciences, Germany
CD45-V450	rat	mouse	BD Biosciences, Germany
CD68	rat	mouse	AbD serotec, USA
CD80-biotinylated	hamster	mouse	BD Biosciences, Germany
CD86-biotinylated	rat	mouse	BD Biosciences, Germany
F4/80-biotinylated	rat	mouse	Serotec, Germany
GFAP	mouse	mouse	abcam
Iba1	rabbit	mouse	Wako, Germany
Siglec-E	rat	mouse	MBL International, Japan

2.1.5.2 Isotype controls

Antibody	Host	Reactivity	Company
isotype IgG2bκ	rat		BD Biosciences, Germany
isotype IgG2bκ-PE	rat		BD Biosciences, Germany
isotype IgG2bκ-V450	rat		BD Biosciences, Germany

2.1.5.3 Secondary Antibodies

Fluorophore	**Host**	**Reactivity**	**Company**
Alexa488	Goat	Rabbit	Invitrogen, Germany
anti-rat-biotinylated	goat	rat	Dianova, Germany
Cy3	Goat	Rat	Dianova, Germany
Cy3	Goat	Mouse	Dianova, Germany
FITC	Goat	Rat	Dianova, Germany
PE	Goat	Rat	JacksonImmuno, USA
PE-Streptavidin			JacksonImmuno, USA
Alexa647-Streptavidin			JacksonImmuno, USA

2.1.5.4 Enzymes, recombinant proteins

Enzyme	**Company**
BamHI (10 U/µl)	Roche, Germany
BglII (10 U/µl)	New England Biolabs, Germany
Catalase	Serva, Germany
DNase I, RNase-free, lyophilized	Qiagen, Germany
EcoRI (10 U/µl)	Roche, Germany
EcoRV (10 U/µl)	Roche, Germany
EndoN (EC 3.2.1.129)	Abcys, France
HindIII (10 U/µl)	Roche, Germany
Neuraminidase (Sialidase; EC 3.2.1.18) from *Arthrobacter ureafaciens*	Roche, Germany
Neuraminidase (EC 3.2.1.18) from *Clostridium perfringens*	New England Biolabs, Germany
Peroxidase from Horseradish	Sigma, Germany
PinAI (AgeI) (10 U/µl)	Roche, Germany
Platinum Taq DNA Polymerase High Fidelity	Invitrogen, Germany
Recombinant mouse Siglec-E Fc chimera, CF	R & D Systems, Germany
Recombinant mouse Siglec-F Fc chimera, CF	R & D Systems, Germany
Reverse Transcriptase (200 U/ml)	Invitrogen, Germany
SfuI (AsuII) (10 U/µl)	Roche, Germany
Superoxide dismutase from bovine	Serva, Germany

erythrocytes	
T4 DNA Ligase	Invitrogen, Germany
XhoI (10 U/µl)	Roche, Germany

2.1.5.5 Stimulants

Stimulant	**Company**
LPS *S. enterica* serotype abortus equi (1000 µg/ml)	Sigma, Germany
Recombinant murine IFN-α, CHO derived (10^6 U/ml)	Hycult Biotechnology, Netherland
Recombinant murine IFN-γ, CHO derived (10^6 U/ml)	Hycult Biotechnology, Netherland
Recombinant murine TNF-α (10 µg/ml)	R & D Systems, Germany

2.1.6 Primer

2.1.6.1 Quantitative Real-Time PCR Primer

Target	**Orientation**	**Sequence**
GAPDH	forward	5’ – ACAACTTTGGCATTGTGGAA – 3’
	reverse	5’ – GTCTTGTAGTAGGGACGTAG – 3’
IL-1β	forward	5’ – ACAACAAAAAAGCCTCGTGCTG – 3’
	reverse	5’ – TGAAAGCTCTCCACCTCAATGG – 3’
iNOS	forward	5’ – AAGCCCCGCTACTACTCCAT – 3’
	reverse	5’ – TTGGATCAGGAACCTGAAGC – 3’
Siglec-E	forward	5’ – TCTGAGGGCCAGTCACTGCGT – 3’
	reverse	5’ – GGACAGAGGTGTCTCGTCACGTT – 3’
TNF- α	forward	5’ – TCTTCTCATTCCTGCTTGTGG – 3’
	reverse	5’ – AGTTCTATGGCCCAGACCCT – 3’

2.1.6.2 Cloning Primer

Target	Orientation	Sequence
Igκ EcoRI fwd	forward	5’ – CATGAATTCACCATGGAGACAGACACACTCCTG – 3’
SigE flag fw XhoI	forward	5’ – CATCTCGAGACCATGCTGCTGTTGCTGCTGC – 3’
SigE flag rv SfuI	reverse	5’ – CATTTCGAATCCTCCTCCTCCTCCTCCTGGCCATGCGGTCCTTTG – 3’
SigE pll fw AgeI	forward	5’ – CATACCGGTACCATGCTGCTGTTGCTGCTGC – 3’
SigE pll rv AgeI	reverse	5’ – GTTTCCTGGCGTACCGGTCCTCCTCCTCCTGGCCATAC – 3’

2.1.6.3 Sequencing Primer

Target	Orientation	Sequence
hIgG1-Fc rv seq	reverse	5’ – CGTAGTGTTTAAAGTGTTTATTTCG – 3’
SigE F1 seq	forward	5’ – CATCATATGCTGCTGTTGCTGCTGC – 3’
SigE F2 seq	forward	5’ – GCTCCAAAGAATCTGACTGTGAC – 3’
SigE R1 seq	reverse	5’ – CGTTGGACTGGACGAGAC – 3’

2.1.7 Consumables

Product	Company
0.22 µm pore size filter stericup	Millipore, USA
100 Sterican 20Gx2 ¾ 0,9x70 mm	Braun Melsungen AG
2 ml, 5 ml, 10 ml, 25 ml plastic pipets	Costar, Germany
5 ml polystyrene round-bottom tubes	BD Falcon, Germany
6-well culture plates	Cellstar, Germany
10 µl, 100 µl, 1000 µl pipette tips	Eppendorf, Germany
10 ml, 50 ml syringe	Braun, Germany
15 ml plastic tubes	Greiner, Germany
24-well culture plates	Greiner, Germany
50 ml plastic tubes	Sarstedt, Germany

BD 5 ml Syringe Luer-lock Tip	BD Syringe, Germany
BD Discardit™ II Spritze	Becton Dickinson GmbH
BD Microlance™ 3	Becton Dickinson GmbH
Bottle top filters, 0.25 µm pore	Millipore, Germany
Cell scraper	Sarstedt, Germany
Cell strainer 40 µm Nylon	BD Falcon, Germany
Cell strainer 70 µm Nylon	BD Falcon, Germany
Chamber slides	Nunc, Germany
Cryovials	VWR International, Germany
Dermaclean Untersuchungshandschuhe	Ansell, Germany
Erlenmeyer flask, 250 ml	Schott-Duran, Germany
Glass cover slides 24x24 mm	VWR International, Germany
Glas pasteur pipettes	Brand, Germany
Injection needles	Braun, Germany
MicroAmp® 96-well Optical Adhesive Film	Applied Biosystems, USA
MicroAmp® optical 96-well plate	Applied Biosystems, USA
NitraTex® Nitril-Untersuchungshandschuhe	Ansell, Germany
Optical Adhesive Covers	Applied Biosystems, USA
PCR tubes, 500 µl	Biozym Diagnostics, Germany
Petri dishes 100x15 mm	BD Falcon, Germany
Tissue culture dish 60x15 mm	Sarstedt, Germany
Tissue culture dish 100x20 mm	Sarstedt, Germany
Tissue culture dish 150x20 mm	TPP, Germany
Tubes 1.5 ml, 2.0 ml	Eppendorf, Germany

2.1.8 Equipment

Equipment	**Company**
Agagel Standard	Biometra, Germany
BD Facs Calibur	BD Bioscience
BD Facs CantoII	BD Bioscience
Biofuge Fresco	Heraeus, Germany
BL 610	Sartorius, Germany
Electrophoresis Power Supply EPS-301	Amersham Bioscience, Germany
Fluoview1000 Confocal microscope	Olympus, Germany

Freezer -80°C Herafreeze	Heraeus, Germany
Heating block	Stuart Scientific, Germany
HeraCell 240	Heraeus, Germany
HI 9321 Microprocessor pH meter	Hanna Instruments, Germany
Kompaktschüttler KS-15 Control	Edmund Bühler, Germany
Mastercycler epgradient S	Eppendorf, Germany
Megafuge, 1.OR.	Heraeus, Germany
Neubauer chamber	Brand, Germany
Operating microscope OPMI-FR	Zeiss, Germany
Pumpdrive 5001	Heidolph, Germany
Roto-Shake Genie	Scientific Industries Inc., USA
Shimadzu RF 5001PC spectrofluorimeter	Shimadzu, USA
Sorvall Discovery 90SE	Hitachi, Germany
Standard Power Pack P25	Biometra, Germany
Thermocycler T3	Biometra, Germany
Thermomixer compact	Eppendorf, Germany
Vortex Genie2	Scientific Industries Inc., USA
Waterbath Modell WB 7	Memmert, Germany
XCell II™ Mini-Cell Blot Module Kit CE Mark	Invitrogen, Germany
XCell II™ Mini-Cell SureLock® Retrofit Kit	Invitrogen, Germany

2.1.9 Kits, Marker and Vectors

Name	**Company**
DNA Molecular Weight Marker XIV (100 bp ladder)	Roche, Germany
pll3.7 U6 removed	Yiner Wang, AG Neumann
PureLink™ HiPure Plasmid Filter Maxiprep Kit	Invitrogen, Germany
QIAprep Spin Miniprep Kit	Qiagen, Germany
QIAquick Gel extraction Kit	Qiagen, Germany
RNeasy Mini Kit	Qiagen, Germany
RNeasy Lipid Tissue Mini Kit	Qiagen, Germany

2.1.10 Software

Software	Company
Adobe Illustrator™CS3	Adobe
Adobe Photoshop™CS3	Adobe
ApE	M. Wayne Davis
EndNote X1	Thomson ISI ResearchSoft, USA
FlowJo 6.4.7	Tree Star, USA
ImageJ 1.43m	National Institute of Health, USA
Microsoft Office	Microsoft, USA
Olympus FluoView 1.4	Olympus, Germany
QuantityOne	Bio-Rad, Germany
SPSS	IBM, Germany

2.2 Methods

2.2.1 Isolation of primary microglia and neurons

Primary neuronal cultures were obtained from embryonic mice at day 14 or 15 of C57BL/6 mice while primary microglia were prepared from brains of postnatal day 3 or 4 (P3 or P4) of C57BL/6 mice. In brief, the brains were isolated and only the two hemispheres were used. The meninges were removed mechanically and cells were dissociated by trituration and cultured in basal medium for 14 days to form a confluent mixed glial monolayer. For neuronal cultures only the hippocampus and cortex were used, for primary microglia both hemispheres without cerebellum and olfactory lobes were prepared.

To collect microglial cells, the cultures were shaken on a rotary shaker (350 rpm) for 3 hours. The detached microglial cells were either used directly for flow cytometry analysis or seeded on poly-L-lysine (pLL) coated culture dishes at 37°C in 5 % CO_2 for stimulation and RNA isolation.

2.2.2 *Ex vivo* isolation of brain cells

Three weeks old C57/BL6 mice were perfused with HBSS and the brain was prepared without cerebellum. The brain was homogenized in HBSS and centrifuged for 7 minutes at 300g. The pellet was resuspended in 37 % percol and loaded onto a percol gradient consisting of HBSS, 30 % percol, 37 % percol and 70 % percol (from top to bottom). Via centrifugation in this percol gradient for 40 minutes at 200g without brake, mononuclear cells of the brain were enriched in a ring between the 37 % and 70 % phase. The mononuclear cells were aspirated and washed three times with HBSS. After the final washing step the cell pellet was resuspended and further stained for flow cytometry with antibodies directed against CD11b, CD45 and Siglec-E. Microglia were gated as CD11b+ and CD45low cells.

2.2.3 Culturing of microglial cells

The microglia line was cultivated in N2 medium in an incubator with 5 % CO_2 at 37°C. Upon 80-90 % confluence the cells were splitted 1:10 using a cell scraper until they were confluent again. For freezing of cells the N2 medium was supplemented with 10 % DMSO and 40 % FBS. Cells were stored for at least three days at -80°C and then transferred to liquid nitrogen for long term storage.

2.2.4 Immunocytochemistry of cultured cells

Cells were fixed on a chamber slide in 4% PFA for 10 minutes, blocked by 10x bovine serum albumin (BSA) and immunostained with a primary antibody in 1x BSA overnight at 4°C followed by the secondary antibody at room temperature for 2 hours. Nuclei of immunostained cells were subsequently labelled with 4', 6-diamidino-2-phenylindole (DAPI) for 30 seconds and slides covered with cover slips and mowiol. Images were collected by confocal laser scanning microscopy (Fluoview 1000, Olympus) or fluorescence microscopy.

2.2.5 Flow cytometry analysis

Microglia were collected from culture dishes by a cell scraper. For flow cytometry analysis of *ex vivo* microglia cells were isolated as described above. After Fc-receptor blocking for 5 minutes with a CD16/32 antibody cells were incubated with an anti-Siglec-E and a biotin-conjugated antibody directed against the Siglec-E antibody. This was followed by a triple staining with a PE-conjugated anti-CD11b, a V450-conjugated anti-CD45 and Alexa647-conjugated streptavidin. Isotype matched control antibodies were used as negative controls. Analysis was done with a FACS Calibur or FACSCantoII flow cytometer (both BD Bioscience) and FlowJo Software (BD Bioscience).

2.2.6 Analysis of gene transcripts by quantitative real-time polymerase chain reaction (qRT-PCR)

Microglia were seeded at a density of 250 000 cells/well in a 6-well plate and for the analysis of Siglec-E transcription they were stimulated with either 500 ng/ml LPS,

100 U/ml IFN-γ, 1000 U/ml IFN-α or 20 ng/ml TNF-α. Unstimulated cells served as a control. After 24 hours of stimulation RNA was isolated using the RNeasy Mini Kit. Reverse transcription of RNA was performed with SuperScript III reverse transcriptase and hexamer random primers according to the Invitrogen protocol for SuperScript First-Strand Synthesis. The concentration of transcribed cDNA was adjusted to 200 ng/µl.

Gene transcripts of the housekeeping gene glyceraldehyde-3-phosphate dehydrogenase (GAPDH) were applied as internal RNA control. qRT-PCR with specific oligonucleotides was performed with SYBR Green PCR Master Mix using the ABI 5700 Sequence Detection System and amplification protocol for the ABI 5700 Sequence Detection System. For quantitative real-time PCR the following mix was prepared in a 96-well-plate:

12.5 µl	SYBR Green Mix
1 µl	forward primer (10pmol/µl)
1 µl	reverse primer (10pmol/µl)
3 µl	cDNA (200 ng/µl)
7.5 µl	aqua destillata (dest.)

For the non-template control the cDNA was replaced with aqua dest. The plate was covered with a plastic lid and analysed with the following program:

Cover T° = 105°C

Initial denature	95°C	08:30 min
Denature	95°C	00:15 min
Annealing	60°C	00:30 min
Elongation	72°C	00:30 min
Amplification	for 40 cycles	

To ensure that a specific product was obtained a dissociation curve analysis was performed using the following program:

	95°C	01:00 min
	55°C	00:15 min
	95°C	00:15 min
ramp rate		20:00 min

Amplification specificity was confirmed by analysis of the melting curves. Results were analysed with the ABI 5700 Sequence Detection System v.1. after establishing the reaction efficiency for each primer pair. Quantification using the δδ-CT method was carried out.

2.2.7 Plasmid construction

The pll3.7 vector was modified to contain a neomycin resistance gene by replacing the U6 promoter with a cassette of phosphoglycerate-kinase (PGK) promoter. Plasmids expressing green fluorescent protein (GFP) or Siglec-E (AG Fleischer, Hamburg) linked to GFP were cloned based on the modified pll3.7 backbone with a cytomegalovirus (CMV) promoter (Figure 2.1).

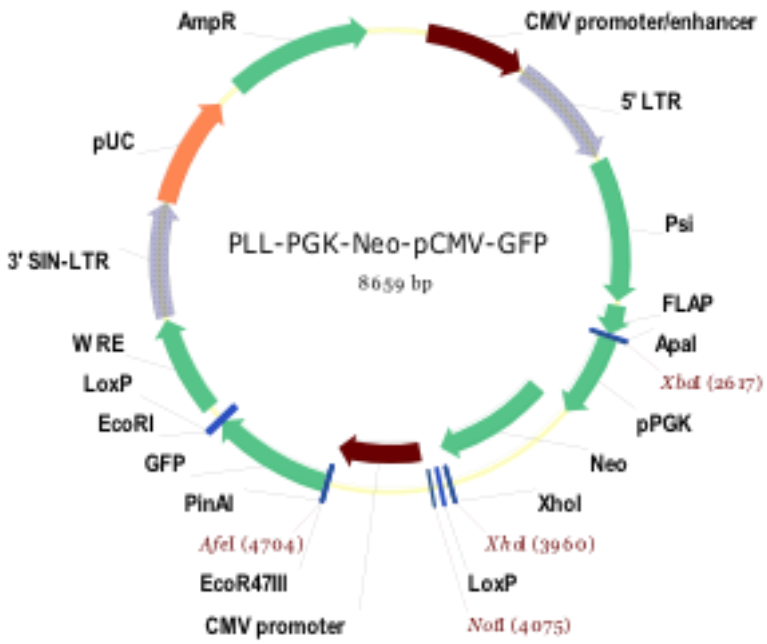

Figure 2.1: Schematic drawing of the vector backbone used for overexpression of Siglec-E. The vector pll3.7 has a CMV promotor, a GFP and a neomycin resistance under the PGK promotor.

Described genes or fragments were obtained from corresponding constructs by PCR using primers including restriction sites allowing the product to be inserted into the vector by specific digest.

The standard PCR mix was as follows:

36.3 µl	aqua dest.
5 µl	10x High Fidelity PCR buffer
2 µl	dNTP mix (10 mM)
2 µl	$MgSO_4$ (50 mM)
2 µl	forward primer (10pmol/µl)
2 µl	reverse primer (10pmol/µl)
0.5 µl	cDNA (1 µg/µl)
0.2 µl	Platinum Taq High Fidelity

The following PCR program was used:

Initial denature	94°C	02:00 min
Denature	94°C	01:30 min
Annealing	according to primer	01:00 min
Elongation	68°C	1 min/1000 bp
Final elongation	68°C	10:00 min
Amplification	for 40 cycles	

The subsequent ligation was performed in a molecular ratio from vector:insert of 1:1, 1:2 and 1:4. The ligated vectors were transformed into Top10 competent bacteria. Positive colonies selected by antibiotics were inoculated in a small volume. Plasmid DNA was isolated and digested using the corresponding restriction enzymes. Colonies having the insert were expanded and purified using PureLink™ HiPure Plasmid Filter Maxiprep Kit. The sequence of each plasmid was verified further by sequencing.

For knock-down of Siglec-E the vectors including the target sequence were obtained by AG Hornung, Bonn (Figure 2.2).

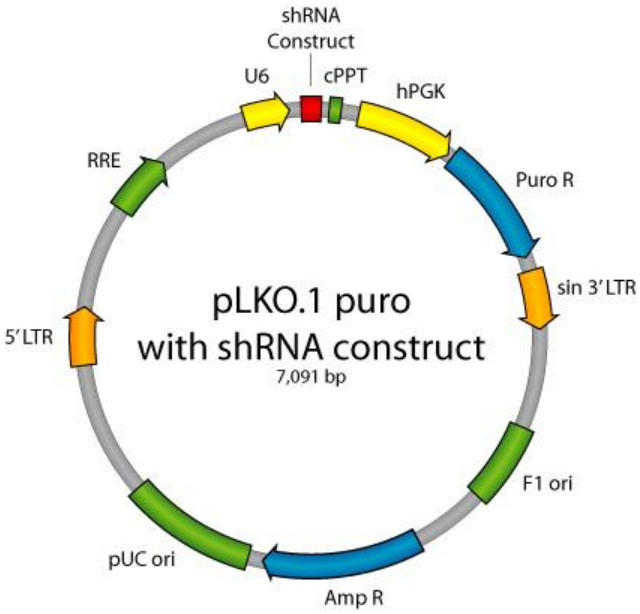

Figure 2.2: Schematic drawing of the vector backbone used for knock-down of Siglec-E. For the production of short hairpin constructs the vector pLKO.1 was used (source: addgene).

2.2.8 Viral particle production

For the production of lentiviral particles 6.5 x 10^6 HEK293FT cells were seeded on 15 cm-dishes pre-coated with pLL. The HEK293FT packaging cell line was kept overnight in MEF medium at 37°C in 5 % CO_2. The following day 25 µg of targeting plasmid together with 25 µg pLP1, 12.5 µg pLP2 and 15 µg pLP/VSVG were incubated with 1047.5 µl ddH_2O, 125 µl 2.5 M $CaCl_2$ and 1250 µl 2x HBS for 25 minutes at room temperature. The transfection mix was added dropwise to the cells. Cells were transfected in Trans-MEF medium containing only 5% FBS and 50 nM chloroquine. Medium was replaced by fresh MEF medium the following day. Viral supernatant was collected at 48 and 72 hours post-transfection and either immediately applied to transduce cells or stored at -80°C.

2.2.9 Lentiviral transduction of the microglia line ESdM

Microglia were seeded at 250 000 cells/well into 6-well plates. In total, 5 ml of lentiviral supernatant was added to the culture and after spinfection at 1500g for 30 minutes at 32°C incubated at 37°C and 5% CO_2. Medium was changed the day after

lentiviral transduction and was replaced by fresh N2 culture medium. The transduction procedure was repeated three times.

2.2.10 Phagocytosis of neural debris

Primary neural cultures were treated with 40 nM okadaic acid for 24 hours, centrifuged, washed three times with PBS and the pellet was frozen at -20°C. After thawing, neural debris was incubated with 1 µM DiI (Derivates for Long-Term cellular Labelling) for 5 minutes at 37°C followed by an incubation time of 15 minutes at 4°C and three washing steps with PBS. Microglia were incubated with neural debris for 2 hours at 37°C and subsequently washed three times with PBS. Cells were fixed with 4 % PFA, washed three times with PBS and blocked with 10 % BSA for 30 minutes. Cells were then incubated with a primary antibody directed to iba1 in 1 % BSA over night at 4°C. The following day cells were washed three times with PBS and stained with a secondary Alexa488-conjugated antibody for 2 hours at room temperature. After DAPI-staining the cells were covered in mowiol. The stainings were stored at 4°C in the dark. For analysis images (normal or *z*-stack, randomly selected areas) were obtained with a confocal laser scanning microscope. For quantification of the phagocytosis rate seven images per condition per experiment and 21 images per condition in total were taken maintaining the same settings. Quantification was performed using ImageJ software comparing phagocytosing to non-phagocytosing cells.

2.2.11 Microglial-neuronal co-culture and immunocytochemistry

Primary hippocampal neuronal cultures were either untreated or treated with 25 mU/ml Neuraminidase for 2.5 hours at 37°C to remove sialic acids from the cell surface and were washed three times subsequently. For the ROS scavenging experiments, 40 nM Trolox was added to the medium before starting the co-culture experiment. Transduced microglia were added and both cell types were co-cultured for 48 hours at 37°C, 5 % CO_2. Cells were fixed with 4 % PFA for 10-15 minutes and washed three times with PBS. Cells were incubated in 10 % BSA for 30 minutes for blocking, followed by an incubation with the primary monoclonal antibody directed to βIII-tubulin over night at 4°C. The next day cells were washed three times with PBS

and stained with the secondary Cy3-conjugated antibody followed by additional three washing steps and then incubated in the second primary antibody directed to iba1 over night at 4°C. Cells were again washed three times with PBS and stained with an Alexa488-conjugated secondary antibody. Cells were stained with DAPI to visualise the nuclei and then covered in mowiol. Five images per condition per experiment (in total 15 images per condition) were collected by confocal laser scanning microscopy or fluorescent microscopy. The mean length of βIII-tubulin positive neurites or the density of βIII-tubulin positive cell bodies were analysed versus iba1 positive cells using ImageJ/NeuronJ software.

2.2.12 Detection of ROS and cytokine transcript analysis during phagocytosis of neural debris

Cultured microglia were incubated with 5 µg/µl neural debris for either 1 hour for dihydroethidium (DHE) staining or 16 hours for RNA isolation and qRT-PCR. For ROS scavenging experiments either 20 µg/ml superoxide dismutase (SOD1) or 40 nM trolox were added at the same time as the neural debris. DHE is cell-permeable and exhibits blue-fluorescence in the cytosol until oxidized. After oxidation it intercalates in the cell's DNA and stains the nucleus in a bright red fluorescence. For detection and quantification of superoxide anion radical production 30 µM DHE were added and incubated at 37°C for 15 minutes. Cells were fixed with 4 % PFA plus 0.25 % glutaraldehyde (GAD) and analysed by confocal laser scanning microscopy. For the quantification of DHE staining intensity six images of each condition per experiment were obtained and analysed with the ImageJ software. The level of background staining was subtracted and the mean values of the staining intensities were compared. Quantification of gene transcripts was done by qRT-PCR (see chapter 2.2.6).

2.2.13 Detection of superoxide by Amplex Red

Analysis was done by AG Kunz, University of Bonn. Quantitative rates of superoxide generation of microglial cells incubated with 10 µg/ml neural debris were determined using a spectrofluorimeter with the Amplex Red/peroxidase-coupled method (1 µM Amplex Red (λ_{ex} = 560 nm, λ_{em} = 590 nm) + 20 units/ml horseradish peroxidase) in

the additional presence of 60 units/ml superoxide dismutase. Presence of an excess superoxide dismutase allows a quantification of superoxide production in hydrogen peroxide equivalents. All measurements were performed at 35° C in oxygen-saturated PBS. The reaction was stopped by addition of 12000 U/ml catalase. The fluorescent signal was calibrated by known H_2O_2 concentrations as described previously (Malinska et al. 2009), allowing to express the superoxide production rate in hydrogen peroxide equivalents. In the calculations of quantitative superoxide generation rates the catalase (12,000 U/ml)-insensitive Amplex Red oxidation rates were always subtracted.

2.2.14 Binding of Siglec-E:Fc fusion protein to primary neurons, astrocytes and microglia

Neurons were either untreated or treated with 25 mU/ml Neuraminidase (*A. ureafaciens*), primary microglia and astrocytes with a combination of 1.4 µl/ml EndoN and 25 U/ml Neuraminidase (*C. perfringens)* for 2.5 hours at 37°C to remove sialic acids from the cell surface. After 2.5 hours cells were washed three times with PBS and then incubated with recombinant Siglec-E:Fc fusion protein or recombinant Siglec-F:Fc fusion protein as a positive control at a final concentration of 2.5 µg/ml (neurons) or 0.1 µg/ml (astrocytes and microglia) for 1 hour at 37°C. Cells were fixed with 4 % PFA, followed by three washing steps with PBS and blocking with 10 % BSA for 30 minutes. The primary monoclonal antibody was directed to βIII-tubulin (neurons), CD68 (microglia) or glial fibrillary acidic protein (GFAP; astrocytes) and applied in 1 % BSA over night at 4°C. The secondary Cy3-conjugated antibody was applied after three washing steps with PBS for 2 hours at room temperature in the dark. After another washing step the primary antibody directed to mouse IgG Fcγ was added over night at 4°C to the stainings with Siglec-E:Fc. An Alexa488-conjugated secondary antibody for Siglec-E:Fc or primary antibody directed to human IgG Fc-FITC against Siglec-F:Fc was applied. Images were collected by confocal laser scanning microscopy.

2.2.15 Statistical analysis

Data are presented as mean ± SEM of at least three independent experiments. Data were analysed by ANOVA followed by Bonferroni using SPSS computer software. *p<0.05; **p<0.01; ***p<0.001.

3. Results

The topic of the present study was to characterize the role microglial Siglec-E plays in neuroinflammatory processes in the brain.

The first steps were to identify Siglec-E transcription and expression on microglia. To get an idea about the function of Siglec-E on microglia, lentiviral overexpression and knock-down constructs were designed and cloned. A microglia line was transduced and further characterized. We used these microglia to study the influence of Siglec-E expression on phagocytic behaviour and the associated burst. After it was proven that the Siglec-E:Fc fusion protein is able to bind sialic acids in the neuronal glycocalyx, co-culture experiments with primary neurons and the modified microglia line were performed. Thereby the implication of the receptor Siglec-E on microglia in neuroinflammatory processes was analysed.

3.1 Siglec-E is a regulator of the immune response

Recent data of gene expression profiles from distinct mouse tissue macrophages suggest that Siglec-E can be also found in microglia (Gautier et al. 2012). Other studies demonstrated the regulatory function on Siglec-E in the immune system. Stimulation with TLRs induced Siglec-E expression and once upregulated it was enabled to control TLR-induced NF-κB and the induction of the antiviral cytokine IFN-β and RANTES. Thereby Siglec-E participated in the regulatory part of the antiviral response to TLRs and maintenance of cytokine levels in state of infection (Boyd et al. 2009). Siglec-E knock-out in mice led to an increased neutrophil recruitment to the lung in an acute lung inflammation model induced by LPS which was mediated by negative regulation of the integrin CD11b by Siglec-E (McMillan et al. 2013).

3.2 Detection of Siglec-E transcription and expression in microglia

3.2.1 Siglec-E expression in ex vivo and primary microglia

So far, expression of Siglec-E on microglia in the CNS has not been described. Therefore the first aim was to investigate the expression of Siglec-E on *ex vivo* and primary mouse microglia. To identify *ex vivo* microglia in a cell population enriched by a percol gradient cells were labelled and gated for $CD45^{low}/CD11b^{+}$ cells. The same labelling was done for primary microglia and both were then stained for Siglec-E. Both *ex vivo* and primary microglia showed low constitutive Siglec-E expression when compared to isotype matched control antibodies (Figure 3.1). In detail the median Siglec-E fluorescence intensity for *ex vivo* microglia was 133.67 ± 40.74 and 452.50 ± 46.62 for primary microglia, respectively.

Therefore, *ex vivo* isolated and primary microglia do both express Siglec-E.

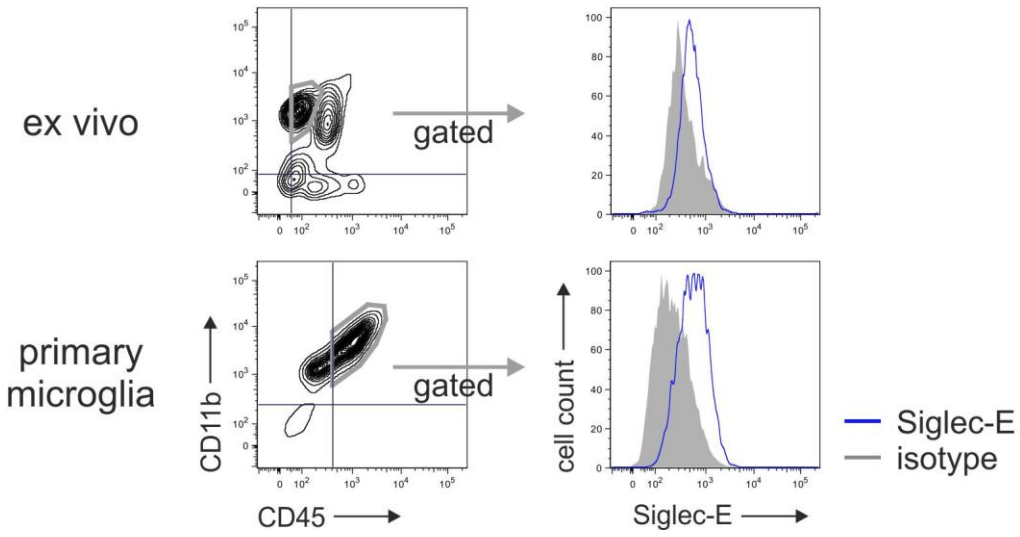

Figure 3.1: Expression of Siglec-E in *ex vivo* and primary microglia. $CD45^{low}/CD11b^{+}$ *ex vivo* and primary microglia were analysed for Siglec-E expression. Both cell types showed low Siglec-E expression on their surface. Representative data out of at least three independent experiments are shown.

3.2.2 Siglec-E transcription in microglia

Primary microglia or the microglia line ESdM were stimulated for 24 hours with either LPS, IFN-γ, IFN-α or TNF-α. mRNA was isolated from primary microglia, the microglia line, spleenocytes and neurons. Spleenocytes are known to have high levels of Siglec-E and were used as a positive control whereas neurons are known to have no Siglec-E and were used as negative control (Zhang et al. 2004).

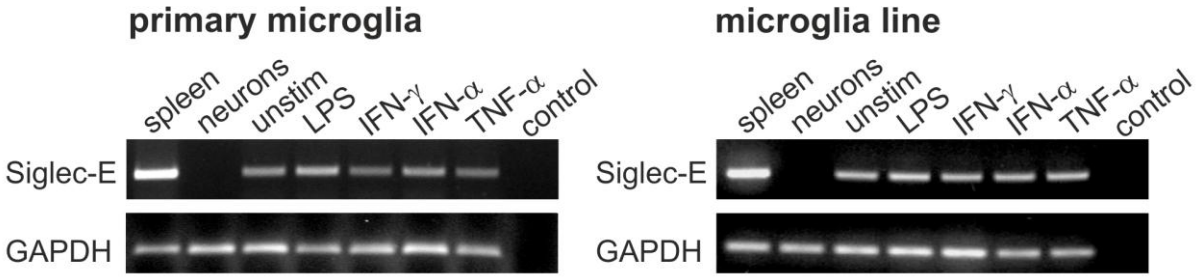

Figure 3.2: Detection of Siglec-E mRNA in microglia by RT-PCR. Siglec-E transcripts were detected in unstimulated primary microglia and in the microglia line ESdM (unstim). Stimulation with LPS, IFN-γ, IFN-α or TNF-α did not alter the transcription level of Siglec-E. The house-keeping gene *Gapdh* was used as an internal loading control. Spleenocytes (spleen) are known to highly express Siglec-E and served as a positive control, in contrast neurons do not express Siglec-E. Representative data out of three independent experiments are shown. Control: reaction mix without cDNA.

PCR of the transcribed cDNA clearly showed that primary microglia and the microglia line ESdM both transcribed Siglec-E (Figure 3.2). Upon stimulation there was no significant difference in the level of Siglec-E transcripts in primary microglia and the microglia line. As expected, the spleenocyte cDNA showed the highest transcription level of Siglec-E mRNA whereas the neuron cDNA had no Siglec-E transcripts.

The outcome of the reverse transcription was further confirmed by quantitative real-time PCR. This method enabled us to quantify changes in the Siglec-E transcription level upon stimulation when compared to unstimulated cells. The values were normalized to the house-keeping gene *Gapdh*. As seen before using RT-PCR, stimulation with the different cytokines IFN-α, IFN-γ, TNF-α or LPS for 24 hours did not result in any significant changes in the mRNA transcription levels of Siglec-E in the microglia line ESdM (Figure 3.3).

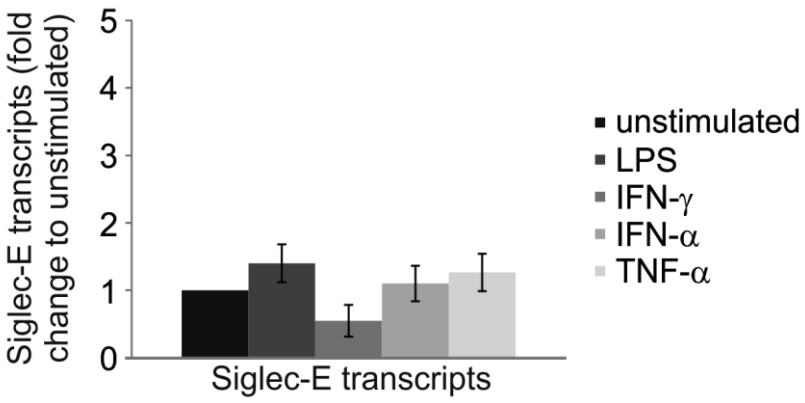

Figure 3.3: Quantitative real-time PCR of stimulated ESdM. Stimulation with LPS or the cytokines IFN-γ, IFN-α or TNF-α did not result in a significant change in the transcription levels of Siglec-E mRNA after 24 hours stimulation. Data was normalized to the gene *Gapdh*.

In conclusion, primary microglia and the microglia line have a detectable level of Siglec-E mRNA of Siglec-E.

3.2.3 Siglec-E expression in microglia upon stimulation

After it was shown that the expression of Siglec-E can be detected in *ex vivo*, primary microglia and the transcription in the microglia line ESdM, the next step was to show Siglec-E expression on the cell surface of microglia. For this purpose primary microglia and ESdM were stimulated with LPS, IFN-γ, IFN-α or TNF-α for 24 hours and then Siglec-E quantified using flow cytometry.

In primary microglia and ESdM, low Siglec-E expression was detected by flow cytometry in unstimulated cells. Upon stimulation with IFN-α, primary microglia showed an upregulation of Siglec-E on their surface whereas the other cytokines and LPS had no effect on the Siglec-E expression level (Figure 3.4). In ESdM both IFN-α and IFN-γ increased the Siglec-E expression levels on the cells, but not the other stimulants.

In summary, only IFN-α and IFN-γ had an impact on the expression level of Siglec-E in primary microglia and the microglia line.

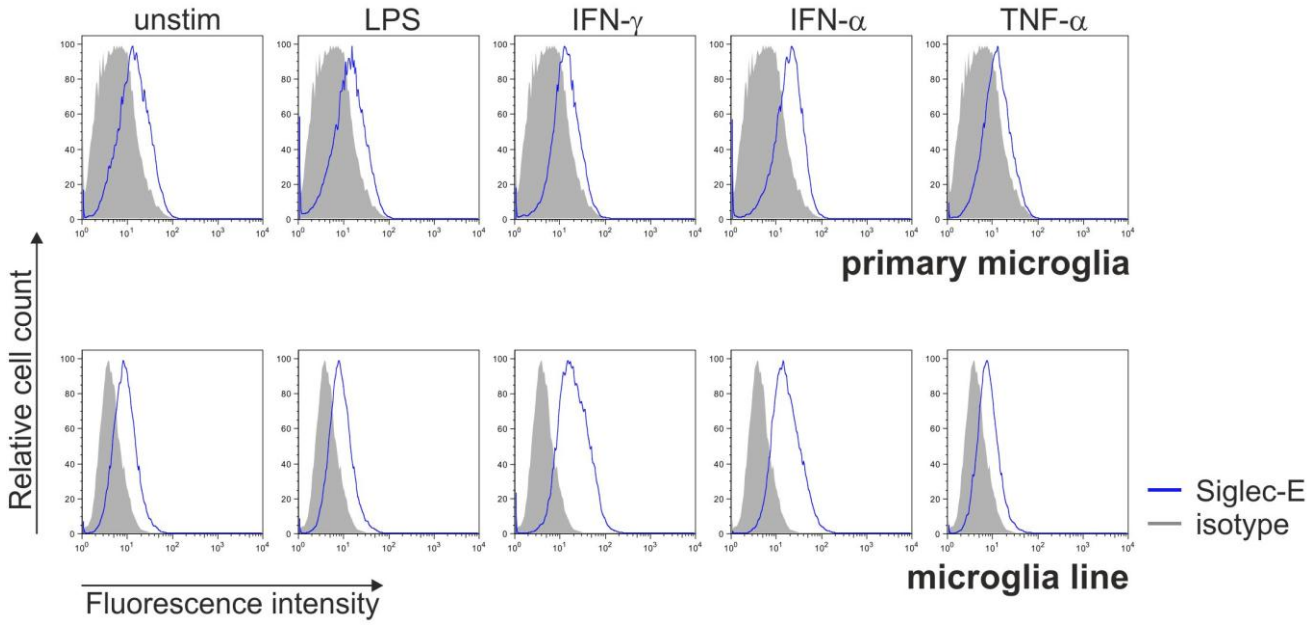

Figure 3.4: Flow Cytometry analysis for Siglec-E expression upon stimulation. Siglec-E was detected on unstimulated (unstim) microglia at low levels. A 24 hour treatment with IFN-γ or IFN-α slightly increased the expression of Siglec-E on the microglia line, while treatment with LPS or TNF-α showed no effect. Representative data out of three independent experiments are shown. unstim: unstimulated cells; isotype: isotype control antibody.

3.3 Lentiviral overexpression and knock-down of Siglec-E in ESdM

Since there are hardly any functional data about Siglec-E, one of the main goals was to achieve a basic understanding of the role Siglec-E plays in microglia. For this purpose a microglia line was transduced with lentiviral particles to overexpress or knock-down Siglec-E. After characterization of these modified cells they were used for further experiments.

3.3.1 Lentiviral over-expression or knock-down of Siglec-E does not change the microglial phenotype

3.3.1.1 Siglec-E overexpression and knock-down constructs

Siglec-E was tagged with GFP under the control of the CMV promotor (abbreviated later as „SigE vector“). It was cloned into the pll3.7 vector with a PGK-neomycin selection gene in front of the Siglec-E related expression cassette. The

corresponding control was the empty vector containing only GFP (abbreviated as “control vector”).

Constructs for lentiviral knock-down of the receptor Siglec-E in the microglia line were obtained from a knock-down library in a pLKO.1 backbone and were kindly provided by Prof. Veit Hornung, Bonn (shRNASigE1: TRCN0000094526, target sequence 5’-CCCAATTCGTAAAGCAGTGAA-3’, abbreviated as „shRNASigE1“; shRNASigE2: TRCN0000094527, target sequence 5’-GCCACAAATAACCCAA TTCGT-3', abbreviated as „shRNASigE2“).

3.3.1.2 Confirmation of successful transduction of microglia

After the transduction of the microglia line with lentiviral particles for either overexpression or knock-down of Siglec-E, the outcome of the procedure was confirmed by qRT-PCR and flow cytometry.

The qRT-PCR results showed that after the transduction with lentiviral particles for Siglec-E overexpression the transcription level was increased when compared to untransduced cells and the control vector. In detail, the transcription was 48.45 $\pm$ 4.06-fold higher than untransduced cells (1.0 $\pm$ 0.08; $p = 2.2 \times 10^{-5}$; $p = 2.2 \times 10^{-5}$ compared to control vector). The control vector showed no significant change in Siglec-E mRNA levels (1.12 $\pm$ 0.11-fold increase) when compared to untransduced microglia (Figure 3.5).

The knock-down efficiency was analysed in comparison to untransduced microglia and microglia having received lentiviral particles of the non-targeting shRNA (“NTshRNA”) control construct. Both transductions with the lentiviral particles of the knock-down constructs resulted in a significant reduction in Siglec-E transcription in the microglia. Siglec-E mRNA levels were decreased from 1.0 $\pm$ 0.07 in untransduced cells and 1.04 $\pm$ 0.01-fold in NTshRNA ($p = 1.4 \times 10^{-11}$) microglia to 0.14 $\pm$ 0.01-fold ($p = 2.0 \times 10^{-11}$; p = xxx to NTshRNA) for shRNASigE1 and 0.15 $\pm$ 0.01-fold for shRNASigE2 ($p = 2.2 \times 10^{-11}$; $p = 1.5 \times 10^{-11}$ to NTshRNA).

Therefore the modification for Siglec-E in the microglia line was proven on the transcriptional level for overexpression and knock-down of Siglec-E.

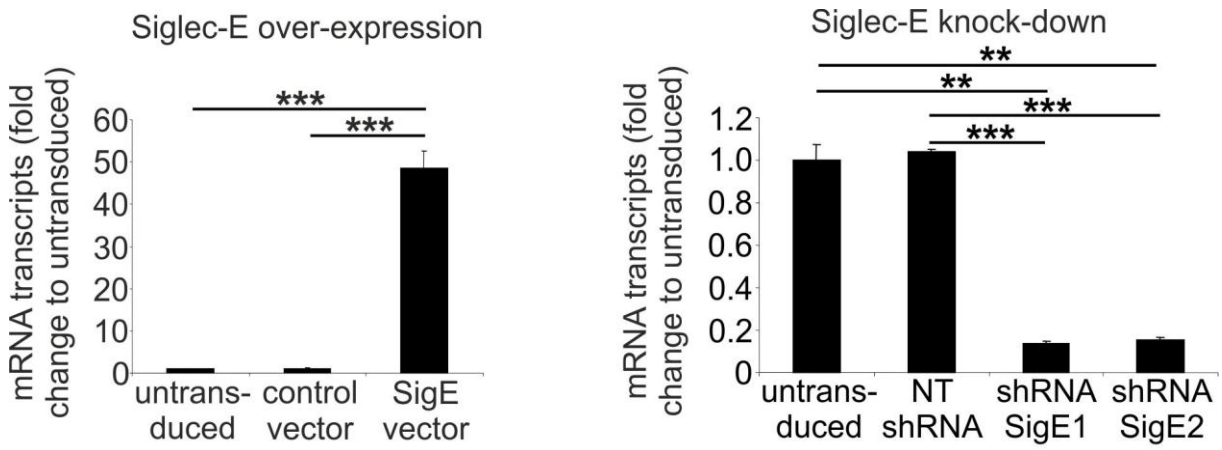

Figure 3.5: Siglec-E transcription level after lentiviral transduction. Microglia were transduced with lentiviral particles of vectors expressing either Siglec-E:GFP (SigE vector) or a control vector. Furthermore, lentiviral knock-down was performed by two different lentiviral short-hairpin constructs targeting Siglec-E (shRNASigE1; shRNASigE2) or a corresponding non-targeting control vector (NTshRNA). qRT-PCR confirmed the successful modification of the microglial line by showing an increase in Siglec-E cDNA levels after lentiviral overexpression of Siglec-E (left graph) or a reduction in gene transcript levels after knock-down of Siglec-E (right graph). Numbers were normalized to the house-keeping gene *Gapdh*.

To analyse the effect of the lentiviral transduction on the protein level as well, flow cytometry with an antibody directed against Siglec-E was performed. The transduction with the particles of the overexpression vector led to much higher Siglec-E expression in the microglia compared to that in untransduced microglia and microglia which only received the control vector (Figure 3.6). In contrast, the viral particles of both knock-down constructs shRNASigE1 and shRNASigE2 showed a diminished Siglec-E surface protein level of the cells when compared to untransduced cells and microglia transduced with the NTshRNA.

Thus, the expression level of Siglec-E was successfully modified in the microglia line.

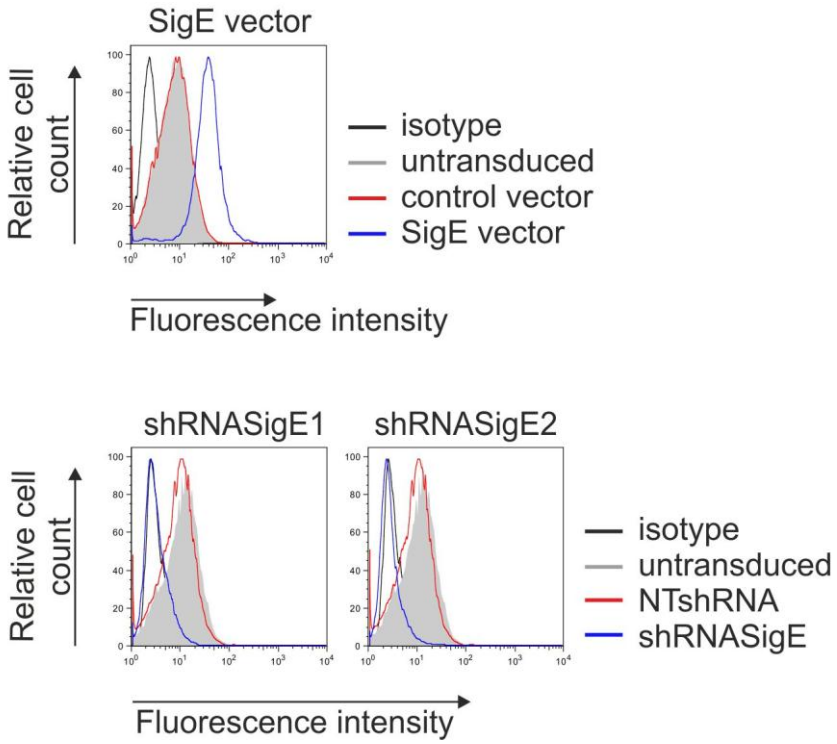

Figure 3.6: Siglec-E surface expression level after lentiviral transduction. Flow cytometry confirmed modification of the microglial line. Lentiviral transduction with the construct for overexpression of Siglec-E (SigE vector) led to an increase in Siglec-E expression (upper graph) compared to untransduced and control vector microglia. Both knock-down vectors (shRNASigE1; shRNASigE2) resulted in a clear decrease of Siglec-E surface expression on microglia (lower graph) when compared to untransduced cells and microglia having received the NTshRNA viral particles.

3.3.1.3 Lentiviral transduction does not change the microglial phenotype

After the altered transcription and expression level of Siglec-E in the modified microglia line was confirmed, it had to be analysed if the lentiviral transduction caused any changes in the microglial phenotype. The microglia were analysed for changes in cytokine transcription and surface marker expression after successful lentiviral transduction.

The transcription profile of IL-1β, NOS2 and TNF-α was analysed by qRT-PCR in the modified microglia and the corresponding control cell lines. As an internal control the gene *Gapdh* was used.

For the Siglec-E overexpressing cells as well as for the Siglec-E knock-down cells, the transcription level of all the cytokines and surface markers analysed remained unchanged when compared to untransduced cells or the corresponding control

vector. In detail, for IL-1β the transcription level after lentiviral overexpression for Siglec-E remained quite stable with a non-significant fold increase from 1.0 ± 0.32 (untransduced cells) to 1.45 ± 0.22 for the control vector and to 1.52 ± 0.51 for Siglec-E overexpression (Figure 3.7).

The same holds true for the knock-down vectors. In this case, the alteration was from 1.0 ± 0.23 (untransduced) or 1.23 ± 0.38 (NTshRNA) to 0.87 ± 0.47-fold (shRNASigE1) and 1.12 ± 0.43 (shRNASigE2), respectively. For NOS2 the mRNA levels remained unchanged from 1.0 ± 0.19 (untransduced) to a 1.38 ± 0.37-fold change (control vector) and to a 0.9 ± 0.3-fold change (SigE vector). The knock-down microglia showed stable transcription levels at a fold change of 1.28 ± 0.35 (shRNASigE1), 1.55 ± 0.16 (shRNASigE2) and 1.2 ± 0.43 (NTshRNA) when compared to untransduced cells (1.0 ± 0.21). TNF-α transcription levels for Siglec-E overexpressing microglia were not affected by the transduction procedure. They remained at a 1.15 ± 0.24-fold change compared to 1.0 ± 0.12 (untransduced) and 1.05 ± 0.07 (control vector). Similarly, TNF-α mRNA levels in Siglec-E knock-down microglia were unaffected by lentiviral transduction. The fold change was from 1.0 ± 0.12 (untransduced) and 1.37 ± 0.41 (NTshRNA) to 1.25 ± 0.65 (shRNASigE1) and 0.96 ± 0.35 (shRNASigE2), respectively.

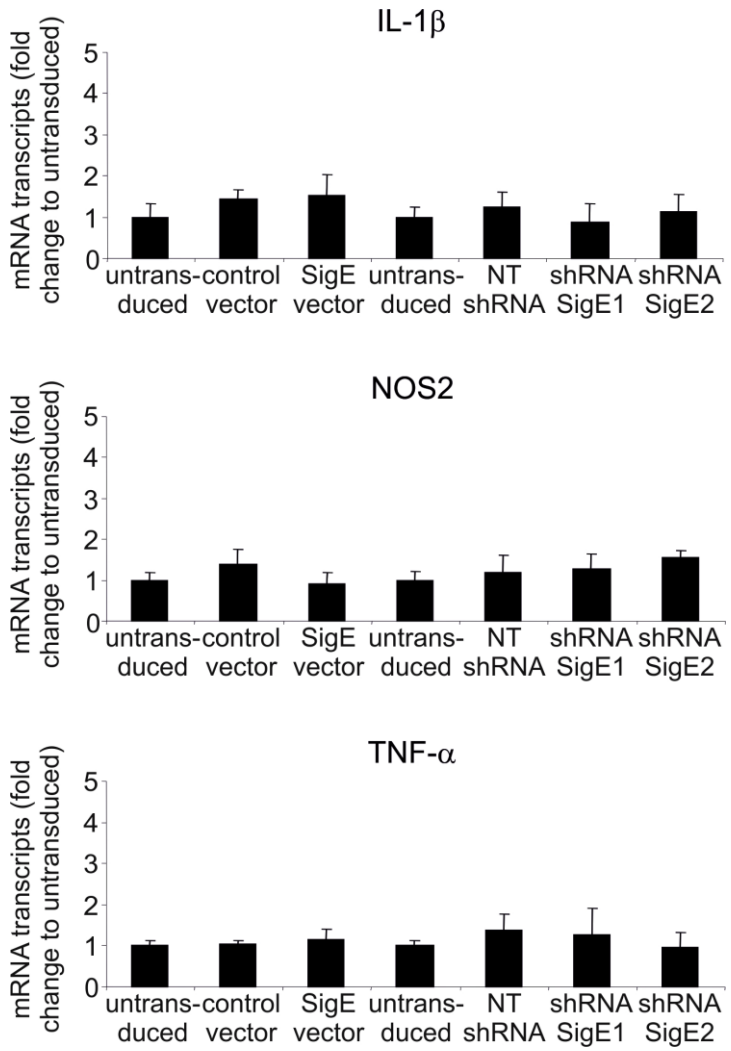

Figure 3.7: No change in cytokine transcription in modified microglia. The transduced microglia were analysed in regard to their inflammatory phenotype. They were analysed for IL-1β, NOS2 and TNF-α mRNA levels by qRT-PCR. Neither Siglec-E overexpressing microglia nor the Siglec-E knock-down cells had any significant change in the transcription level of the cytokines. Data were normalized to the house-keeping gene *Gapdh*.

In addition, a flow cytometry experiment was performed to display the surface marker expression profile of the modified microglia. The expression levels of CD11b, CD11c, CD18, CD31, CD34, CD45, CD80, CD86 and F4/80 were measured. CD31 and CD34 are markers of not fully differentiated cells and therefore no expression of these markers was expected. In contrast, the microglia line is known to express high levels of CD11b and CD45 on their surface. Overall the surface marker expression profile of the Siglec-E overexpressing microglia was comparable to that of

untransduced and control vector transduced cells (Figure 3.8a). The same holds true for both of the knock-down constructs shRNASigE1 (Figure 3.8b) and shRNASigE2 (Figure 3.8c) when compared to the untransduced and NTshRNA microglia.

In conclusion, the lentiviral transduction procedure did not alter the microglia phenotype.

See next page:

Figure 3.8: Microglia surface marker expression profile remains unchanged after lentiviral transduction. After the transduction procedure, surface marker expression of the modified microglia was analysed. **a** The expression level of the surface markers was not influenced by overexpression of Siglec-E on microglia or by the control vector. **b** The construct shRNASigE1 showed a comparable expression profile to that of untransduced and NTshRNA microglia. **c** shRNASigE2 transduction did not affect marker expression levels on microglia. Representative data out of three independent experiments are shown.

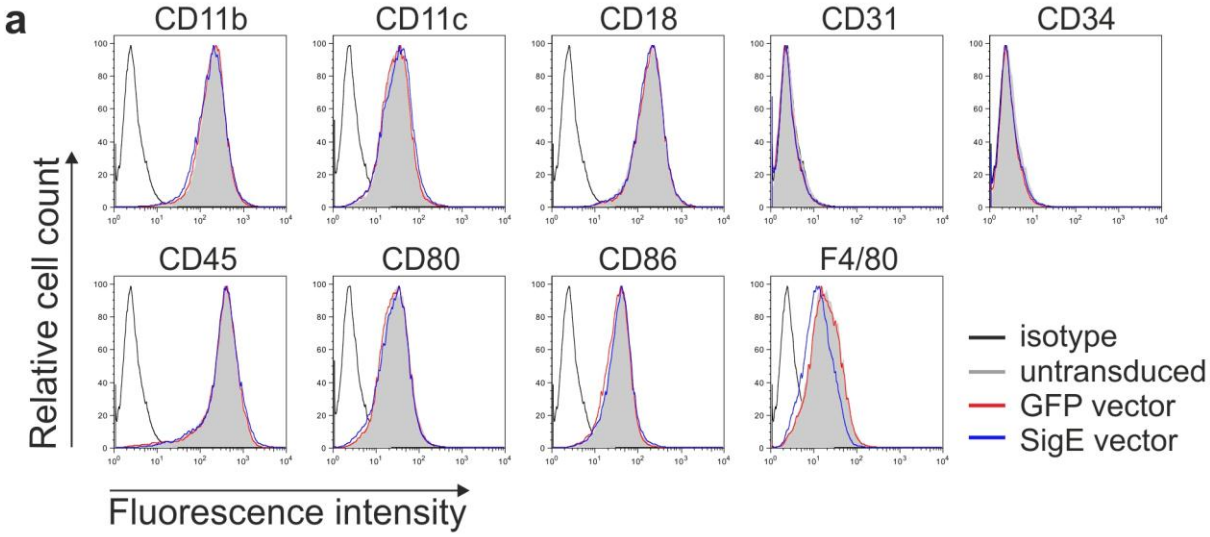
a
CD11b
CD11c
CD18
CD31
CD34
CD45
CD80
CD86
F4/80
Relative cell count
Fluorescence intensity
isotype
untransduced
GFP vector
SigE vector

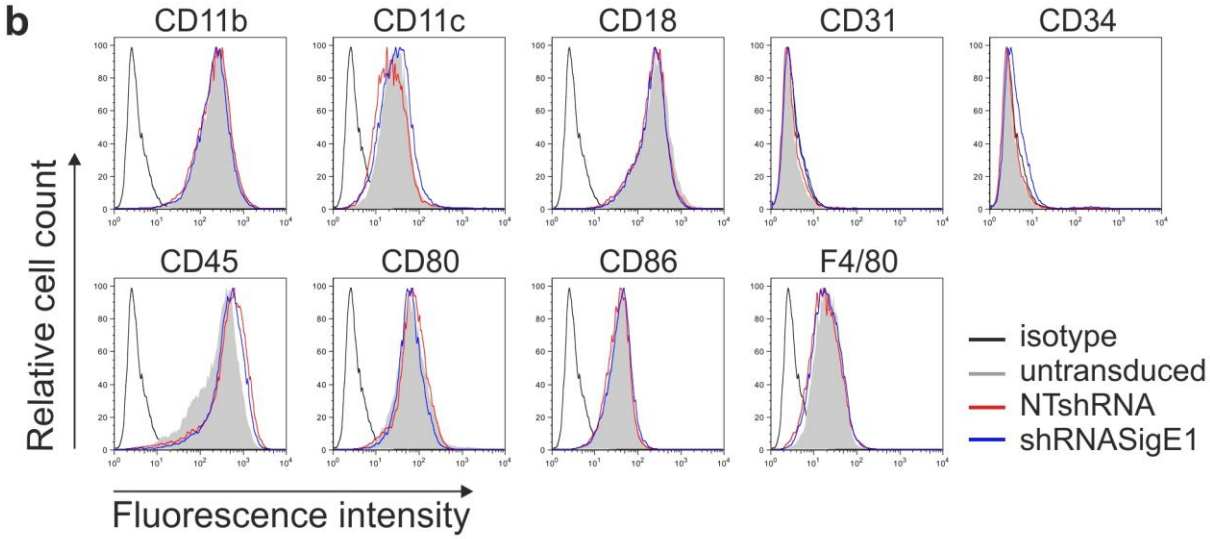
b
CD11b
CD11c
CD18
CD31
CD34
CD45
CD80
CD86
F4/80
Relative cell count
Fluorescence intensity
isotype
untransduced
NTshRNA
shRNASigE1

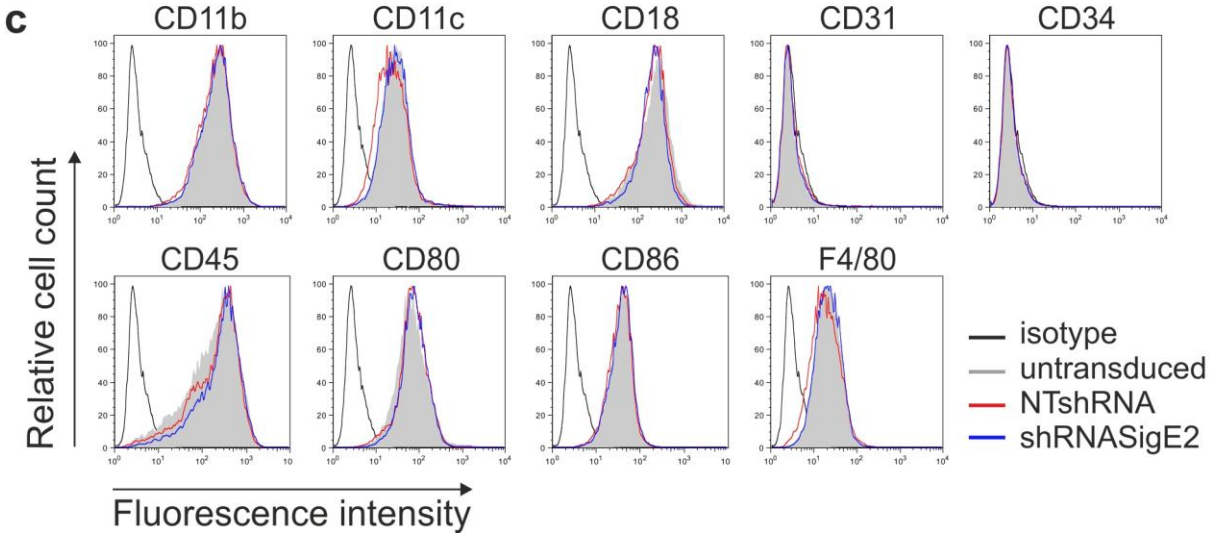
c
CD11b
CD11c
CD18
CD31
CD34
CD45
CD80
CD86
F4/80
Relative cell count
Fluorescence intensity
isotype
untransduced
NTshRNA
shRNASigE2

3.4 Phagocytosis of neural debris by microglia

Microglia are the phagocyting cells of the brain. They can phagocyte cellular debris and secrete anti-inflammatory cytokines. By this mechanism they prevent inflammatory processes caused by apoptotic cells and thereby help maintain a healthy environment for all the brain cells especially for the neurons in the CNS. Since this is one of the key functions of microglia, the modified microglia were analysed as to whether the introduced modifications in the expression level of Siglec-E might influence this main characteristic.

3.4.1 Siglec-E expression levels influence phagocytosis rate of microglia

The modified microglia were challenged with neural debris and phagocytosis was analysed under the microscope. The merged images show overlays of microglia and neural debris indicating the event of phagocytosis.

Microglia expressing GFP display a higher rate of phagocytosis of neural debris when compared to microglia overexpressing Siglec-E. In contrast, microglia having received the NTshRNA show less overlay events compared to microglia with a Siglec-E knock-down. When considering the number of phagocytosed neural debris particles per phagocytosing cell, microglia with a knock-down of Siglec-E seem to have a higher number of phagocytosed neural debris particles per phagocytosing cell compared to microglia, which had been transduced with the NTshRNA control (Figure 3.9).

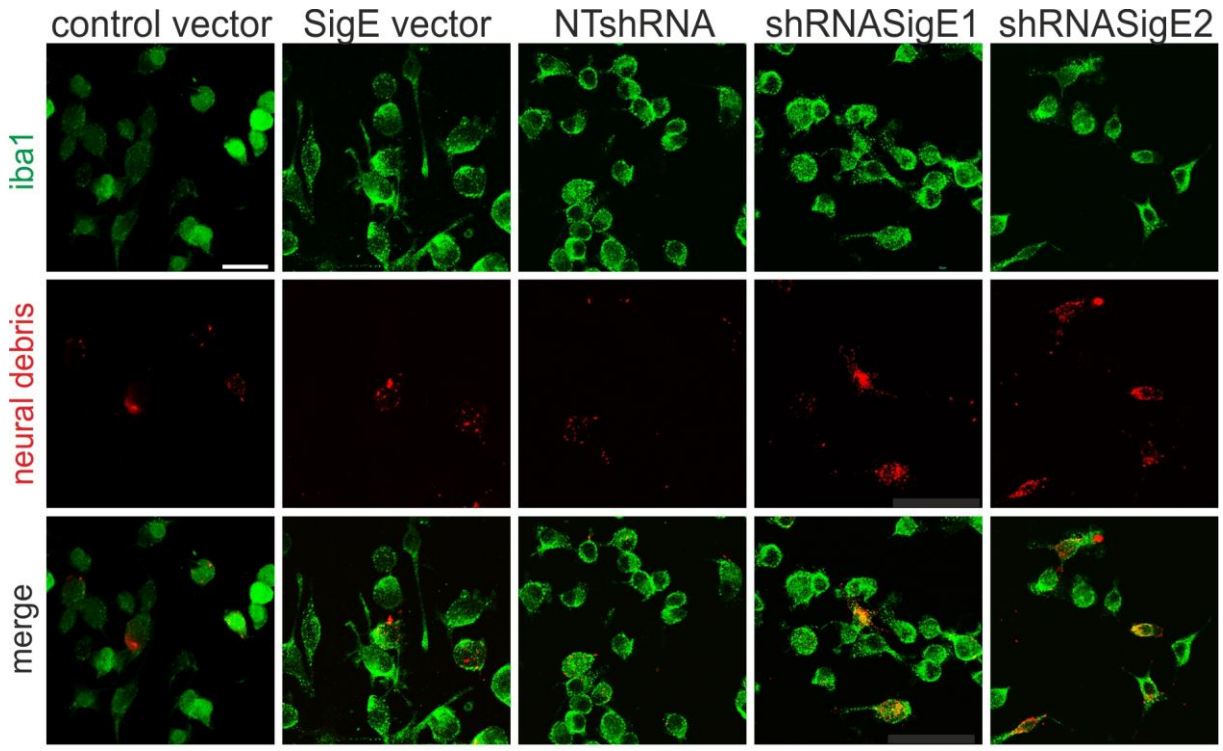

Figure 3.9: Phagocytosis of neural debris by modified microglia. Lentiviral transduced microglia with different expression levels of Siglec-E were challenged with neural debris. Phagocytosis of the neural debris was analysed. Siglec-E overexpressing microglia (SigE vector) showed less phagocytosis than their corresponding control (control vector). Siglec-E knock-down microglia (shRNASigE1; shRNASigE2) had more phagocytosis events when compared to their control (NTshRNA). Representative images out of three independent experiments are shown. Scale bar: 30 µm.

To prove that the neural debris was indeed in the microglia, three-dimensional reconstruction images were taken. The images showed that the neural debris was indeed inside the cells. The control lines (control vector; NTshRNA) demonstrated a comparable amount of phagocytosed neural debris, whereas Siglec-E overexpressing microglia had only few neural debris particles. Siglec-E knock-down microglia had the highest number of neural debris when compared to the other cells (Figure 3.10a).

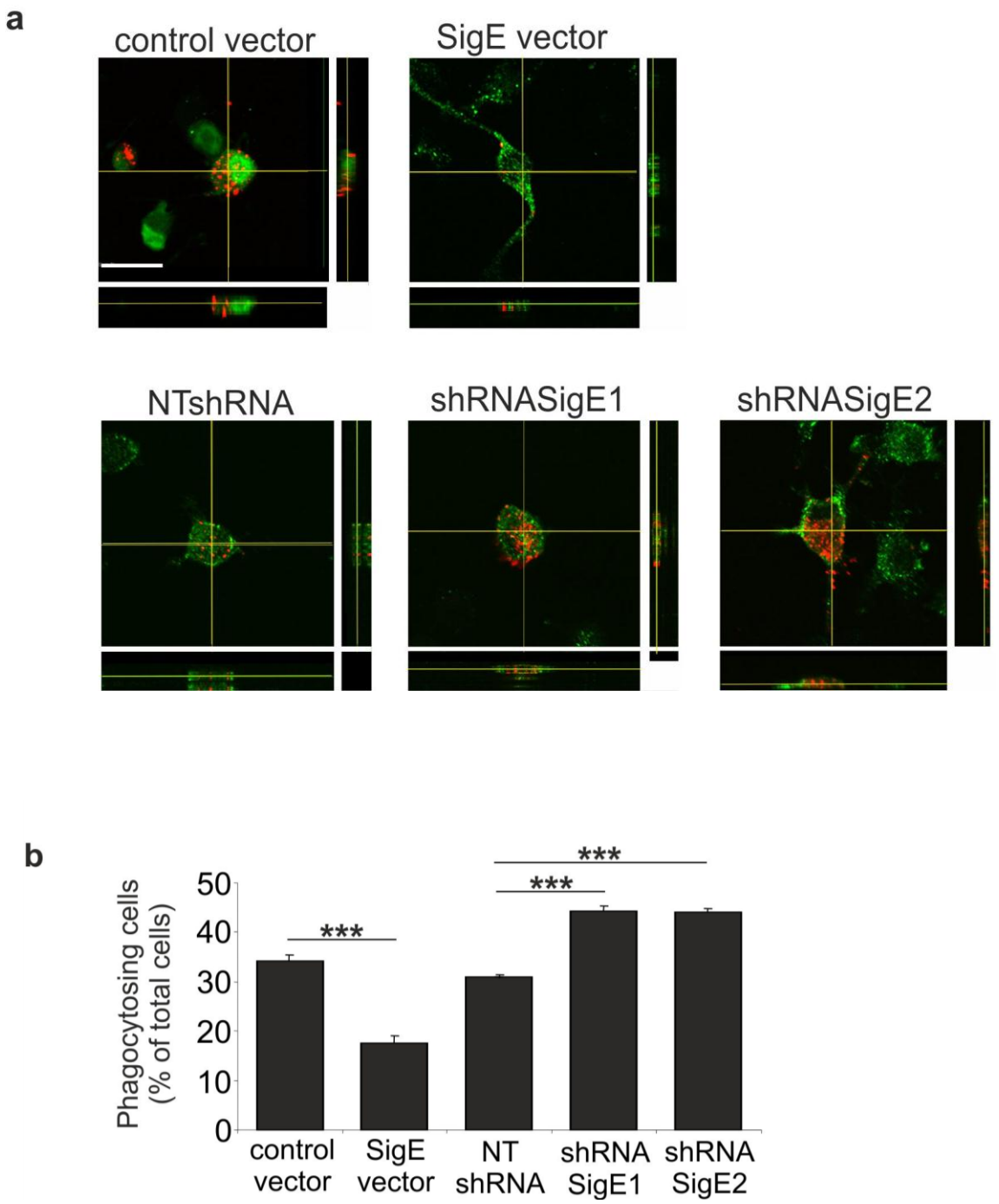

Figure 3.10: Siglec-E overexpression prevents phagocytosis of neural debris. a Uptake of red fluorescent labelled neural debris (red) into microglia (green) was analysed by confocal microscopy and 3D-reconstruction. Microglial cells were lentiviral transduced with either the control vector, the Siglec-E over-expressing vector (SigE vector), the Siglec-E knock-down constructs (shRNASigE1; shRNASigE2) or the non-targeting vector (NTshRNA). Representative images out of three independent experiments are shown. Scale bar: 20 µm. **b** The phagocytosis rate of the microglia was quantified. Overexpression of Siglec-E on the cell surface led to a reduction in phagocytosis rate, while knock-down of Siglec-E increased the uptake of neural debris.

Quantification of neural debris uptake revealed that an overexpression of Siglec-E on the microglia resulted in a decrease in phagocytosis rate from 34.17 ± 1.30 % (control vector; $p = 1.65 \times 10^{-8}$) down to 17.55 ± 1.30 % of phagocytosing cells. On the contrary, knock-down of Siglec-E in the microglia line led to an increase in the uptake of neural debris. In detail, microglia transduced with the NTshRNA vector showed a phagocytosis rate of 31.0 ± 0.06 % whereas cells being modified with shRNASigE1 lentiviral particles had a phagocytosis rate of 44.32 ± 0.86 % ($p = 6.93 \times 10^{-7}$) and transduction with shRNASigE2 particles led to 44.03 ± 0.71 % ($p = 9.86 \times 10^{-7}$) phagocytosis (Figure 3.10b).

While Siglec-E overexpressing microglia showed a decreased phagocytosis rate, Siglec-E knock-down microglia had a higher phagocytosis rate.

3.4.2 Siglec-E knock-down leads to an increase in superoxide production in microglia

Phagocytosis is frequently associated with a burst of reactive oxygen species. As Siglec-E expression levels had an influence on the phagocytosis rate in microglia, it was of further interest whether Siglec-E has an impact on the production of reactive oxygen species as well.

Microglia modified with the knock-down constructs shRNASigE1 and shRNASigE2 displayed the highest fluorescence intensity for DHE ROS staining whereas microglia overexpressing Siglec-E (SigE vector) or microglia having been transduced with the non-targeting shRNA (NTshRNA) showed lower fluorescent intensities (Figure 3.11a). Quantification of the fluorescence intensities showed that the increase in ROS production after addition of neural debris was strongest in microglia with the lowest Siglec-E expression levels (shRNASigE1; shRNASigE2). In detail, the mean fluorescence intensity increased from 1.38 ± 0.03 for the NTshRNA microglia treated with neural debris to 2.25 ± 0.19 for shRNASigE1 ($p = 2.24 \times 10^{-11}$) incubated with neural debris and to 2.44 ± 0.21 for microglia modified by lentiviral particles of the construct shRNASigE2 stimulated with neural debris ($p = 3.19 \times 10^{-16}$). Microglia, which have been transduced with a control vector, only had a moderate increase of superoxide production after challenge with neural debris to 1.26 ± 0.05. Siglec-E

overexpressing microglia did not even show a significant increase in ROS production after treatment with neural debris (0.98 ± 0.11; Figure 3.11b).

Since only the knock-down constructs led to a significant increase in ROS production after stimulation with neural debris, these cells were chosen for the scavenging experiments. While challenging microglia with neural debris, the addition of one of the free radical scavenger, SOD1 or trolox, led to comparable levels of ROS production as cells which received no neural debris (Figure 3.11c). In detail, ROS production after cultivation of NTshRNA microglia in the presence of neural debris was decreased from 1.35 ± 0.06 to 0.72 ± 0.10 ($p = 1.6 \times 10^{-5}$) with addition of SOD1 and to 0.73 ± 0.07 ($p = 3.0 \times 10^{-5}$) with trolox. For shRNASigE1 the reduction was from 2.13 ± 0.07 to 0.79 ± 0.09 (SOD1; $p = 5.36 \times 10^{-24}$) and to 0.72 ± 0.10 (trolox; $p = 2.86 \times 10^{-26}$), respectively. The shRNASigE2 microglia showed a similar diminution of DHE staining intensity from 2.09 ± 0.11 to 0.77 ± 0.07 for SOD1 ($p = 2.89 \times 10^{-23}$) and to 0.70 ± 0.06 for incubation in the presence of the scavenger trolox ($p = 1.58 \times 10^{-25}$).

Siglec-E has an impact on the microglial phagocytosis rate and the associated oxidative burst. This event can be rescued by addition of a scavenger like SOD1 or trolox.

See next page:

Figure 3.11: Siglec-E prevents the phagocytosis associated reactive oxygen burst after challenge with neural debris. a DHE staining of modified microglia. Siglec-E overexpressing vector (SigE vector), Siglec-E knock-down constructs (shRNASigE1; shRNASigE2), non-targeting vector (NTshRNA). Control vector, Siglec-E overexpressing microglia and NTshRNA microglia displayed a moderate increase in fluorescence intensity after stimulation with neural debris. In contrast, knock-down microglia showed an increase of fluorescence intensity after challenge with neural debris. Representative images out of five independent experiments are shown. Scale bar: 30 µm. **b** Quantification of superoxide production in microglia after challenge with neural debris. Lack of Siglec-E on microglia led to increased levels of ROS production when compared with NTshRNA. **c** Analysis of superoxide levels in Siglec-E knock-down microglia challenged with neural debris in either the presence of SOD1 or trolox. Both scavengers were able to restore the elevated ROS production after knock-down of Siglec-E in microglia and treatment with neural debris back to the ROS production level of untreated cells.

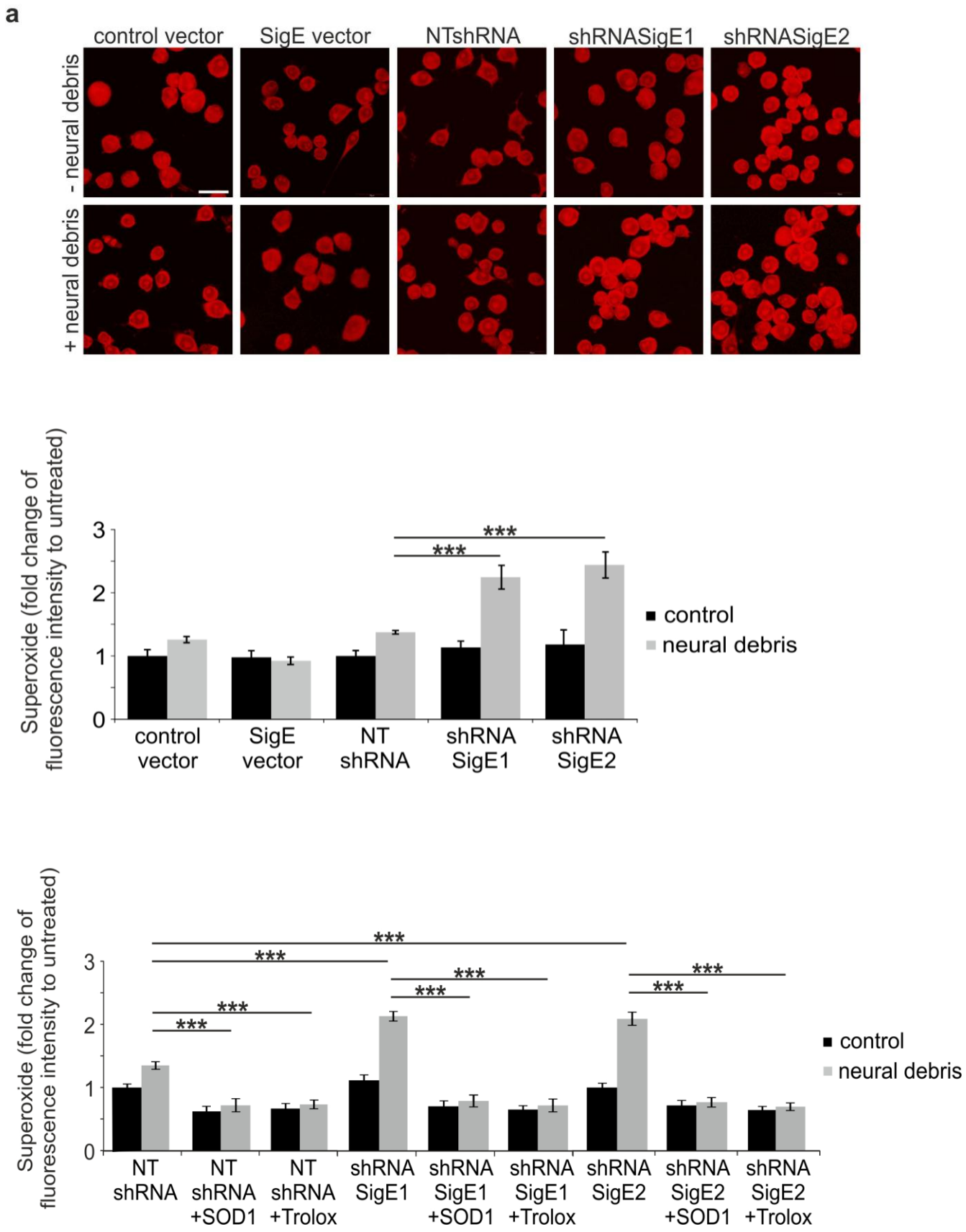
a
control vector
SigE vector
NTshRNA
shRNASigE1
shRNASigE2
- neural debris
+ neural debris
b
Superoxide (fold change of fluorescence intensity to untreated)
3
2
1
0
***
***
control
neural debris
control vector
SigE vector
NT shRNA
shRNA SigE1
shRNA SigE2
c
Superoxide (fold change of fluorescence intensity to untreated)
3
2
1
0
***
***
***
***
***
***
***
***
control
neural debris
NT shRNA
NT shRNA +SOD1
NT shRNA +Trolox
shRNA SigE1
shRNA SigE1 +SOD1
shRNA SigE1 +Trolox
shRNA SigE2
shRNA SigE2 +SOD1
shRNA SigE2 +Trolox

To prove the outcome of the experiments with DHE, another method was used. Amplex Red is able to react with H_2O_2 to produce resorufin, which can be measured by a spectrofluorimeter. Cells were incubated with neural debris in suspension and H_2O_2 production was quantified by converting superoxide to H_2O_2 with SOD1. Similar to the DHE experiments, incubation with neural debris stimulated ROS production in microglia only about 1.1-fold in the control vector transduced microglia, whereas knock-down of Siglec-E resulted in a 2 to 3-fold increase in superoxide level (Figure 3.12). In detail, production of 12.10 ± 1.10 pmol H_2O_2 equivalents/min/mg protein in untreated control cells (NTshRNA) increased to 13.6 ± 1.34 pmol H_2O_2 equivalents/min/mg protein after addition of neural debris. In microglial cells with a knock down of Siglec-E by shRNASigE1 release of superoxide increased from 15.43 ± 0.47 pmol H_2O_2 equivalents/min/mg protein to 32.39 ± 0.39 pmol H_2O_2 equivalents/min/mg protein following stimulation with neural debris ($p = 1.89 \times 10^{-26}$). A similar increase in superoxide production was observed in neural debris treated cells after knock down with shRNASigE1 (from 16.13 ± 0.65 pmol H_2O_2 equivalents/min/mg protein to 28.15 ± 1.12 ; $p = 1.16 \times 10^{-15}$).

Thus, the Amplex Red method confirmed the outcome of the DHE method.

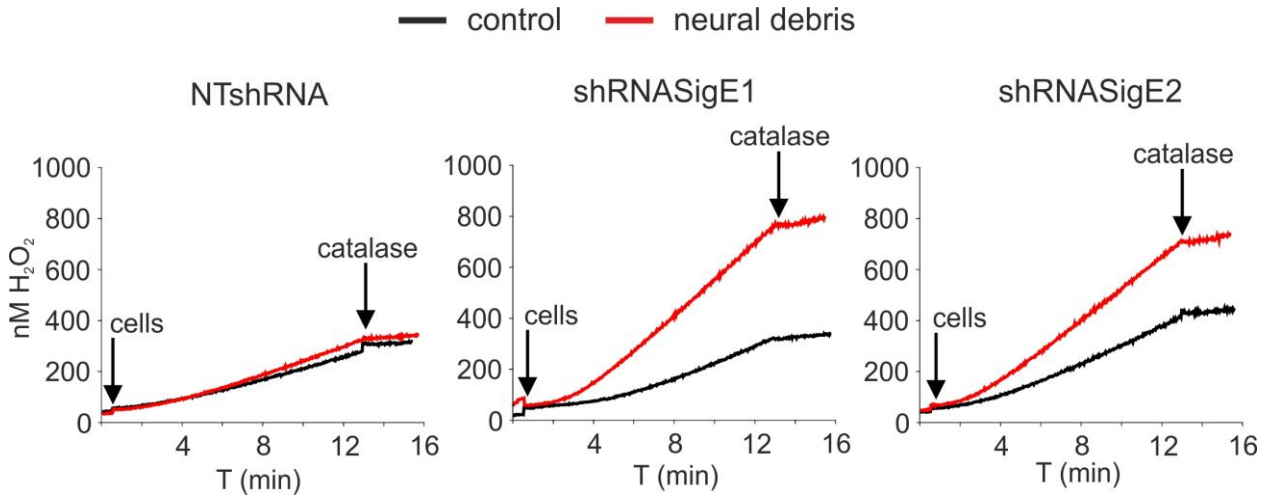

Figure 3.12: Siglec-E knock-down microglia have increased production of superoxide following incubation with neural debris. Quantification of superoxide production in microglia by a spectrofluorimeter. Siglec-E knock-down microglia had increased levels of ROS production when challenged with neural debris compared with NTshRNA. cells: addition of cells; catalase: addition of catalase to stop the reaction

3.4.3 Siglec-E overexpression reduces production of proinflammatory cytokines triggered by neural debris

The next question was whether Siglec-E also plays a role in the production of proinflammatory cytokines triggered by the 16 hours treatment with neural debris.

The transcriptional levels of IL-1β and TNF-α were significantly increased after stimulation with neural debris in Siglec-E knock-down microglia compared to control cells (NTshRNA) that have been stimulated with neural debris, while there was no effect on the mRNA level of NOS2 (Figure 3.13). In detail, gene transcription of IL-1β was increased from 10.0 ± 0.13 to 17.42 ± 2.26 after knock-down with shRNASigE1 ($p = 0.001$) and to 16.56 ± 1.10 after knock-down with shRNASigE2 ($p = 0.003$). The mRNA level of TNF-α was increased from 9.07 ± 1.39 to 14.21 ± 0.73 after knock-down with shRNASigE1 ($p = 0.011$) and to 15.27 ± 1.15 after knock-down with shRNASigE2 ($p = 0.001$). Overexpression of Siglec-E had no significant effect on the gene transcription of proinflammatory mediators after neural debris challenge when compared to control cells (control vector).

In summary, Siglec-E on microglia acted anti-inflammatory by preventing the production of the pro-inflammatory cytokines IL-1β and TNF-α after 16 hours challenge with neural debris.

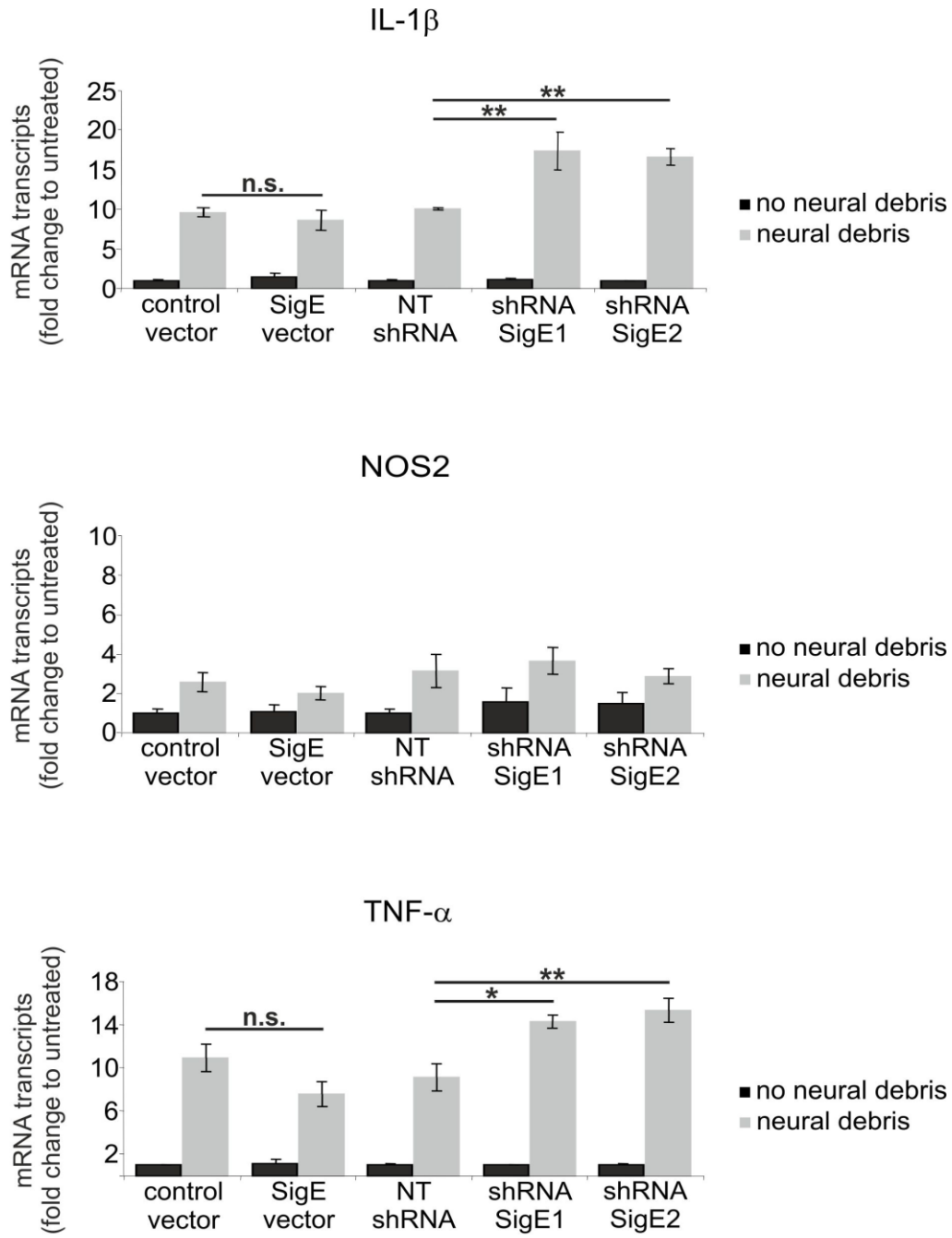

Figure 3.13: Siglec-E overexpressing microglia show diminished production of proinflammatory cytokines after treatment with neural debris. qRT-PCR to detect IL-1β, TNF-α and NOS2 transcription levels after 16 hours incubation of modified microglia with neural debris. Microglia with knock-down of Siglec-E (shRNASigE1; shRNASigE2) showed a significant increase in gene transcription of IL-1β and TNF-α after incubation with neural debris compared to the control vector (NTshRNA). n.s. not significant.

3.5 Siglec-E:Fc fusion protein binding to primary cells

It is known that Siglec-E can bind different linkages of sialic acid with a binding preference for α2-8 linked sialic acid to α2-6 and α2-3 linked sialic acid. Polysialic acid (PSA) is a polymer of α2-8 linked sialic acid, which can be found attached to the neural cell adhesion molecule (NCAM). A fusion protein of Siglec-E consisting of only the extracellular part of Siglec-E fused to a mouse immunoglobulin domain was used to investigate the binding behaviour of Siglec-E to polysialic acids chains in the glycocalyx of astrocytes and neurons.

3.5.1 Siglec-E:Fc binds to neurons

Primary neurons were either treated or untreated with sialidase to remove sialic acid from their cell surface. After the treatment, the fusion proteins Siglec-F:Fc and Siglec-E:Fc were applied to analyse their binding capacity. For Siglec-F:Fc it has been previously shown in our lab that it is capable of binding to neurons and that this feature is abrogated after treatment with sialidase (Linnartz et al. 2012a). Therefore it was used as a positive control for this experiment.

Without sialidase treatment both fusion proteins Siglec-F:Fc and Siglec-E:Fc were able to bind sialic acid on the neuronal surface as indicated by the co-staining with the neurons (Figure 3.14). However, after the enzymatic removal of sialic acid from the neuronal glycocalyx none of the fusion proteins was binding to the neurons. Thus, sialic acid is a crucial factor in the neuronal glycocalyx to allow the binding of Siglec-F and Siglec-E to the cell surface.

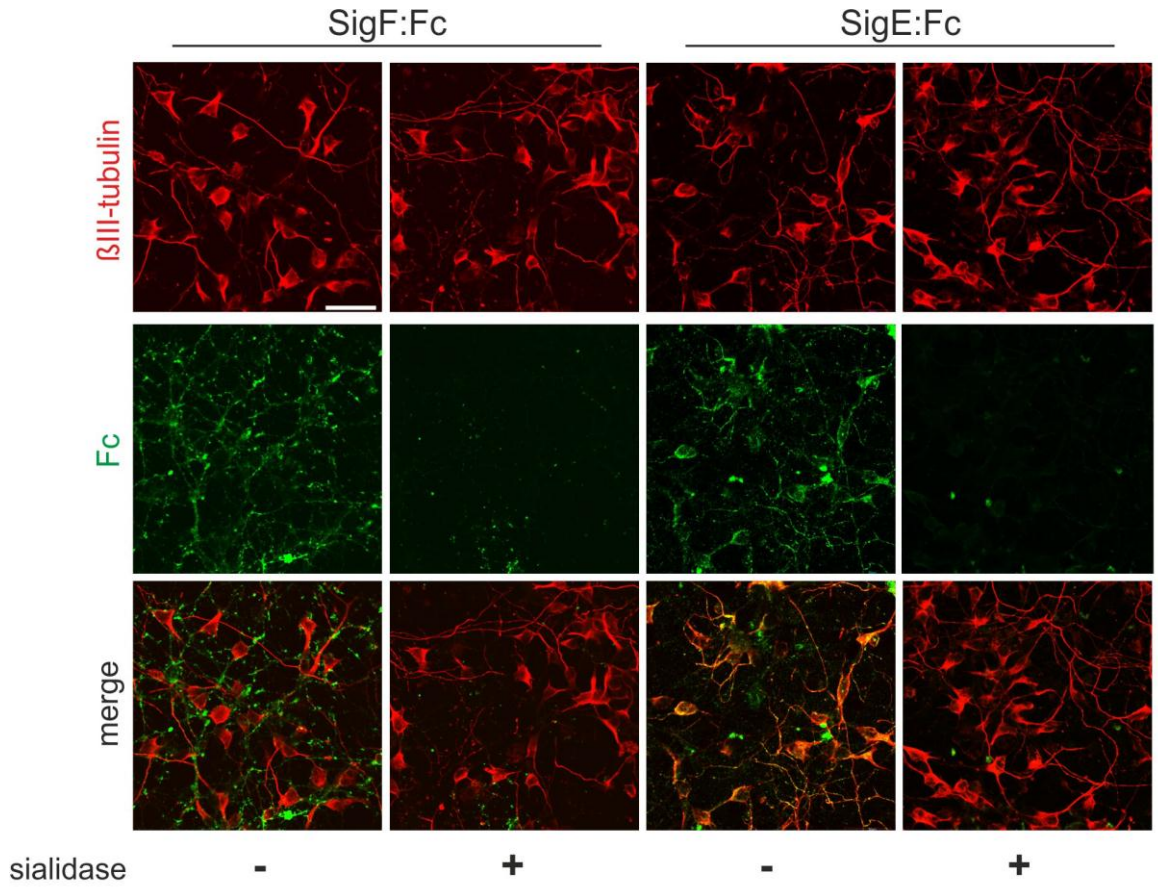

Figure 3.14: Binding of Siglec-F:Fc and Siglec-E:Fc fusion protein to neurons. Neurons were either untreated or treated with sialidase to remove sialic acid from the cell surface. The removal of sialic acid resulted in a reduction of the binding capacity of Siglec-F:Fc and Siglec-E:Fc to neurons. Representative images out of three independent experiments are shown. Scale bar: 30 µm.

3.5.2 Siglec-E:Fc binds to astrocytes and primary microglia

Primary astrocytes or microglia were either untreated or treated with a combination of neuraminidase and EndoN for 2.5 hours to enzymatically remove sialic acid. Subsequently cells were cultured with a recombinant Siglec-E:Fc fusion protein for 1 hour. The outcome was analysed by confocal microscopy. The analysis revealed that Siglec-E:Fc bound to primary astrocytes and microglia (Figure 3.15). Enzymatic removal of sialic acid residues by EndoN and neuraminidase treatment resulted in an abrogation of the binding capacity of Siglec-E:Fc to both cell types, indicating that sialic acid residues in the glycocalyx of the cells were needed for Siglec-E:Fc fusion protein to bind to the cells.

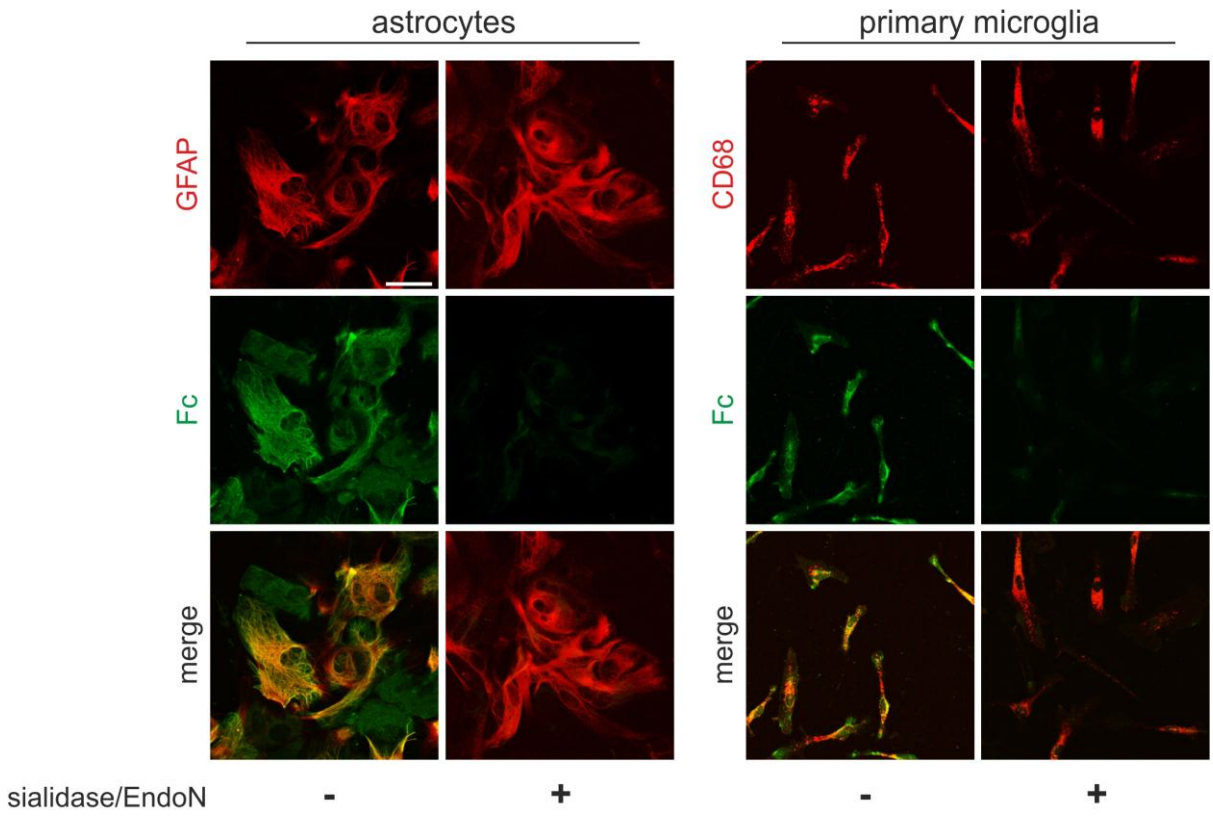

Figure 3.15: Siglec-E:Fc binds to primary astrocytes and microglia. The fusion protein Siglec-E:Fc was cultured with astrocytes or primary microglia for 1 hour. Staining showed that Siglec-E:Fc was able to bind to astrocytes and primary microglia. Enzymatic removal of sialic acid led to a reduction in the binding capacity of the recombinant Siglec-E:Fc fusion protein. Representative images out of three independent experiments are shown. Scale bar: 30 µm.

3.6 Co-culture of primary neurons and microglia

After it had been proven that Siglec-E is indeed capable of binding to the neuronal glycocalyx in a sialic acid-dependent manner, the next point of interest was to investigate the impact of the modification in Siglec-E expression levels on microglia in a neuron-microglia co-culture system. For this purpose primary neurons and modified microglia of the microglia line were co-cultured for 48 hours.

3.6.1 Siglec-E is neuroprotective in a neuron-microglia co-culture system

Primary neurons were either untreated or treated with the enzyme sialidase to remove sialic acid from the cell surface. Following the treatment, the neurons were

co-cultured with microglia having different expression levels of Siglec-E on their surface for 48 hours. Cells were stained by immunocytochemistry and the change in relative neurite length was quantified. Overexpression of Siglec-E increased the relative neurite length while knock-down of Siglec-E reduced it (Figure 3.16a). In detail, the neurite length was increased from 100 % ± 9.97 % (control vector) to 150 % ± 2.19 % following overexpression of Siglec-E on microglia ($p = 1.07 \times 10^{-13}$; Figure 3.16b). Siglec-E knock-down on microglia reduced the relative neurite length from 100 % ± 5.31 % (NTshRNA) to 70 % ± 1.45 % (shRNASigE1, $p = 1.62 \times 10^{-9}$) and to 69 % ± 1.2 % (shRNASigE2, $p = 6.06 \times 10^{-10}$). Enzymatic removal of the glycocalyx's sialic acid abolished both of the effects and led to a reduction in the relative neurite length of the neurons in all the control conditions and the microglia with the modified Siglec-E expression level.

To exclude side effects due to changes in the cell-cell ratio, the neuronal cell body density with respect to percentage in the co-culture system was quantified. The outcome clearly showed that there was no change in the neuronal cell body density for all the different settings in this experiment (Figure 3.16c).

In conclusion, microglia were able to sense sialic acid in the neuronal glycocalyx by their Siglec-E receptors. Siglec-E overexpression on microglia led to an increase of the relative neurite length in the co-culture system whereas knock-down increased the cytotoxicity with respect to the neurons, resulting in a reduction of the relative neurite length.

See next page:

Figure 3.16: Siglec-E overexpressing microglia act neuroprotective in a neuron-microglia co-culture system. a Neurons were co-cultured for 48 hours with microglia expressing different amounts of Siglec-E. In co-culture with Siglec-E overexpressing microglia, neurons seemed to have longer neurites, whereas in the presence of Siglec-E knock-down microglia, neurons had shorter neurites. Representative images without sialidase treatment out of three independent experiments are shown. Scale bar 30 µm. **b** Quantification of relative neurite length. Siglec-E overexpression led to an increase in relative neurite length whereas knock-down of Siglec-E caused a reduction in relative neurite length. After enzymatic removal of sialic acid the relative neurite length was significantly reduced when compared to untreated neurons. **c** Neuronal cell body density in relation to microglia was counted to exclude side effects due to changes in the cell-cell ratio. There was no significant difference in the neuronal cell body density.

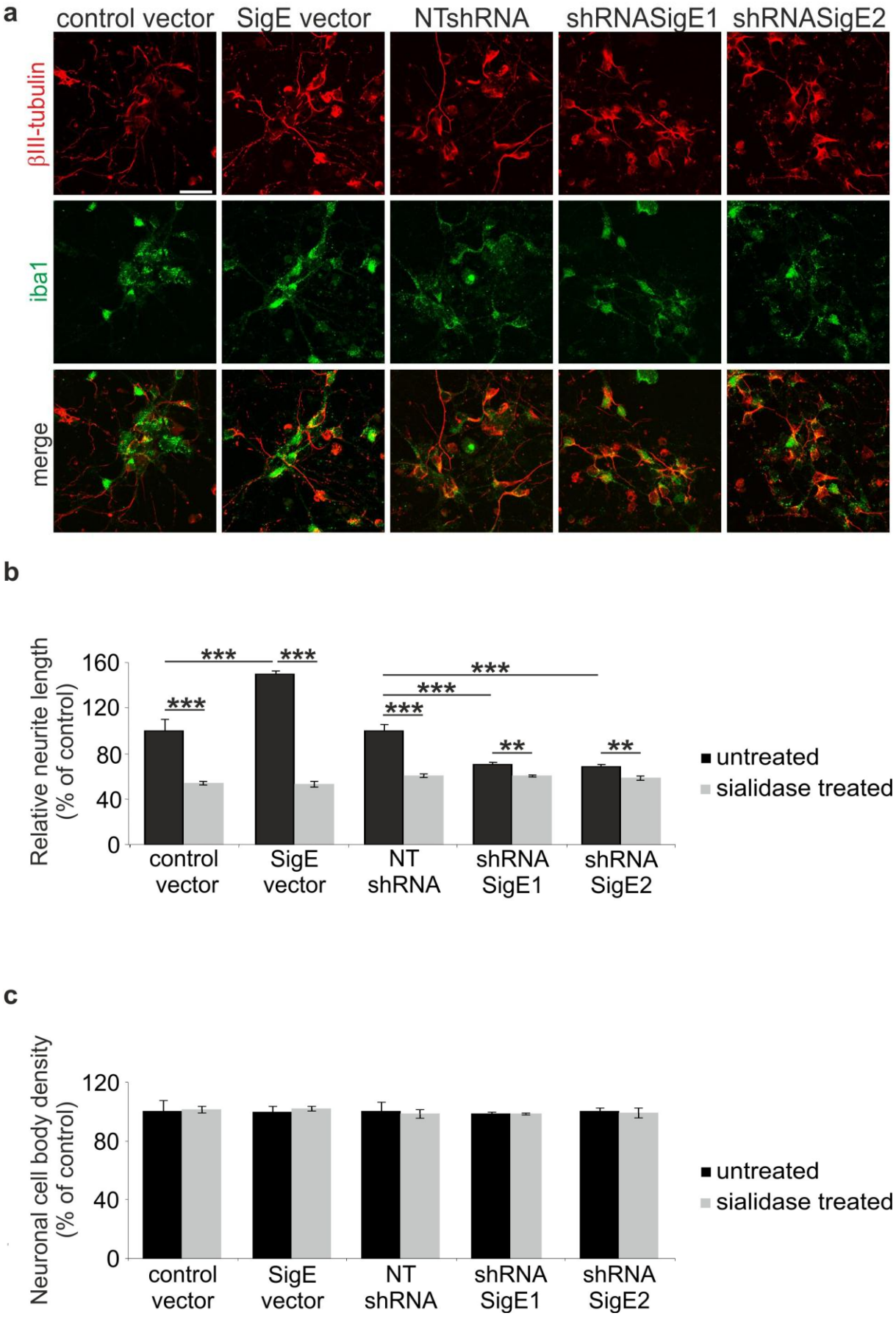
a
control vector
SigE vector
NTshRNA
shRNASigE1
shRNASigE2
βIII-tubulin
iba1
merge
b
Relative neurite length (% of control)
160
120
80
40
0
***
***
***
***
***
**
**
control vector
SigE vector
NT shRNA
shRNA SigE1
shRNA SigE2
untreated
sialidase treated
c
Neuronal cell body density (% of control)
120
80
40
0
control vector
SigE vector
NT shRNA
shRNA SigE1
shRNA SigE2
untreated
sialidase treated

3.6.2 Siglec-E exerts its neuroprotective effect by attenuation of reactive oxygen species release

Primary neurons were co-cultured with modified microglia either in the presence or absence of 40 nM Trolox for 48 hours. Trolox is a vitamin E analogue, which is an antioxidant and capable of scavenging superoxide anions. After 48 hours cells were stained and analysed for their relative neurite length (Figure 3.17a). In the presence of the scavenger trolox, the relative neurite length of neurons in co-culture with Siglec-E knock-down microglia was restored to 97 % ± 2.91 % for knock-down with shRNASigE1 (NTshRNA 103 % ± 1.53 %), and 94 % ± 2.85 % for shRNASigE2 (Figure 3.17b). In co-culture with Siglec-E overexpressing microglia the relative neurite length seemed to be unaffected by Trolox treatment. Quantification of the neuronal cell body density again showed that there was no change in the cell-cell ratio in the different experimental settings (Figure 3.17c).

Thus, the cytotoxicity of Siglec-E knock-down microglia on the relative neurite length could be scavenged by addition of 40 nM Trolox in the co-culture system. This indicates that Siglec-E participates in the regulation of the microglial oxidative burst.

See next page:

Figure 3.17: Siglec-E exerts its neuroprotective effect by attenuating the production of reactive oxygen species. a Neurons were treated with 40 nM Trolox and then co-cultured for 48 hours with microglia expressing different levels of Siglec-E on their surface. The neurites of the neurons being co-cultured with Siglec-E overexpressing microglia had the longest neurites. The other conditions (control vector, NTshRNA, shRNASigE1 and shRNASigE2) displayed comparable neurites lengths. Representative images with Trolox treatment out of three independent experiments are shown. Scale bar 30 µm. **b** Quantification of relative neurite length. The relative neurite length was restored after the treatment with 40 nM Trolox by which the release of ROS and their harmful effect was diminished. **c** Neuronal cell body density in relation to microglia was counted to exclude side effects due to changes in the cell-cell ratio. There was no significant difference in the neuronal cell body density.

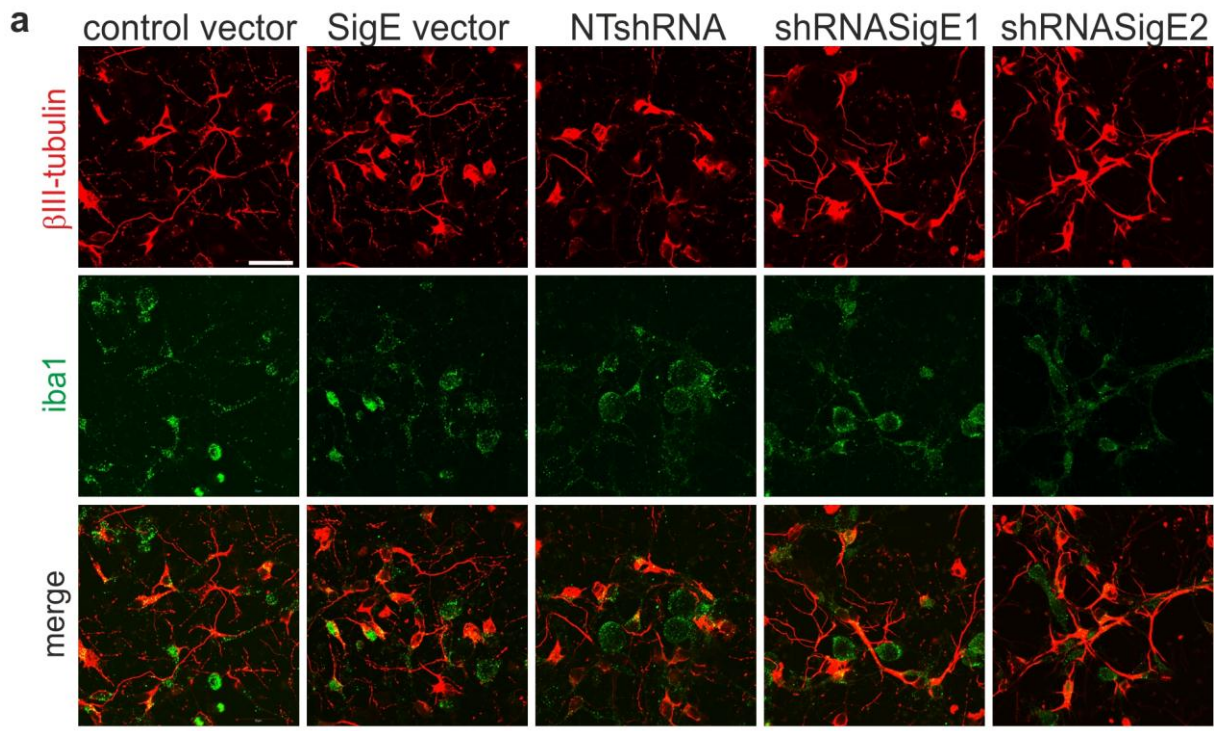
a
control vector
SigE vector
NTshRNA
shRNASigE1
shRNASigE2
βIII-tubulin
iba1
merge

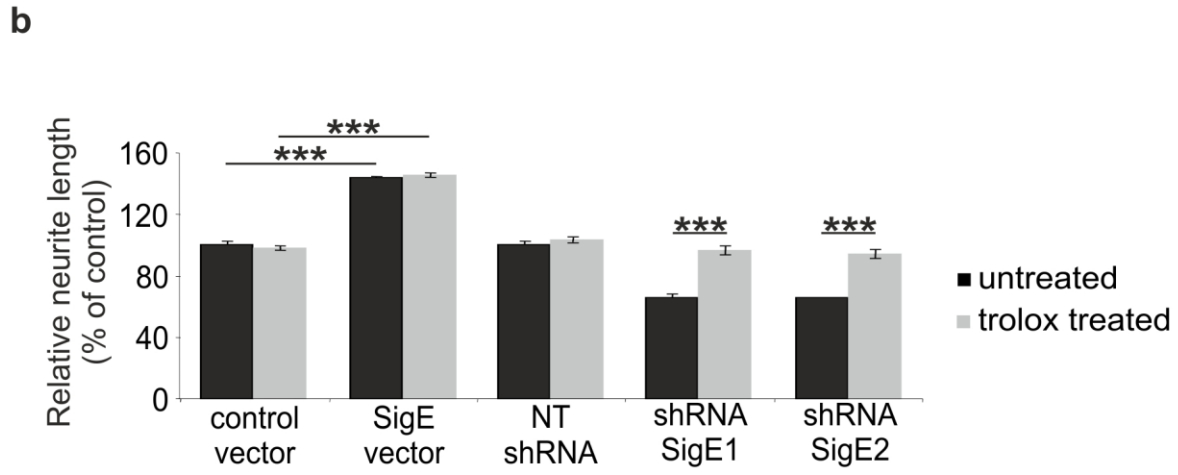
b
Relative neurite length (% of control)
160
120
80
40
0
***
***
***
***
control vector
SigE vector
NT shRNA
shRNA SigE1
shRNA SigE2
untreated
trolox treated

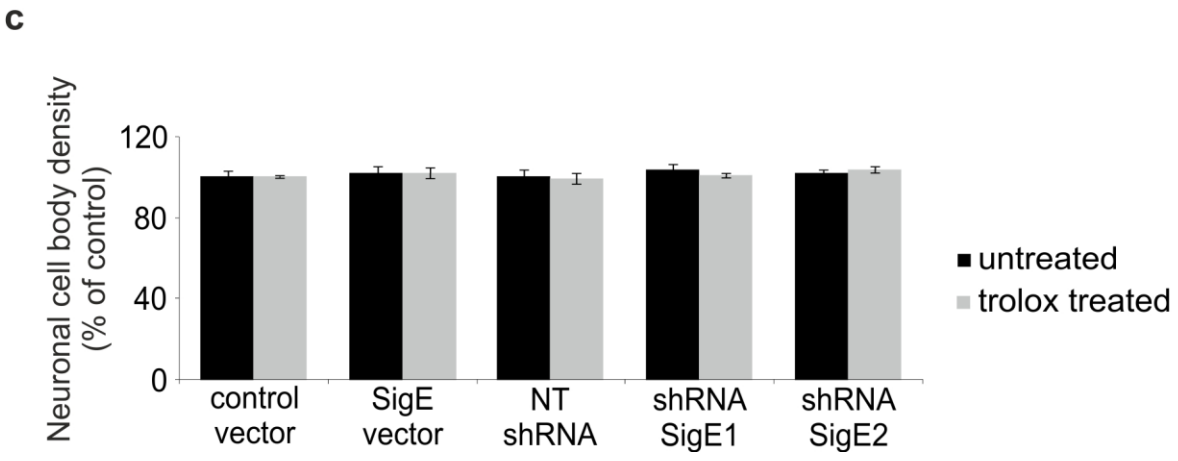
c
Neuronal cell body density (% of control)
120
80
40
0
control vector
SigE vector
NT shRNA
shRNA SigE1
shRNA SigE2
untreated
trolox treated

4. Discussion

4.1 Siglecs in mouse and human

The mouse Siglec family consists of nine members from which four belong to the common Siglecs (Siglec-1, Siglec-2, Siglec-4, Siglec-15) and five to the family of the CD33-related Siglecs (Siglec-3, Siglec-E, Siglec-F, Siglec-G, Siglec-H). Among them four have an ITIM and ITIM-like motifs in their cytoplasmic tail (Siglec-2, Siglec-E, Siglec-F, Siglec-G) whereas Siglec-3 has only an ITIM-like motif in the cytoplasmic domain (Pillai et al. 2011). Some Siglecs are expressed on a single cell type of the immune system, like Siglec-2/CD22 and Siglec-G, which are exclusively expressed on B cells, and Siglec-F, which is expressed solely on eosinophils. Others like Siglec-3 and Siglec-E can be found on a different set of cells of the myeloid line, for example Siglec-E can be found on neutrophils, monocytes and dendritic cells (Crocker et al. 2007). The present study now reveals that Siglec-E is transcribed and expressed in mouse microglia as well.

In contrast, 15 Siglecs can be found in humans. The human common Siglecs have the same nomenclature as the mouse ones. The CD33-related Siglecs are Siglec-3, Siglec-5 to Siglec-16. Among the human Siglecs, ten have ITIM and ITIM-like motifs (Siglec-2, Siglec-3, Siglec-5 to Siglec-12) and three have just an ITIM-like motif (Siglec-14 to Siglec-16) (Pillai et al. 2011). The human Siglec-11 is another Siglec, which is expressed on microglia in the brain like Siglec-E (Hayakawa et al. 2005). A study showed that Siglec-11 is capable of interacting with the neuronal glycocalyx by recognizing α2-8-linked sialic acid and thereby prevents neurotoxic effects (Wang and Neumann 2010). But Siglec-11 has no homolog in the mouse system.

Siglec-E is most similar in its sequence to the human Siglec-7, Siglec-8 and Siglec-9 but in its expression profile Siglec-E mostly resembles Siglec-7 and Siglec-9. Siglec-E shows the same preference for α2-8-linked sialic acid like Siglec-7 or Siglec-11. However, there is no homolog for Siglec-E in the human system (Wang and Neumann 2010; Zhang et al. 2004). A study of gene expression profiles revealed that Siglec-11 and Siglec-E are not the only inhibitory Siglecs, which are expressed on microglia or macrophages. CD33/Siglec-3 expression can be found in spleen macrophages, Siglec-5 is transcribed in microglia, Siglec-1 is expressed in lung and

spleenic macrophages and Siglec-F can be found in lung macrophages (Gautier et al. 2012). Existing data now suggest that the leukocytes from the innate immune system have inhibitory Siglec receptors on their cell surface, which are able to sense the sialic acid caps in an intact glycocalyx and by this to distinguish between “self” and “non-self” (Varki 2011). Binding of a so-called “self”-ligand leads to the inhibition of an immune response via the ITIM counteracting an activating ITAM signal (Linnartz et al. 2010).

Our data now suggest that Siglec-E is a receptor recognizing the intact glycocalyx of primary neurons and thereby identifies if the neuron is “healthy” or harmed. This function is in line with a previous study of Siglec-11 in a co-culture system with primary hippocampal neurons (Wang and Neumann 2010). The study found out that Siglec-11 had a neuroprotective function as long as the neurons had sialic acid in the glycocalyx. Enzymatic removal of the sialic acid cap resulted in a loss of the neuroprotective function of Siglec-11 in microglia. According to our data, Siglec-E seems not to belong to either of the microglia receptor groups, which recognize pathogen-associated molecular patterns (PAMPs), or to the group, which senses danger-associated molecular patterns (DAMPs). Siglec-E rather belongs to a type of receptor, which recognizes self-associated molecular patterns (SAMPs) like the sialic acid cap (Varki 2011). A study demonstrated that Siglec-E has a preference for the sialic acid N-acetyl-neuraminic acid (Redelinghuys et al. 2011). By this property Siglec-E on microglia is well adapted for recognizing the microenvironment in the mouse brain as the murine brain solely expresses N-acetyl-neuraminic acid (Varki and Schauer 2009).

4.2 Siglec-E has anti-inflammatory properties

Siglec-E has been shown before to play a role in the regulation of the immune response. Following stimulation with LPS or other TLR agonists, Siglec-E on macrophages was upregulated in a MyD88-dependent mechanism and phosphorylated. Cross-linking of Siglec-E on macrophages led to a significantly decreased production of the NF-κB-dependent cytokines TNF-α and IL-6. Further, the overexpression of Siglec-E inhibited the TIR domain containing adaptor inducing IFN-β, (TRIF)-driven IFN-β and RANTES whereas the knock-down displayed an increase in RANTES production. Therefore, Siglec-E seemed to take part in the

control of the antiviral response to TLRs by helping to maintain the cytokine balance after infection (Boyd et al. 2009).

In a more recent publication Siglec-E was demonstrated to be crucial for the regulation of neutrophil recruitment to the lung under pathological conditions. A knock-out mouse model showed a more rapid and greater migration of neutrophils and macrophages in the airways in an aerosolised LPS-induced acute lung airway inflammation model. The same holds true for stimulation with zymosan, demonstrating that this effect was not exclusively for LPS but it was shown to be selective for the lung. Additional investigations revealed that Siglec-E is a negative regulator of the integrin CD11b-dependent adhesive function by suppressing the phosphorylation and thereby the activation of the Src family kinase Syk and p38 MAP kinase (McMillan et al. 2013).

In line with the former observations, the stimulation with neural debris led in this study to elevated levels of the proinflammatory cytokines IL-1β and TNF-α in Siglec-E knocked-down microglia and to decreased levels in microglia overexpressing Siglec-E. This immunoregulatory property of Siglecs under pathological conditions is not unknown in literature. Thus, CD22 has been demonstrated to be strongly expressed in gastrointestinal lamina propria eosinophils in the upper gastrointestinal tract with highest amounts in the jejunum. Overexpression of IL-5 was accompanied by downregulation of CD22 expression. In a state of gastrointestinal inflammation CD22 expression on eosinophils was reduced as well. CD22 knock-out mice showed a higher percentage of eosinophils among total lamina propria cells. This negative correlation of CD22 expression levels and the percentage of eosinophils in the intestines suggests an important role of CD22 in the regulation of tissue eosinophilia in the gastrointestinal tract (Wen et al. 2011). A similar property was detected for the murine Siglec-F, which is known to be expressed on eosinophils (Zhang et al. 2007). Chronic challenge with ovalbumin (OVA) led to an increase in bronchoalveolar lavage (BAL), peribronchial, bone marrow and peripheral blood eosinophils in Siglec-F deficient mice. Additionally, the OVA treated Siglec-F deficient mice had elevated levels of airway mucus, a higher amount of lung collagen, increased smooth muscle peribronchial thickness and the area stained for trichome was increased as well suggesting an increase in peribronchial fibrosis. Furthermore, mice lacking Siglec-F had more peribronchial

cells positive for TGF-β1 and levels of eotaxin-1 and RANTES were elevated as well. Treatment with the cytokines IL-4 and IL-13 increased the level of Siglec-F ligands in WT mice. Summarizing, Siglec-F deficient mice had a stronger immune response and displayed altered cytokines levels in favour of pro-inflammatory cytokines similar to that demonstrated for the knock-down of Siglec-E in microglia. Taken together, these data illustrated once more the importance of Siglec receptors in maintaining the balance in the inflammatory response (Cho et al. 2010).

For the human receptor CD33, which is expressed on peripheral human blood monocytes, the release of high levels of the proinflammatory cytokines IL-1β, IL-8 and TNF-α was triggered by the challenge with a specific monoclonal antibody directed to CD33. The same happened through specific gene silencing of CD33. Activation of monocytes led to a downregulation of CD33, suggesting that CD33 has repressive properties on human monocytes (Lajaunias et al. 2005).

Siglec-9 on immature dendritic cells, the human orthologue to Siglec-E, was shown to be capable of binding to tumour-produced mucins. Treatment with LPS in the presence of tumour mucins or treatment with an anti-Siglec-9 antibody resulted in a reduced production of IL-12 (Ohta et al. 2010). In another study with macrophages overexpressing Siglec-9, the stimulation with LPS or peptidoglycan only led to moderate levels of TNF-α production whereas control macrophages reacted with a high amount of TNF-α production to stimulation of TLRs. The same held true for IL-6 and IFN-β upon stimulation with either LPS or peptidoglycan. Mutations in the ITIM motifs of Siglec-9 abolished this effect. In contrast, the expression levels of the anti-inflammatory cytokine IL-10 induced by TLRs were reduced in Siglec-9 overexpressing macrophages. In the same study it was found out that Siglec-5 had similar effects when overexpressed on macrophages after stimulation with TLR agonists, IL-10 production was upregulated whereas TNF-α production was diminished (Ando et al. 2008). This data is in line with the altered cytokine expression levels of stimulated microglia expressing different amounts of Siglec-E on their cell surface.

Altogether, the data of the present study once more proves that ITIM-bearing Siglecs like Siglec-E play an important role in the regulation of the immune response to different threats such as the stimulation with neural debris. It is important for a

healthy microenvironment in the brain that apoptotic cells and debris are removed without over-activation of the immune system. Over-activation could lead to the overproduction of pro-inflammatory cytokines what in the end could damage the neurons in the CNS. The Siglec-E overexpression and knock-down approach on microglia showed that Siglec-E is a member of this tightly regulated system to keep a balanced cytokine level in the brain to ensure its functionality. This was demonstrated by stimulation with neural debris and the quantification of cytokine levels. The data of this study suggest that Siglec-E exerts its inhibitory function by negative regulation of pro-inflammatory cytokines like IL-1β and TNF-α to prevent an over-activation of the immune response.

4.3 Siglec-E is a regulator of phagocytosis and the associated oxidative burst

This study shows that Siglec-E overexpression on microglia led to a decreased phagocytosis rate of neural debris and attenuation of the associated oxidative burst. In contrast, knock-down of microglial Siglec-E resulted in an increased phagocytosis rate of neural debris and higher production of superoxide.

One of the main characteristics of microglia is phagocytosis of either pathogens or of cells that underwent apoptosis and cellular debris during development and in pathology and regeneration. Microglia are assumed to remove synapses in the developing brain and take part in neuronal pruning in the postnatal brain (Stevens et al. 2007). In neurodegenerative diseases like Alzheimer's disease (AD) microglia clearance is of great importance as well. Microglia take up the soluble and fibrillar amyloid-beta, which is harmful for the neurons in the brain by pinocytosis or phagocytosis (Lee and Landreth 2010). Apoptotic cells attract microglia by displaying different signals. One prominent so-called "eat-me" signal is phosphatidylserine. Phosphatidylserine is transferred from the inner leaflet of the cell membrane to the outer leaflet by scramblases and flippases and serves as a signal for the microglia to find apoptotic cells (Ravichandran 2003; Ravichandran and Lorenz 2007).

Changes in the glycocalyx can serve as a signal for phagocytosis as well. The induction of apoptosis in lymphoblasts led to a decrease of sialic acids on the cell surface (Meesmann et al. 2010). This process increased the binding of sialic acid

binding plant lectins to the apoptotic cell-derived membranes and the subsequent engulfment by monocyte-derived phagocytes. Furthermore, a sialidase treatment of apoptotic cells increased the uptake compared to untreated cells. Even the incubation of neuraminidase treated viable lymphoblasts with monocyte-derived phagocytes led to an engulfment of the lymphoblasts. Therefore, the glycosylation status of a cell can act as a signal for phagocytes (Meesmann et al. 2010).

The importance of ITAM and ITIM-signalling like from the Siglec receptors and their involvement in immune processes like phagocytosis was shown in model organisms like *Caenorhabditis elegans* and *Drosophila melanogaster*. A study in *Caenorhabditis elegans* showed that the receptor CED-1 is an important component in the engulfment of apoptotic cells (Zhou et al. 2001). The mechanism, which lies behind, is crucial for the uptake of necrotic cells, developmentally pruned axons and dendrites. The CED-1 orthologue in *Drosophila* is Draper. The phosphorylation of Draper was increased by a kinase from Src kinase family, the same kinase family that phosphorylates the ITAMs and ITIMs of Siglecs. This phosphorylation step was essential for glial phagocytic activity. Phosphorylated Draper associated with the tyrosine kinase Shark, which is similar to the mammalian Syk kinase, through an ITAM motif in the intracellular domain (Ziegenfuss et al. 2008). The activity of Shark was required for Draper-mediated signalling like recruitment of glial membranes to damaged neurons and the phagocytosis of axonal debris and neuronal corpses by glia (Ziegenfuss et al. 2008). A follow-up study found out that in *Drosophila* there are different splice variants of Draper (Logan et al. 2012). The draper-I isoform seemed to be necessary for phagocytosis of axonal debris and is expressed in embryos, larval brains and larval body wall tissue whereas the Draper-II isoform is solely expressed in adults. Isoform-I is the only splice variant harbouring an ITAM sequence in its intracellular part. In contrast, the Draper-II isoform contains an ITIM sequence in its intracellular part. Overexpression of splice variant II resulted in a complete block of glial clearance function. Furthermore Logan and colleagues discovered that the ITIM-bearing isoform-II associates with Corkscrew, the *Drosophila* homolog of vertebrate SHP-1 and SHP-2. Taken together, they proposed a model where Draper-II and Corkscrew inhibit glial engulfment activity by diminishing the activity of Draper-I and its signalling effectors like Shark by dephosphorylation (Logan et al. 2012). This present study nicely shows that the same mechanism is conserved in Siglec signalling. ITIM-bearing Siglecs like Siglec-E counter-regulate the activatory

signals from ITAMs resulting in the inhibition of processes like phagocytosis, as was shown for Siglec-E overexpression on microglia in this study. Like ITIM-bearing Siglecs the isoform-II associated with a homolog of SHP-1 or SHP-2 to exert its inhibitory function.

Other examples for the counter-regulation of an ITAM and an ITIM motif are the human receptors FcγRIIA and FcγRIIB. The ITIM receptor FcγRIIB was shown to inhibit the FcγR-mediated phagocytic pathways (Huang et al. 2003). Clustering of the human FcγRIIA and the receptor FcγRIIB led to a reduction in the efficiency of FcγRIIA-mediated phagocytosis of IgG-coated erythrocytes up to 50 %. Co-transfection of FcγRIIB and the phosphatases SHP-1 or SHIP-1 further amplified this effect up to 85 % of phagocytosis inhibition. Transfection of FcγRIIA with one of the phosphatases was capable of decreasing the phagocytosis rate even in the absence of FcγRIIB by more than 50 %. In contrast, the overexpression of Syk kinase enhances phagocytosis in transfected epithelial cells (Huang et al. 2003). Like Siglec-E, FcγRIIB decreased the phagocytosis rate by counteracting the activating signal of the FcγRIIA. The association with SHP-1 or SHIP-1 was important as known for the ITIM-bearing Siglec receptors.

The ITIM bearing human Siglec-5 and the mouse Siglec-1/Sn have been shown to be capable of binding to sialylated bacteria (Jones et al. 2003). The difference in the binding of Siglec-5 to non-sialylated or sialylated bacteria was 30- and 10-fold for two *Neisseria meningitides* strains. Significantly larger numbers of bacteria were taken up when they were sialylated. This effect could be inhibited by a Siglec-5 blocking antibody. When the uptake of bacteria of wild-type versus macrophages from Sn-deficient mice was compared, the wild-type macrophages displayed an enhanced uptake of sialylated bacteria over a 30 minutes time course. In conclusion, this demonstrates that Siglecs can interact with sialylated pathogens and are able to engulf them (Jones et al. 2003).

Thus, in line with these studies, the present experimental results suggest, that the microglial ITIM-containing receptor Siglec-E is a negative regulator of phagocytosis of microglia probably by counteracting an activatory ITAM signalling receptor and by recognition of the sialylation status of a cell. The removal of sialic acid was a triggering factor as seen in the co-culture approach with primary hippocampal

neurons. Mimicking the state of apoptotic or damaged cells by removal of sialic acid resulted in a decrease of the relative neurite length, which was mediated by the microglia. The amount of the decrease in the relative neurite length was dependent on the level of Siglec-E expression on the microglia. Similar to the Draper isoform II and FcγRIIB, Siglec-E seemed to have a negative regulating function in the context of phagocytosis. Overexpression of Siglec-E resulted in a diminished phagocytosis rate of neural debris whereas the knock-down of Siglec-E on microglia led to an increased phagocytosis rate. The outcome of the knock-down approach suggests that if the inhibitory counterpart of the ITAM-ITIM-regulation is missing, an over-activation of the immune response could be the consequence like the one which was seen by the increase in the phagocytosis rate.

Associated with phagocytosis is the production of reactive oxygen species. In neutrophils and macrophages, double-knock-out of DAP12 and FcRγ resulted in the lack of the ability to mediate the integrin induced respiratory burst by the ITAM-Syk pathway (Mocsai et al. 2006). The ITAM-Syk pathway is initiated by the ITAM-bearing receptor DAP12 and FcRγ and signals via the Vav family of Rho guanine nucleotide exchange factors. This leads to the activation of the NADPH oxidase (NOX2) complex and production of reactive oxygen species (Graham et al. 2007). Siglecs bearing an inhibitory ITIM motif are thought to counteract the activatory signals by ITIM receptors like DAP12, suggesting an involvement on the regulation of the NOX2 complex.

In another approach the participation of SHP-1 in the regulation of superoxide formation was investigated. SHP-1 is recruited by phosphorylated Siglec-E to counteract activatory signals of ITAM receptors. In the study by Krotz and colleagues blocking of SHP-1 in endothelial cells by distinct mechanisms resulted in increased basal superoxide release. The same held true for knock-down of SHP-1 with RNA interference. This effect was abolished by a nicotinamide adenine dinucleotide (phosphate) (NAD(P)H)-oxidase inhibitor and by a phosphatidyl-inositol-3-kinase (PI3K) inhibitor, suggesting that SHP-1 negatively regulates PI3K followed by attenuation of NAD(P)H-oxidase-dependent superoxide production (Krotz et al. 2005).

The importance of ITAM-Syk and therefore counter-regulating ITIM receptors in ROS production has been exemplified by numerous studies. The C-type lectin Dectin-2 is crucial for NF-κB activation and anti-fungal immune response. Silencing of Dectin-2 or Syk had the consequence that THP-1 macrophages stimulated with swollen conidia of the fungus *Aspergillus fumigatus* were no more capable to react with a respiratory burst, which was seen for control THP-1 cells. Treatment with a Syk inhibitor resulted in the same outcome in WT macrophages demonstrating the essential role Syk plays in the ROS production mediated by Dectin-2 in response to a fungus infection (Sun et al. 2013).

Another research group took a closer look at the mechanism lying behind the Syk-pathway and the respiratory burst. Two different phases of the production of ROS could be identified. In platelets the first initial phase seemed to be independent of the Syk-pathway whereas the second phase involved the Syk-pathway. Furthermore, a blocking antibody of the ITAM receptor FcγRIIa was able to abolish the FcγRIIa-induced ROS production in platelets indicating that the respiratory burst in platelets was dependent on the interaction with FcγRIIa. ITIM receptors like Siglec-E could have a similar effect on ROS production as the overexpression and knock-down studies with Siglec-E showed. Overexpression of Siglec-E and thus the inhibitory stimulus for the activating ITAM-Syk pathway led to a remarkable decrease in ROS production. The platelet-specific collagen receptor GPVI/FcRγ is known to trigger ROS production in platelets. Generation of ROS induced by agonists of the receptor GPVI could be inhibited by a Syk inhibitor. In contrast, co-treatment with a GPVI and a FcγRIIa agonist increased ROS production, which in turn was inhibited by the same Syk inhibitor. In summary, ROS generation in platelets could be induced by either GPVI/FcRγ or FcγRIIa agonists but both are involved in the ITAM-Syk-pathway (Arthur et al. 2012), which could be regulated by receptors with an ITIM sequence.

Hyperglycaemic conditions were shown to down-regulate CD33/Siglec-3 expression on primary human monocytes. This went along with an increase in the expression of proinflammatory cytokines like TNF-α, which is in line with the results of the Siglec-E knock-down in microglia, showing elevated level of proinflammatory cytokines like IL-1β and TNF-α. Treatment with the antioxidant α-tocopherol reversed the down-regulation of CD33 and the elevated TNF-α production, suggesting a mechanism by which ROS generation is induced by high glucose concentrations and the

subsequent down-regulation of CD33 linking ROS production to CD33 expression levels (Gonzalez et al. 2012). In microglia the level of Siglec-E expression could be linked to the amount of ROS production as well. Knock-down of Siglec-E had similar results like the down-regulation of CD33/Siglec-3 namely elevated ROS production and increased release of proinflammatory cytokines.

The CD22/Siglec-2 blocking antibody HB22.7 was recently applied in a study with Bortezomib treated lymphoma cells. Bortezomib is a proteasome inhibitor with anti-lymphoma properties exerting its influence by generation of ROS and by induction of apoptosis. A sequential treatment of lymphoma cells with HB22.7 and Bortezomib reduced the number of viable cells by about 95 % and increased ROS production by more than 40 %, suggesting a synergistic cytotoxic effect via raised apoptosis and ROS production. This links the blocking of another Siglec to an increase in ROS production (Martin et al. 2011) like it was shown for Siglec-E in this study.

Siglec-8 sharing a high sequence homology with Siglec-E is known to induce apoptosis in eosinophils via caspase-8 and/or caspase-9 (Nutku et al. 2003). Cross-linking of Siglec-8 triggered caspase-3, caspase-8 and caspase-9 cleavage and led to an increase in annexin-V staining. Caspase inhibitors reduced Siglec-8-induced apoptosis in eosinophils. Additionally, Siglec-8 cross-linking resulted in mitochondrial dissipation, which is a characteristic of apoptosis. An inhibitor of ROS production was capable of completely inhibiting Siglec-8-mediated apoptosis and the associated mitochondria dissipation, indicating that ROS production is indispensable for Siglec-8-triggered apoptosis and precedes mitochondrial injury (Nutku et al. 2005). These results are in line with the analysis of ROS production in microglia with knock-down of Siglec-E, which had higher ROS production than control cells. This effect could be reversed by addition of a scavenger like SOD1 or trolox. Additionally, in the co-culture approach of neurons with microglia, trolox was able to abolish the neurotoxic effect of Siglec-E knock-down microglia and restore the relative neurite length back to control levels.

Concluding, the ITAM-Syk pathway seems to be of great importance for the initiation of ROS production in various cell types. Inhibition or knock-down of either Syk or a component bearing an ITAM sequence like the receptor DAP12 leads to a diminished respiratory burst. That Siglecs can indeed be linked to the respiratory burst was proven by the studies with CD33/Siglec-3, CD22/Siglec-2 and Siglec-8 (Gonzalez et

al. 2012; Martin et al. 2011; Nutku et al. 2005). As Siglec-E is an ITIM-containing receptor, which counter-balances activatory signals from ITAM receptors, it is not surprising to see that overexpression of Siglec-E on microglia resulted in a strongly reduced level of ROS whereas the knock-down of the inhibiting receptor Siglec-E led to an overproduction of ROS. Another indication for the involvement of Siglec-E in ROS production is that the elevated ROS production after knock-down of Siglec-E on microglia and treatment with neural debris could be rescued by addition of either the scavenger trolox or SOD1 to the system. This suggests, that for the knock-down of Siglec-E on microglia, the regulating part of this mechanism was missing, as was also shown in a study with SHP-1, leading to the increased amount of ROS production (Krotz et al. 2005).

4.4 Microglial Siglec-E has neuroprotective properties in co-culture with neurons

Experiments with a Siglec-E:Fc fusion protein demonstrated that Siglec-E binds to ligands on neurons, astrocytes and primary microglia. Overexpression of Siglec-E on microglia led to an increase in relative neurite length in a co-culture system indicating a neuroprotective function of Siglec-E in the co-culture system whereas knock-down of Siglec-E on microglia resulted in a diminished relative neurite length, arguing for a neurotoxic influence. Upon removal of sialic acid the binding capacity as well as the neuroprotective effect was abolished, demonstrating that the *trans* interaction with its ligands on the neurons was needed for Siglec-E to exert neuroprotection. Strikingly, co-culture of Siglec-E knock-down microglia and neurons in the presence of the ROS scavenger trolox reversed the neurotoxic effect, demonstrating that the neurotoxic effect was mediated via ROS. Thus, the data of this study suggest that microglial Siglec-E has neuroprotective properties by preventing ROS production.

A similar effect was shown for murine microglia being modified to express human Siglec-11. Transduction of microglia with human Siglec-11 resulted in an elevation of relative neurite length and a higher neuronal cell body density in a co-culture system with neurons pointing to an alleviation of microglial neurotoxicity (Wang and Neumann 2010).

The idea of microglia playing an important role in brain homeostasis is not new. They can either be beneficial and neuroprotective or detrimental and neurotoxic. The frontier between the two is narrow since acute neuroinflammation can be necessary to clear a site of injury and minimize further injury but chronic neuroinflammation can be harmful by promoting neurodegenerative diseases like AD, Parkinson's disease (PD) and amyotrophic lateral sclerosis (ALS). Activation of microglia in response to a threat includes phagocytosis (Napoli and Neumann 2009), antigen processing and presentation (Aloisi 2001), release of pro- and anti-inflammatory cytokines and of neurotoxic and neurotrophic factors (Walter and Neumann 2009).

Microglia are the main source of the proinflammatory cytokine TNF-α in the brain (Sawada et al. 1989). That TNF-α can be harmful in neuropathogenesis has been shown before (Abo-Ouf et al. 2013). Rodriguez and colleagues used either the anti-inflammatory agent minocycline or prednisolone or a combination of minocycline and prednisolone to treat the 6-hydroxydopamine hamster model. The treatment led to reduced levels of TNF-α and iNOS, which resulted in better recovery of dopaminergic neurons after the neurotoxic stimulus (Rodriguez et al. 2013). In a co-culture system of neurons and p38α-deficient microglia neurons were protected against LPS-induced synaptic loss, neurite degeneration and neuronal death. The p38α-deficient microglia produced decreased levels of TNF-α. Strikingly, addition of TNF-α to the system re-established LPS-induced neuron damage. Neutralization of TNF-α in a co-culture system with wildtype microglia prevented neuron damage. This demonstrates once more that microglia are the key mediators of LPS-induced neuronal and synaptic dysfunction partially through upregulation of TNF-α (Xing et al. 2011). Another study used the immunosuppressive antibiotic rifampicin in co-culture of microglia and neurons. Stimulation of microglia with rifampicin led to reduced release of iNOS, TNF-α, IL-1β and less production of NO. This resulted in reduced neurotoxicity and improved neuron survival (Bi et al. 2011). Fluoxetine is a selective serotonin re-uptake inhibitor. In a rat neuron-glia culture, fluoxetine was capable of attenuating LPS-induced chronic neurodegeneration as it inhibited activation of microglia and their release of proinflammatory cytokines like TNF-α and IL-1β and the neurotoxic factors NO and ROS. Thereby, fluoxetine exerted a neuroprotective effect by preventing microglial neurotoxicity (Zhang et al. 2012). The Siglec-E expression level on microglia influenced the production of TNF-α and IL-1β following

stimulation with neural debris. As the results of the before mentioned studies revealed, the release of cytokines like TNF-α needs a tight control. Therefore, it can be assumed that Siglec-E is a regulator of the production of cytokines and thereby helps to prevent overproduction of proinflammatory cytokines, which could become harmful if not tightly regulated. That IL-1β is another cytokine with devastating potential like TNF-α was shown in other studies. Ghrelin is a compound, which displayed neuroprotective properties in a PD model (Moon et al. 2009). An inducible IL-1β-overexpressing mouse model showed a significant increase in tau phosphorylation and a fourfold to sixfold increase in microglia associating with plaques. The microglia at the site of injury seemed more activated (Ghosh et al. 2013). Long-lasting expression of TNF-α in the substantia nigra caused death of dopaminergic neurons, irreversible akinesia and microglia activation (De Lella Ezcurra et al. 2010).

That no activation of microglia can be beneficial was demonstrated by a study where it was shown, that when there is no activation of microglia in the substantia nigra there is no activation of the NADPH oxidase, no ROS production and no production of proinflammatory cytokines and that this was advantageous for the dopaminergic neurons in the substantia nigra (Chung et al. 2012). Another study showed, that application of a free radical scavenger like SOD1 can be protective for dopaminergic neurons (Zhang et al. 2009). The study at hand demonstrated the neurotoxic effect of microglia using a knock-down of Siglec-E for neurons and showed that this effect was mediated by ROS since it could be reversed by the scavenger trolox. These results provide new insights to the impact of the Siglec-E expression level in microglia for ROS production and thereby its role for determining a neuroprotective or neurotoxic phenotype.

In conclusion, activation of microglia is essential to clear a site of injury. This process involves release of cytokines and neurotrophic factors. On the other hand, the activation of microglia can become harmful to neurons when this event is not tightly regulated by counter-balancing mechanisms. Siglec-E seems to be part of the mechanism by which the immune response is regulated by microglia as overexpression led to reduced release of pro-inflammatory cytokines and a diminished production of free radicals. In a co-culture system, this beneficial effect could be demonstrated by an increase in relative neurite length after overexpression

of Siglec-E on microglia, suggesting that Siglec-E has neuroprotective properties. The glycosylation pattern of the neurons was important to mediate the inhibitory effect of Siglec-E serving as a signal for the microglia to detect the healthy state of the neurons.

The outcome of this study could be of great importance for diseases that are accompanied by chronic inflammation like AD, PD or ALS as the chronic activation of microglia promotes the course of the diseases. For CD33/Siglec-3 it was shown that a specific CD33/Siglec-3 SNP in AD patients, which was correlated with higher expression of CD33 on microglia, was associated with an increase of insoluble Aβ42 levels and amyloid plaque load. Inactivation of CD33/Siglec-3 enhanced the uptake of amyloid beta whereas increase in CD33/Siglec-3 levels inhibited the uptake of amyloid beta by microglia (Griciuc et al. 2013). Siglec-E belongs to the CD33-related Siglecs and is expressed on microglia in the brain. As shown by this study, Siglec-E takes part in the regulation of microglia activity by inhibiting the release of pro-inflammatory cytokines like TNF-α and IL-1β and diminishes phagocytosis and the associated production of reactive oxygen species. Therefore, Siglec-E is likely to be another Siglec that associates with neurodegenerative diseases and may play an important role in the immune response. Further study in the context of neurodegenerative diseases might thus be interesting, since Siglec-E appears to be a Siglec with neuroprotective properties.

4.5 Outlook

The present study shows that Siglec-E is a murine Siglec with immunomodulatory properties on microglia. Through the influence on the transcription level of proinflammatory cytokines and the production of ROS following stimulation, the expression level of Siglec-E on microglia seems to be crucial for the phenotype. In a co-culture system with neurons, the expression level of Siglec-E determined if the microglia were neuroprotective or neurotoxic. The sialic acid cap on the glycocalyx of the neurons was important to mediate the binding of Siglec-E.

As this study provides solely *in vitro* data, the next interesting step would be to have a look into the *in vivo* situation. A study with Siglec-E knock-out mice already demonstrated that Siglec-E is crucial for the regulation of neutrophil recruitment in the lung (McMillan et al. 2013). But the impact of the Siglec-E knock-out on microglia

in the brain remains unknown so far. Further insights could be gained by analysing the influence of a Siglec-E overexpression on a neuroinflammatory disease model like experimental autoimmune disease (EAE) for Multiple Sclerosis to see, for example, whether pro-inflammatory cytokines are downregulated and whether the disease progression is reduced to a slower proceeding paralysis. Since Siglec-E overexpression was shown to lead to a more anti-inflammatory phenotype of microglia, a Siglec-E overexpressing mouse model might influence the disease progression to a milder disease course.

The level of ROS production by microglia was affected by modulation of Siglec-E expression. ALS is a disease, which is linked to elevated ROS production and frequently associated with a mutation in SOD1. The NADPH oxidase is a source of ROS and was shown to be regulated by SOD1. This regulation is defective in mutated SOD1 leading to elevated levels of superoxide (Harraz et al. 2008). Siglec-E knock-down resulted in increased levels of ROS production by microglia. Hence, a Siglec-E knock-out might enhance the disease course by additional superoxide release. Siglec-E under a constitutively higher expressed promoter specific for microglia like iba1 might thus be beneficial for the disease course. A similar experimental setup is conceivable in a mouse model of PD or AD as ROS production is known to play a detrimental role in the progression of these diseases. The ROS released by microglia is harmful for the surrounding neurons and thereby accelerates the disease course of PD and AD (Shimohama et al. 2000; Wu et al. 2003). A mouse model overexpressing Siglec-E in microglia might be beneficial as it might have decreased ROS production and therefore less neurotoxicity.

The process of phagocytosis is essential for a healthy brain. In the study at hand Siglec-E was demonstrated to influence the phagocytosis rate of microglia, depending on the expression status of Siglec-E on the microglial surface. AD is one of the most prominent neurodegenerative diseases where microglial phagocytosis is needed to clear amyloid plaques (Nicoll et al. 2006). Therefore, a mouse model of AD could be used to study whether Siglec-E knock-out or overexpression of Siglec-E leads to alterations in the plaque load in the brain. The human orthologue Siglec-9 was shown to be expressed on macrophages and an effect of Siglec-E in AD might provide indication of a possible involvement of Siglec-9 in AD as well (Ando et al. 2008).

Concluding, Siglec-E is a modulator of the microglial immune response concerning the release of proinflammatory cytokines like IL-1β and TNF-α, phagocytosis of cell debris and the production of ROS. With these features, Siglec-E should be an interesting topic for further studies in the context of different diseases involving neuroinflammation, phagocytosis and superoxide production. Since Siglec-E was shown to have neuroprotective properties in a co-culture system with neurons, it might be a promising target in the therapy and treatment of neurodegenerative diseases like PD or AD. More knowledge on the function of Siglec-E is needed to better understand its role in the modulation of the immune response. The outcome of studies concerning Siglec-E might be interesting for its human orthologues Siglec-7 and Siglec-9 as well.

5. Summary

The aim of this study was to investigate and understand the function of the receptor Siglec-E on microglial cells under neuroinflammatory conditions. So far, no data about Siglec-E on microglia are available. Therefore the initial step was to prove the transcription and expression of Siglec-E in microglia. *Ex vivo,* primary microglia as well as the microglial line were shown to express Siglec-E. To gain knowledge on the function of Siglec-E, lentiviral transductions were performed to obtain microglia lines either overexpressing Siglec-E or expressing less (knock-down) Siglec-E and the corresponding controls. The modified microglia did not show any changes in surface marker expression or cytokine transcription after the transduction procedure.

As phagocytosis is one of the main features of microglia, the phagocytic behaviour of the modified microglia was the first to be analysed. Microglia overexpressing Siglec-E had a decreased phagocytosis rate of neural debris whereas microglia with a knock-down of Siglec-E had an increased phagocytosis rate when compared to the corresponding controls. The phagocytosis-associated oxidative burst was relatively mild after stimulation with neural debris in microglia overexpressing Siglec-E and was more prominent in Siglec-E knock-down microglia being fed with neural debris. Quantification of mRNA levels of IL-1β, iNOS and TNF-α after stimulation with neural debris revealed that the Siglec-E overexpressing microglia showed no change in cytokine production while Siglec-E knock-down microglia showed a significant increase of IL-1β and TNF-α production following the stimulation.

Since neurons display high levels of the Siglec-E ligand sialic acid on their glycocalyx, the binding capacity of a Siglec-E:Fc fusion protein to neurons was tested. While the Siglec-E fusion proteins bound to neurons, this effect was abolished after enzymatic removal of sialic acid from the neuronal cell surface by sialidase. A co-culture experiment with primary hippocampal neurons and the different modified microglia showed that neurons, which had been cultured with microglia overexpressing Siglec-E, had the highest relative neurite length. In contrast, co-culture of microglia with knock-down of Siglec-E and neurons resulted in the lowest relative neurite length. Enzymatic removal of sialic acid on the neuronal glycocalyx led to an overall comparable decrease in relative neurite length. When the ROS

scavenger trolox was added to the co-culture system, the decrease in relative neurite length after knock-down of Siglec-E on microglia was restored to the level of the corresponding control.

In summary, these data show that Siglec-E is a regulatory receptor, which plays a role in phagocytosis and the associated oxidative burst. In the co-culture experiments the overexpression of Siglec-E on the microglia resulted in a neuroprotective phenotype by preventing the removal of neurites. The knock-down approach revealed that the ROS scavenger trolox is capable of restoring the detrimental effect in the co-culture system. Therefore, the neuroprotective effect of Siglec-E was mediated by attenuation of reactive oxygen species release. Thus, Siglec-E might be an interesting target in diseases associated with neuroinflammation and neurodegeneration.

6. References

Abo-Ouf H, Hooper AW, White EJ, van Rensburg HJ, Trigatti BL, Igdoura SA. 2013. Deletion of tumor necrosis factor-alpha ameliorates neurodegeneration in Sandhoff disease mice. Hum Mol Genet.

Alliot F, Lecain E, Grima B, Pessac B. 1991. Microglial progenitors with a high proliferative potential in the embryonic and adult mouse brain. Proc Natl Acad Sci U S A 88(4):1541-5.

Aloisi F. 2001. Immune function of microglia. Glia 36(2):165-79.

Ando M, Tu W, Nishijima K, Iijima S. 2008. Siglec-9 enhances IL-10 production in macrophages via tyrosine-based motifs. Biochem Biophys Res Commun 369(3):878-83.

Arthur JF, Qiao J, Shen Y, Davis AK, Dunne E, Berndt MC, Gardiner EE, Andrews RK. 2012. ITAM receptor-mediated generation of reactive oxygen species in human platelets occurs via Syk-dependent and Syk-independent pathways. J Thromb Haemost 10(6):1133-41.

Barron KD. 1995. The microglial cell. A historical review. J Neurol Sci 134 Suppl:57-68.

Bechmann I, Galea I, Perry VH. 2007. What is the blood-brain barrier (not)? Trends Immunol 28(1):5-11.

Bi W, Zhu L, Wang C, Liang Y, Liu J, Shi Q, Tao E. 2011. Rifampicin inhibits microglial inflammation and improves neuron survival against inflammation. Brain Res 1395:12-20.

Boyd CR, Orr SJ, Spence S, Burrows JF, Elliott J, Carroll HP, Brennan K, Ni Gabhann J, Coulter WA, Jones C and others. 2009. Siglec-E is up-regulated and phosphorylated following lipopolysaccharide stimulation in order to limit TLR-driven cytokine production. J Immunol 183(12):7703-9.

Bruhns P, Vely F, Malbec O, Fridman WH, Vivier E, Daeron M. 2000. Molecular basis of the recruitment of the SH2 domain-containing inositol 5-phosphatases SHIP1 and SHIP2 by fcgamma RIIB. J Biol Chem 275(48):37357-64.

Burshtyn DN, Yang W, Yi T, Long EO. 1997. A novel phosphotyrosine motif with a critical amino acid at position -2 for the SH2 domain-mediated activation of the tyrosine phosphatase SHP-1. J Biol Chem 272(20):13066-72.

Cardona AE, Pioro EP, Sasse ME, Kostenko V, Cardona SM, Dijkstra IM, Huang D, Kidd G, Dombrowski S, Dutta R and others. 2006. Control of microglial neurotoxicity by the fractalkine receptor. Nat Neurosci 9(7):917-24.

Chan WY, Kohsaka S, Rezaie P. 2007. The origin and cell lineage of microglia: new concepts. Brain Res Rev 53(2):344-54.

Cho JY, Song DJ, Pham A, Rosenthal P, Miller M, Dayan S, Doherty TA, Varki A, Broide DH. 2010. Chronic OVA allergen challenged Siglec-F deficient mice have increased mucus, remodeling, and epithelial Siglec-F ligands which are up-regulated by IL-4 and IL-13. Respir Res 11:154.

Chung ES, Bok E, Chung YC, Baik HH, Jin BK. 2012. Cannabinoids prevent lipopolysaccharide-induced neurodegeneration in the rat substantia nigra in vivo through inhibition of microglial activation and NADPH oxidase. Brain Res 1451:110-6.

Cicmil M, Thomas JM, Leduc M, Bon C, Gibbins JM. 2002. Platelet endothelial cell adhesion molecule-1 signaling inhibits the activation of human platelets. Blood 99(1):137-44.

Crocker PR. 2002. Siglecs: sialic-acid-binding immunoglobulin-like lectins in cell-cell interactions and signalling. Curr Opin Struct Biol 12(5):609-15.

Crocker PR, Clark EA, Filbin M, Gordon S, Jones Y, Kehrl JH, Kelm S, Le Douarin N, Powell L, Roder J and others. 1998. Siglecs: a family of sialic-acid binding lectins. Glycobiology 8(2):v.

Crocker PR, Freeman S, Gordon S, Kelm S. 1995. Sialoadhesin binds preferentially to cells of the granulocytic lineage. J Clin Invest 95(2):635-43.

Crocker PR, Gordon S. 1986. Properties and distribution of a lectin-like hemagglutinin differentially expressed by murine stromal tissue macrophages. J Exp Med 164(6):1862-75.

Crocker PR, Paulson JC, Varki A. 2007. Siglecs and their roles in the immune system. Nat Rev Immunol 7(4):255-66.

Crocker PR, Varki A. 2001a. Siglecs in the immune system. Immunology 103(2):137-45.

Crocker PR, Varki A. 2001b. Siglecs, sialic acids and innate immunity. Trends Immunol 22(6):337-42.

Daeron M, Jaeger S, Du Pasquier L, Vivier E. 2008. Immunoreceptor tyrosine-based inhibition motifs: a quest in the past and future. Immunol Rev 224:11-43.

Davalos D, Grutzendler J, Yang G, Kim JV, Zuo Y, Jung S, Littman DR, Dustin ML, Gan WB. 2005. ATP mediates rapid microglial response to local brain injury in vivo. Nat Neurosci 8(6):752-8.

De Lella Ezcurra AL, Chertoff M, Ferrari C, Graciarena M, Pitossi F. 2010. Chronic expression of low levels of tumor necrosis factor-alpha in the substantia nigra elicits progressive neurodegeneration, delayed motor symptoms and microglia/macrophage activation. Neurobiol Dis 37(3):630-40.

del Rio-Hortega P. 1919. El "tercer elemento" de los centros nerviosus. Bol Soc Esp Biol 9:69-120.

del Rio-Hortega P. 1932. Microglia. Penfield 2:483-534.

del Rio-Hortega P, Penfield W. 1927. Cerebral cicatrix. The reaction of neuroglia and microglia to brain wounds. Bull Johns Hopkins Hosp 41:278-282.

Falco M, Biassoni R, Bottino C, Vitale M, Sivori S, Augugliaro R, Moretta L, Moretta A. 1999. Identification and molecular cloning of p75/AIRM1, a novel member of the sialoadhesin family that functions as an inhibitory receptor in human natural killer cells. J Exp Med 190(6):793-802.

Ferlazzo G, Spaggiari GM, Semino C, Melioli G, Moretta L. 2000. Engagement of CD33 surface molecules prevents the generation of dendritic cells from both monocytes and CD34+ myeloid precursors. Eur J Immunol 30(3):827-33.

Floyd H, Ni J, Cornish AL, Zeng Z, Liu D, Carter KC, Steel J, Crocker PR. 2000. Siglec-8. A novel eosinophil-specific member of the immunoglobulin superfamily. J Biol Chem 275(2):861-6.

Gautier EL, Shay T, Miller J, Greter M, Jakubzick C, Ivanov S, Helft J, Chow A, Elpek KG, Gordonov S and others. 2012. Gene-expression profiles and transcriptional regulatory pathways that underlie the identity and diversity of mouse tissue macrophages. Nat Immunol 13(11):1118-28.

Ghosh S, Wu MD, Shaftel SS, Kyrkanides S, LaFerla FM, Olschowka JA, O'Banion MK. 2013. Sustained interleukin-1beta overexpression exacerbates tau pathology despite reduced amyloid burden in an Alzheimer's mouse model. J Neurosci 33(11):5053-64.

Ginhoux F, Greter M, Leboeuf M, Nandi S, See P, Gokhan S, Mehler MF, Conway SJ, Ng LG, Stanley ER and others. 2010. Fate mapping analysis reveals that adult microglia derive from primitive macrophages. Science 330(6005):841-5.

Gonzalez Y, Herrera MT, Soldevila G, Garcia-Garcia L, Fabian G, Perez-Armendariz EM, Bobadilla K, Guzman-Beltran S, Sada E, Torres M. 2012. High glucose concentrations induce TNF-alpha production through the down-regulation of CD33 in primary human monocytes. BMC Immunol 13:19.

Graham DB, Stephenson LM, Lam SK, Brim K, Lee HM, Bautista J, Gilfillan S, Akilesh S, Fujikawa K, Swat W. 2007. An ITAM-signaling pathway controls cross-presentation of particulate but not soluble antigens in dendritic cells. J Exp Med 204(12):2889-97.

Griciuc A, Serrano-Pozo A, Parrado AR, Lesinski AN, Asselin CN, Mullin K, Hooli B, Choi SH, Hyman BT, Tanzi RE. 2013. Alzheimer's disease risk gene CD33 inhibits microglial uptake of amyloid beta. Neuron 78(4):631-43.

Hanisch UK. 2002. Microglia as a source and target of cytokines. Glia 40(2):140-55.

Hanisch UK, Kettenmann H. 2007. Microglia: active sensor and versatile effector cells in the normal and pathologic brain. Nat Neurosci 10(11):1387-94.

Harraz MM, Marden JJ, Zhou W, Zhang Y, Williams A, Sharov VS, Nelson K, Luo M, Paulson H, Schoneich C and others. 2008. SOD1 mutations disrupt redox-sensitive Rac regulation of NADPH oxidase in a familial ALS model. J Clin Invest 118(2):659-70.

Hayakawa T, Angata T, Lewis AL, Mikkelsen TS, Varki NM, Varki A. 2005. A human-specific gene in microglia. Science 309(5741):1693.

Huang ZY, Hunter S, Kim MK, Indik ZK, Schreiber AD. 2003. The effect of phosphatases SHP-1 and SHIP-1 on signaling by the ITIM- and ITAM-containing Fcgamma receptors FcgammaRIIB and FcgammaRIIA. J Leukoc Biol 73(6):823-9.

Jones C, Virji M, Crocker PR. 2003. Recognition of sialylated meningococcal lipopolysaccharide by siglecs expressed on myeloid cells leads to enhanced bacterial uptake. Mol Microbiol 49(5):1213-25.

Kelm S, Gerlach J, Brossmer R, Danzer CP, Nitschke L. 2002. The ligand-binding domain of CD22 is needed for inhibition of the B cell receptor signal, as demonstrated by a novel human CD22-specific inhibitor compound. J Exp Med 195(9):1207-13.

Kelm S, Schauer R. 1997. Sialic acids in molecular and cellular interactions. Int Rev Cytol 175:137-240.

Kierdorf K, Erny D, Goldmann T, Sander V, Schulz C, Perdiguero EG, Wieghofer P, Heinrich A, Riemke P, Holscher C and others. 2013. Microglia emerge from erythromyeloid precursors via Pu.1- and Irf8-dependent pathways. Nat Neurosci 16(3):273-80.

Koizumi S, Shigemoto-Mogami Y, Nasu-Tada K, Shinozaki Y, Ohsawa K, Tsuda M, Joshi BV, Jacobson KA, Kohsaka S, Inoue K. 2007. UDP acting at P2Y6 receptors is a mediator of microglial phagocytosis. Nature 446(7139):1091-5.

Kono T, Imai Y, Yasuda S, Ohmori K, Fukui H, Ichikawa K, Tomita S, Imura J, Kuroda Y, Ueda Y and others. 2008. The CD155/poliovirus receptor enhances the proliferation of ras-mutated cells. Int J Cancer 122(2):317-24.

Krotz F, Engelbrecht B, Buerkle MA, Bassermann F, Bridell H, Gloe T, Duyster J, Pohl U, Sohn HY. 2005. The tyrosine phosphatase, SHP-1, is a negative regulator of endothelial superoxide formation. J Am Coll Cardiol 45(10):1700-6.

Lajaunias F, Dayer JM, Chizzolini C. 2005. Constitutive repressor activity of CD33 on human monocytes requires sialic acid recognition and phosphoinositide 3-kinase-mediated intracellular signaling. Eur J Immunol 35(1):243-51.

Lawson LJ, Perry VH, Dri P, Gordon S. 1990. Heterogeneity in the distribution and morphology of microglia in the normal adult mouse brain. Neuroscience 39(1):151-70.

Lee CY, Landreth GE. 2010. The role of microglia in amyloid clearance from the AD brain. J Neural Transm 117(8):949-60.

Lehnardt S. 2010. Innate immunity and neuroinflammation in the CNS: the role of microglia in Toll-like receptor-mediated neuronal injury. Glia 58(3):253-63.

Linnartz B, Kopatz J, Tenner AJ, Neumann H. 2012a. Sialic acid on the neuronal glycocalyx prevents complement C1 binding and complement receptor-3-mediated removal by microglia. J Neurosci 32(3):946-52.

Linnartz B, Wang Y, Neumann H. 2010. Microglial immunoreceptor tyrosine-based activation and inhibition motif signaling in neuroinflammation. Int J Alzheimers Dis 2010.

Logan MA, Hackett R, Doherty J, Sheehan A, Speese SD, Freeman MR. 2012. Negative regulation of glial engulfment activity by Draper terminates glial responses to axon injury. Nat Neurosci 15(5):722-30.

Malinska D, Kudin AP, Debska-Vielhaber G, Vielhaber S, Kunz WS. 2009. Chapter 23 Quantification of superoxide production by mouse brain and skeletal muscle mitochondria. Methods Enzymol 456:419-37.

Martin SM, Churchill E, McKnight H, Mahaffey CM, Ma Y, O'Donnell RT, Tuscano JM. 2011. The HB22.7 Anti-CD22 monoclonal antibody enhances bortezomib-mediated lymphomacidal activity in a sequence dependent manner. J Hematol Oncol 4:49.

McMillan SJ, Sharma RS, McKenzie EJ, Richards HE, Zhang J, Prescott A, Crocker PR. 2013. Siglec-E is a negative regulator of acute pulmonary neutrophil inflammation and suppresses CD11b beta2-integrin-dependent signaling. Blood 121(11):2084-94.

Meesmann HM, Fehr EM, Kierschke S, Herrmann M, Bilyy R, Heyder P, Blank N, Krienke S, Lorenz HM, Schiller M. 2010. Decrease of sialic acid residues as an eat-me signal on the surface of apoptotic lymphocytes. J Cell Sci 123(Pt 19):3347-56.

Mocsai A, Abram CL, Jakus Z, Hu Y, Lanier LL, Lowell CA. 2006. Integrin signaling in neutrophils and macrophages uses adaptors containing immunoreceptor tyrosine-based activation motifs. Nat Immunol 7(12):1326-33.

Moon M, Kim HG, Hwang L, Seo JH, Kim S, Hwang S, Lee D, Chung H, Oh MS, Lee KT and others. 2009. Neuroprotective effect of ghrelin in the 1-methyl-4-phenyl-1,2,3,6-tetrahydropyridine mouse model of Parkinson's disease by blocking microglial activation. Neurotox Res 15(4):332-47.

Nagaishi T, Pao L, Lin SH, Iijima H, Kaser A, Qiao SW, Chen Z, Glickman J, Najjar SM, Nakajima A and others. 2006. SHP1 phosphatase-dependent T cell inhibition by CEACAM1 adhesion molecule isoforms. Immunity 25(5):769-81.

Napoli I, Neumann H. 2009. Microglial clearance function in health and disease. Neuroscience 158(3):1030-8.

Nicoll JA, Barton E, Boche D, Neal JW, Ferrer I, Thompson P, Vlachouli C, Wilkinson D, Bayer A, Games D and others. 2006. Abeta species removal after abeta42 immunization. J Neuropathol Exp Neurol 65(11):1040-8.

Nimmerjahn A, Kirchhoff F, Helmchen F. 2005. Resting microglial cells are highly dynamic surveillants of brain parenchyma in vivo. Science 308(5726):1314-8.

Nutku E, Aizawa H, Hudson SA, Bochner BS. 2003. Ligation of Siglec-8: a selective mechanism for induction of human eosinophil apoptosis. Blood 101(12):5014-20.

Nutku E, Hudson SA, Bochner BS. 2005. Mechanism of Siglec-8-induced human eosinophil apoptosis: role of caspases and mitochondrial injury. Biochem Biophys Res Commun 336(3):918-24.

Ohta M, Ishida A, Toda M, Akita K, Inoue M, Yamashita K, Watanabe M, Murata T, Usui T, Nakada H. 2010. Immunomodulation of monocyte-derived dendritic cells through ligation of tumor-produced mucins to Siglec-9. Biochem Biophys Res Commun 402(4):663-9.

Olcese L, Lang P, Vely F, Cambiaggi A, Marguet D, Blery M, Hippen KL, Biassoni R, Moretta A, Moretta L and others. 1996. Human and mouse killer-cell inhibitory receptors recruit PTP1C and PTP1D protein tyrosine phosphatases. J Immunol 156(12):4531-4.

Pillai S, Netravali IA, Cariappa A, Mattoo H. 2011. Siglecs and Immune Regulation. Annu Rev Immunol.

Ransohoff RM, Perry VH. 2009. Microglial physiology: unique stimuli, specialized responses. Annu Rev Immunol 27:119-45.

Rathore V, Stapleton MA, Hillery CA, Montgomery RR, Nichols TC, Merricks EP, Newman DK, Newman PJ. 2003. PECAM-1 negatively regulates GPIb/V/IX signaling in murine platelets. Blood 102(10):3658-64.

Ravichandran KS. 2003. "Recruitment signals" from apoptotic cells: invitation to a quiet meal. Cell 113(7):817-20.

Ravichandran KS, Lorenz U. 2007. Engulfment of apoptotic cells: signals for a good meal. Nat Rev Immunol 7(12):964-74.

Redelinghuys P, Antonopoulos A, Liu Y, Campanero-Rhodes MA, McKenzie E, Haslam SM, Dell A, Feizi T, Crocker PR. 2011. Early murine T-lymphocyte activation is accompanied by a switch from N-glycolyl- to N-acetyl-neuraminic acid and generation of ligands for siglec-E. J Biol Chem.

Rodriguez S, Uchida K, Nakayama H. 2013. Striatal TH-immunopositive fibers recover after an intrastriatal injection of 6-hydroxydopamine in golden hamsters treated with prednisolone: roles of tumor necrosis factor-alpha and inducible nitric oxide synthase in neurodegeneration. Neurosci Res 76(1-2):83-92.

Sawada M, Kondo N, Suzumura A, Marunouchi T. 1989. Production of tumor necrosis factor-alpha by microglia and astrocytes in culture. Brain Res 491(2):394-7.

Schauer R, Kamerling J. 1997. Chemistry, biochemistry and biology of sialic acids. Glycoproteins II:243-402.

Schnaar RL. 2004. Glycolipid-mediated cell-cell recognition in inflammation and nerve regeneration. Arch Biochem Biophys 426(2):163-72.

Shimohama S, Tanino H, Kawakami N, Okamura N, Kodama H, Yamaguchi T, Hayakawa T, Nunomura A, Chiba S, Perry G and others. 2000. Activation of NADPH oxidase in Alzheimer's disease brains. Biochem Biophys Res Commun 273(1):5-9.

Stamenkovic I, Seed B. 1990. The B-cell antigen CD22 mediates monocyte and erythrocyte adhesion. Nature 345(6270):74-7.

Stevens B, Allen NJ, Vazquez LE, Howell GR, Christopherson KS, Nouri N, Micheva KD, Mehalow AK, Huberman AD, Stafford B and others. 2007. The classical complement cascade mediates CNS synapse elimination. Cell 131(6):1164-78.

Sun H, Xu XY, Tian XL, Shao HT, Wu XD, Wang Q, Su X, Shi Y. 2013. Activation of NF-kappaB and respiratory burst following Aspergillus fumigatus stimulation of macrophages. Immunobiology.

Takizawa H, Manz MG. 2007. Macrophage tolerance: CD47-SIRP-alpha-mediated signals matter. Nat Immunol 8(12):1287-9.

Ulyanova T, Shah DD, Thomas ML. 2001. Molecular cloning of MIS, a myeloid inhibitory siglec, that binds protein-tyrosine phosphatases SHP-1 and SHP-2. J Biol Chem 276(17):14451-8.

Van Den Herik-Oudijk IE, Westerdaal NA, Henriquez NV, Capel PJ, Van De Winkel JG. 1994. Functional analysis of human Fc gamma RII (CD32) isoforms expressed in B lymphocytes. J Immunol 152(2):574-85.

Varki A. 2011. Since there are PAMPs and DAMPs, there must be SAMPs? Glycan "self-associated molecular patterns" dampen innate immunity, but pathogens can mimic them. Glycobiology 21(9):1121-4.

Varki A, Schauer R. 2009. Sialic Acids.

Vely F, Olivero S, Olcese L, Moretta A, Damen JE, Liu L, Krystal G, Cambier JC, Daeron M, Vivier E. 1997. Differential association of phosphatases with hematopoietic co-receptors bearing immunoreceptor tyrosine-based inhibition motifs. Eur J Immunol 27(8):1994-2000.

Vitale C, Romagnani C, Falco M, Ponte M, Vitale M, Moretta A, Bacigalupo A, Moretta L, Mingari MC. 1999. Engagement of p75/AIRM1 or CD33 inhibits the proliferation of normal or leukemic myeloid cells. Proc Natl Acad Sci U S A 96(26):15091-6.

Vivier E, Daeron M. 1997. Immunoreceptor tyrosine-based inhibition motifs. Immunol Today 18(6):286-91.

Voisin T, El Firar A, Rouyer-Fessard C, Gratio V, Laburthe M. 2008. A hallmark of immunoreceptor, the tyrosine-based inhibitory motif ITIM, is present in the G protein-coupled receptor OX1R for orexins and drives apoptosis: a novel mechanism. Faseb J 22(6):1993-2002.

Walter L, Neumann H. 2009. Role of microglia in neuronal degeneration and regeneration. Semin Immunopathol 31(4):513-25.

Wang Y, Neumann H. 2010. Alleviation of neurotoxicity by microglial human Siglec-11. J Neurosci 30(9):3482-8.

Wen T, Mingler MK, Blanchard C, Wahl B, Pabst O, Rothenberg ME. 2011. The Pan-B Cell Marker CD22 Is Expressed on Gastrointestinal Eosinophils and Negatively Regulates Tissue Eosinophilia. J Immunol.

Wu DC, Teismann P, Tieu K, Vila M, Jackson-Lewis V, Ischiropoulos H, Przedborski S. 2003. NADPH oxidase mediates oxidative stress in the 1-methyl-4-phenyl-1,2,3,6-tetrahydropyridine model of Parkinson's disease. Proc Natl Acad Sci U S A 100(10):6145-50.

Xing B, Bachstetter AD, Van Eldik LJ. 2011. Microglial p38alpha MAPK is critical for LPS-induced neuron degeneration, through a mechanism involving TNFalpha. Mol Neurodegener 6:84.

Yamaji T, Teranishi T, Alphey MS, Crocker PR, Hashimoto Y. 2002. A small region of the natural killer cell receptor, Siglec-7, is responsible for its preferred binding to alpha 2,8-disialyl and branched alpha 2,6-sialyl residues. A comparison with Siglec-9. J Biol Chem 277(8):6324-32.

Yu Z, Maoui M, Wu L, Banville D, Shen S. 2001. mSiglec-E, a novel mouse CD33-related siglec (sialic acid-binding immunoglobulin-like lectin) that recruits Src homology 2 (SH2)-domain-containing protein tyrosine phosphatases SHP-1 and SHP-2. Biochem J 353(Pt 3):483-92.

Zhang F, Zhou H, Wilson BC, Shi JS, Hong JS, Gao HM. 2012. Fluoxetine protects neurons against microglial activation-mediated neurotoxicity. Parkinsonism Relat Disord 18 Suppl 1:S213-7.

Zhang JQ, Biedermann B, Nitschke L, Crocker PR. 2004. The murine inhibitory receptor mSiglec-E is expressed broadly on cells of the innate immune system whereas mSiglec-F is restricted to eosinophils. Eur J Immunol 34(4):1175-84.

Zhang JQ, Nicoll G, Jones C, Crocker PR. 2000. Siglec-9, a novel sialic acid binding member of the immunoglobulin superfamily expressed broadly on human blood leukocytes. J Biol Chem 275(29):22121-6.

Zhang M, Angata T, Cho JY, Miller M, Broide DH, Varki A. 2007. Defining the in vivo function of Siglec-F, a CD33-related Siglec expressed on mouse eosinophils. Blood 109(10):4280-7.

Zhang P, Wong TA, Lokuta KM, Turner DE, Vujisic K, Liu B. 2009. Microglia enhance manganese chloride-induced dopaminergic neurodegeneration: role of free radical generation. Exp Neurol 217(1):219-30.

Zhou Z, Hartwieg E, Horvitz HR. 2001. CED-1 is a transmembrane receptor that mediates cell corpse engulfment in C. elegans. Cell 104(1):43-56.

Ziegenfuss JS, Biswas R, Avery MA, Hong K, Sheehan AE, Yeung YG, Stanley ER, Freeman MR. 2008. Draper-dependent glial phagocytic activity is mediated by Src and Syk family kinase signalling. Nature 453(7197):935-9.

7. Acknowledgement

First I would like to thank Prof. Dr. Harald Neumann for giving me the opportunity to work in his group on such an interesting and fascinating topic, for his supervision and support. I also thank Prof. Dr. Joachim Schultze for being my second supervisor. Prof. Dr. Oliver Brüstle provided a stimulating working environment and encouraged exchange among colleagues.
Many thanks go to our collaborators Prof. Dr. Wolfram Kunz and Dr. Alexei Kudin. Of great support was our Postdoc Dr. Bettina Linnartz-Gerlach who was always there for discussion and advice when it was needed, thanks for that. Special thanks to Jessica Schumacher and Rita Hass for excellent technical support and help when I needed a second hand.

Thank you very much to my lab members who were not only colleagues but as well friends. They made work much more fun and were always there for discussion, support and sharing sweets. Special thanks to Jessica, Rita, Mona, Marcus and Johannes who always made me laugh and with whom I spent a great time in and outside the lab.

And last but not least my family and friends. They accompanied me not only during the years of my doctoral studies but the whole way to get there, most of them since school days. I am truly grateful for my parents who made it possible for me to get here and all their love and support. Special thanks go to my sister and Johannes Engert who were the greatest support during my studies of the last years, their company and understanding made a lot of things easier.

8. Erklärung/Declaration

I, Janine Claude, hereby confirm that this work submitted is my own. This thesis has been written independently and with no other sources and aids than stated. The presented thesis has not been submitted to another university and I have not applied for a doctorate procedure so far.

Hiermit versichere ich, dass die vorgelegte Arbeit – abgesehen von den ausdrücklich bezeichneten Hilfsmitteln – persönlich, selbständig und ohne Benutzung anderer als der angegebenen Hilfsmittel angefertigt wurde. Aus anderen Quellen direkt oder indirekt übernommene Daten und Konzepte sind unter Angabe der Quelle kenntlich gemacht worden. Die vorliegende Arbeit wurde an keiner anderen Hochschule als Dissertation eingereicht. Ich habe früher noch keinen Promotionsversuch unternommen.

Bonn, September 2013

_____

Janine Claude

9. Curriculum vitae

Computer skills

MS Office	excellent
SPSS	good knowledge
Corel Draw	good knowledge
Adobe Photoshop	good knowledge
EndNote	good knowledge

10. List of publications

Publication in peer-reviewed journals:

Kopatz J, Beutner C, Welle K, Bodea LG, Reinhardt J, **Claude J**, Linnartz-Gerlach B, Neumann H (2013): Siglec-h on activated microglia for recognition and engulfment of glioma cells. Glia 61(7):1122-33.

Manuscript in revision:

Claude J, Linnartz-Gerlach B, Kudin A, Kunz W, Neumann H (2013): Microglial CD33-related Siglec-E inhibits neurotoxicity by preventing the phagocytosis associated oxidative burst.

Abstracts:

Linnartz B, Bodea L-G, **Claude J**, Neumann H (2010): Complement opsonization and microglial removal of asialylated neuronal processes. 10th International Congress of Neuroimmunology, Sitges.

Wang Y, **Claude J**, Linnartz B, Neumann H (2010): Neuroprotective function of the microglial immunoreceptor tyrosine-based inhibitory motif-signaling receptor Siglec-11. 10th International Congress of Neuroimmunology, Sitges.

Claude J, Neumann H (2011): The implication of microglial sialic acid-binding immunoglobulin-like lectin-E (Siglec-E) in neuroinflammation. BFB Jahrestreffen, Bonn.

Claude J, Linnartz-Gerlach B, Neumann H (2013): Neuroprotective function of microglial Siglec-E. 11th European Meeting on Glial Cells in Health and Disease, Berlin.